

*Republic of Iraq  
Ministry of Higher Education  
and Scientific Research  
University of Kerbala  
College of Engineering*



**Experimental and Numerical Study of an Adsorption  
Water Desalination System Utilizing Low-grade Heat  
Sources**

*A Thesis*

*Submitted to the College of Engineering / University of  
Kerbala in Partial Fulfillment of the Requierments for a  
Master of Science Degree in Mechanical Engineering –  
Thermofluids Field*

*By*

**ESRAA ABBAS HUSSEIN**

Supervised By

**Asst. Prof. Dr. Mohammed Wahhab Al-Jibory**

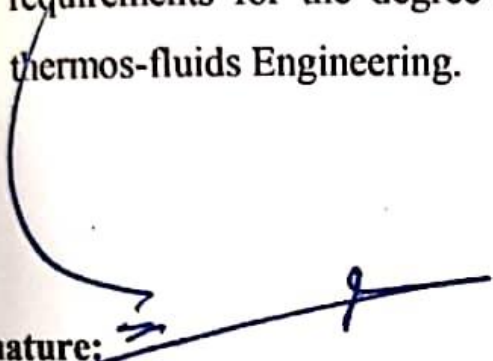
**Asst. Prof. Dr. Fadhel Noraldeen Abed Al-Mousawi**

**2021 A.D.**

**1443 A.H.**

## Supervisors Certification

We hereby certify that thesis entitled "Experimental and Numerical Study of an Adsorption Water Desalination System Utilizing Low-grade Heat Sources" prepared by ESRAA ABBAS HUSSIEN had been carried out completely under our supervision at the University of Kerbela, the Mechanical Engineering Department, for the partial fulfillment of the requirements for the degree of Master of Sciences in the Mechanical thermos-fluids Engineering.

Signature: 

Name: Asst. Prof. Dr. Mohammed Wahhab Al-Jibory

Date: 26/ 4/ 2022

Signature: 

Name: Asst. Prof. Dr. Fadhel Noraldeen Abed Al-Mousawi

Date: 26/ 4/ 2022

---

## **Linguistic certification**

I certify that this dissertation entitled (**Experimental and Numerical Study of an Adsorption Water Desalination System Utilizing Low-grade Heat Sources**) which has been submitted by (**Ms. Esraa Abbas Hussein**) has been prepared under my linguistic supervision. Its language has been edited to meet the basic linguistic requirement.

Signature: 

Name: **Dr. Ali Ahmed Abed Al rasul**

Title: Linguistic editor


Mechanical Engineering Department


University of Kerbela

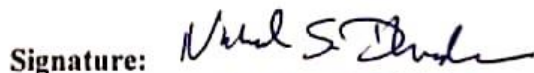
Date: 26/4/2022

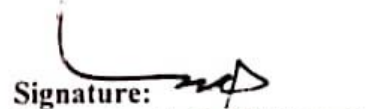
**Examining Committee Certification**


We certify that we have read this thesis entitled " **Experimental and Numerical Study of an Adsorption Water Desalination System Utilizing Low-grade Heat Sources** " and as an examining committee, examined the student " **Esraa Abbas Hussein** " in its content and what related to it, and that in our opinion it meets the standard of a thesis for the Degree of Master of Science in Mechanical Engineering.

Signature:   
Name: Asst. Prof. Dr. Mohammed Wahhab Al-Jibory  
(Member and Supervisor)  
Date: 26/4/2022


Signature:   
Name: Asst. Prof. Dr. Fadhel Noraldeen Abed Al-Mousawi  
(Member and Supervisor)  
Date: 26/4/2022

Signature:   
Name: Asst. Prof. Nabeel S. Dhaidan  
(Member)  
Date: 26/4/2022

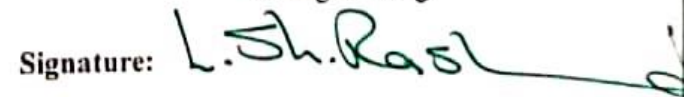
Signature:   
Name: Dr. Jaafar Ali Mahdi  
(Member)  
Date: 26/4/2022

Signature:   
Name: Prof. Dr. Alaa Abbas Mahdi  
(Chairman)  
Date: 26/4/2022

Approval of Mechanical Engineering Department

Signature:   
Name: Asst. Prof. Dr. Hayder Jabbar Kurji  
(Head of Mechanical Engineering Department)  
Date: 8/5/2022.

Approval of Deanery of College of Engineering

Signature:   
Name: Prof. Dr. Laith Shakir Rasheed  
(Dean of the College of Engineering)  
Date: 8/5/2022.

بِسْمِ اللّٰهِ الرَّحْمٰنِ الرَّحِیْمِ

﴿وَقُلْ اَعْمَلُوا فِی سَبِیْلِ اللّٰهِ  
عَمَلَكُمْ وَرِسُوْلَهُ وَالْمُؤْمِنُوْنَ  
وَسَتُرَدُّوْنَ اِلَى عَالَمِ الْغَیْبِ  
وَالشَّهَادَةِ فِیْنَبِیْكُمْ بِمَا كُنْتُمْ  
تَعْمَلُوْنَ﴾

.سورة النوبة (105)

صدق الله العلي العظيم

## *Dedication*

*Praise be to God first for all his blessings and gifts.*

*To the one who seeks success with his supplication always in front of my time (Al-Hujjah Ibn Al-Hassan), may God Almighty hasten his reappearance.*

*To the one who supported me and walked with me in every step (my husband).*

*To those who are the reason for my existence in life (my dear father, my dear mother).*

*To the candles that burn to light our ways for everyone who taught me the letter (my teachers).*

*To everyone who helped and encouraged me, my colleagues, and friends.*

*I dedicate this research, hoping that it will be accepted and successful.*

**ESRAA ABBAS**

**2022 A.D**

## *Acknowledgments*

First, I would like to express my sincere gratitude and thanks to ALLAH (be glorious) for the guidance through this work and for all the blessings bestowed upon me.

I would like to gratefully and sincerely thank my supervisors for their invaluable help, advice, guidance, understanding, and encouragement during this work.

I sincerely thank all the staff of the Mechanical Engineering.

Department of the University of Kerbela for their support and teaching.

I thank my family for their support which made me as ambitious as I wanted. I hope they always are well and able to get their satisfaction.

Finally, and most importantly, I would like to thank all my friends. Their continuous help, support, and encouragement enabled me to complete this thesis.

*ESRAA ABBAS*

*2022 A.D*

## **Abstract**

Drinking water scarcity is a widespread issue in several countries, affecting millions of people's life quality. Although desalination technologies can help solving the problem of water scarcity, they need a lot of energy and to emit a lot of (CO<sub>2</sub>). This study was carried out constructing a test apparatus and MATLAB SIMULINK model for the adsorption desalination and cooling system, monitoring the system's performance under various operating conditions, and determining the best operating conditions. The system was investigated experimentally and numerically under steady conditions.

The test rig consists of main parts and accessories. The adsorption bed, condenser, and evaporator are the main components of the system. While the pumps, tanks, and measuring devices with various kinds are secondary parts.

MATLAB Simulink has been utilized in this work to simulate the different components of the proposed system using Silica-gel and water as an adsorption pair. Due to the lab and cost limitations, the experimental facility contains only one adsorbent bed in addition to the condenser and evaporator, while the numerical model simulates two adsorbent beds besides the condenser and evaporator.



The simulation model has been validated with previously published experimental research. The performance of the system is monitored by its outputs, which are the specific daily water production (SDWP) and the specific cooling power (SCP). The effect of the working fluid temperatures in the condenser, evaporator, and bed, as well as the half cycle time, has been studied.

The experimental results showed that the SDWP and SCP of the system increase with the hot bed temperature by (2.43-6.21 l/kg<sub>ads</sub>/day), (87.95-100.88 W/kg<sub>ads</sub>), respectively and with the temperature of the evaporator by (4.5-6.3 l/kg<sub>ads</sub>/day), (72.43-103.47 W/kg<sub>ads</sub>) respectively, while they decrease with the water temperature of the condenser by (6.03-5.49 l/kg<sub>ads</sub>/day), (99.59-98.3 W/kg<sub>ads</sub>) respectively and with the half-cycle time by (4.59-2.97 l/kg<sub>ads</sub>/day), (95.71-72.43 W/kg<sub>ads</sub>) respectively.

Rising the heating temperature from (70°C to 90°C) results in a (60 %) growing in (SDWP) and a (12.8 %) increase in (SCP). (SDWP) and (SCP) have been improved by (28.5 %) and (30 %), respectively, when the evaporator water temperature raises from (30°C to 38°C). (SDWP) and (SCP) values are reduced by (55 % and 32 %), respectively, when the half-cycle period is increased from (300 to 500 sec).

The results highlight the potential of producing potable water and cooling system utilizing low grade temperatures helping millions of people around the world.

# Table of Contents

<b>Abstract</b>	<b>VII</b>
<b>Table of Contents</b>	<b>X</b>
<b>Nomenclature</b>	<b>XV</b>
<b>Chapter One – Introduction</b>	<b>1</b>
1.1 Background	1
1.2 Conventional desalination technologies	3
1.3 Adsorption technology	6
1.3.1 Adsorption materials	8
1.3.1.1 Physical, chemical and compound adsorbent materials	8
1.3.1.2 Advanced physical adsorbent materials	9
1.3.2 Adsorption cooling system	11
1.3.3 Adsorption desalination system	12
1.4 Aims and objectives of the present work	13
1.5 Research area	14
<b>Chapter Two - Literature Review</b>	<b>16</b>
2.1 Introduction	16
2.2 Traditional desalination system	16
2.2.1 Reverse osmosis technology	16
2.2.2 Solar distillation system	17
2.3 Adsorption desalination	18
2.3.1 Numerical studies	18
2.3.2 Experimental studies	29
2.4 Summary of literature review	35
2.5 Scope of the Present Work	39
<b>Chapter Three - Simulation of Adsorption System for Desalination and Cooling</b>	<b>40</b>
3.1 Introduction	40
3.2 System modeling	41
3.2.1 Adsorber /desorber bed energy balance equation	44
3.2.2 Evaporator energy balance equation	45
3.2.3 Condenser energy balance equation	46
3.2.4 Mass balance equations	47
3.2.5 Cycle performance formula	49
3.3 MATLAB SIMULINK model	49
3.4 SIMULINK model validation	50
3.5 Summary	53
<b>Chapter Four- Experimental Facility</b>	<b>54</b>
4.1 Introduction	54
4.2 System description	54

4.2.1 Adsorber bed	58
4.2.2 Evaporator	62
4.2.3 Condenser	64
4.2.4 Chiller/heater unit	65
4.2.5 Water pumps	67
4.2.6 Flow control valves	68
4.2.7 Hot and cold-water tanks	70
4.2.8 Vacuum system	71
4.3 Measuring devices	72
4.3.1 Pressure measurements	73
4.3.2 Temperature measurements	74
4.3.3 Flow rate measurements	75
4.4 Test rig checking	76
4.5 Experimental procedure	77
4.5.1 Initial preparations	77
4.5.2 Starting the test	78
4.5.3 Output readings	79
4.6 Summary	79
<b>Chapter Five - Results and Discussion</b>	<b>80</b>
5.1 Introduction	80
5.2 Numerical results	80
5.2.1 Half cycle time effect	81
5.2.2 Bed hot water temperature effect	83
5.2.3 Condenser inlet water temperature effect	84
5.2.4 Evaporator inlet water temperature effect	86
5.3 Experimental results	87
5.3.1 Half cycle time effect	88
5.3.2 Bed hot water temperature effect	90
5.3.3 Condenser inlet water temperature effect	91
5.3.4 Evaporator inlet water temperature effect	92
5.4 Summary	94
<b>Chapter Six- Conclusions and Suggestion for Future Works</b>	<b>95</b>
6.1 Conclusions	95
6.2 Suggestion for Future Works	96
<b>References</b>	<b>98</b>
<b>Appendix A</b>	<b>A-1</b>
<b>Adsorption bed design</b>	<b>A-1</b>
<b>Condenser design</b>	<b>A-2</b>
<b>Evaporator design</b>	<b>A-3</b>
<b>Appendix B</b>	<b>B-1</b>
<b>The Calibration of Instruments Used in Thesis</b>	<b>B-1</b>
<b>Data Logger and Thermocouples Calibration</b>	<b>B-2</b>

<b>Results of calibration</b>	<b>B-3</b>
<b>Appendix C</b>	<b>C-1</b>
<b>Published Research</b>	<b>C-1</b>
<b>Conference Published</b>	<b>C-2</b>
<b>Appendix D</b>	<b>D-1</b>
<b>Appendix E</b>	<b>E-1</b>

## List of Figures

Figure (1.1): Water in the earth.	<b>2</b>
Figure (1.2): Availability of drinkable water around the world.	<b>2</b>
Figure (1.3): Classification of desalination technologies.	<b>6</b>
Figure (1.4): Adsorption – Desorption mechanism.	<b>8</b>
Figure (1.5): major components of AD system.	<b>13</b>
Figure (1.6): Research area of this study.	<b>15</b>
Figure (2.1): Layouts of the introduced combined power and desalination systems.	<b>19</b>
Figure (2.2): Schematic of main components and variables in the batch RO system.	<b>21</b>
Figure (2.3): Using of carbon black and air laid paper-based evaporator.	<b>25</b>
Figure (2.4): Schematic design of the two-bed ADS.	<b>32</b>
Figure (3.1): Adsorption Desalination and cooling system.	<b>40</b>
Figure (3.2): Adsorber Bed Schematic diagram.	<b>44</b>
Figure (3.3): Schematic diagram of the evaporator.	<b>45</b>
Figure (3.4): Condenser schematic diagram.	<b>47</b>
Figure (3.5): Validation of Simulink, temperature profiles of adsorber beds, evaporator and condenser.	<b>51</b>
Figure (3.6): Flow chart for the Simulink model of the 2-bed adsorption desalination cycle.	<b>52</b>
Figure (4.1): Schematic scheme for the evaluation facility of the single bed.	<b>56</b>
Figure (4.2): An image of the single-bed testing facility.	<b>57</b>
Figure (4.3): Heat exchanger module.	<b>58</b>
Figure (4.4): Manufacturing of the adsorbent bed.	<b>60</b>
Figure (4.5): Adsorbent bed heat exchanger (left) before installing the mesh (middle & right) after installing the mesh.	<b>61</b>
Figure (4.6): XRD-6000 X-ray Diffractometer.	<b>61</b>
Figure (4.7): Evaporator used in test rig.	<b>63</b>
Figure (4.8): Condenser used in test rig.	<b>64</b>
Figure (4.9): Chiller/heater unit utilised in this study	<b>66</b>
Figure (4.10) temperature controller used in the chiller/heater unit	<b>66</b>
Figure (4.11): adsorber bed pump.	<b>68</b>

Figure (4.12) evaporator & condenser pump.	<b>68</b>
Figure (4.13): Manual Valve.	<b>69</b>
Figure (4.14): Hot water automatic valve.	<b>69</b>
Figure (4.15): Cold water automatic valve.	<b>69</b>
Figure (4.16): Double electric timer.	<b>69</b>
Figure (4.17): Cold water tank.	<b>70</b>
Figure (4.18): Hot water boiler.	<b>70</b>
Figure (4.19): Electric boiler temperature controller.	<b>71</b>
Figure (4.20): Vacuum Pump.	<b>71</b>
Figure (4.21): Vacuum System accessories.	<b>72</b>
Figure (4.22): Vacuum system manifold.	<b>72</b>
Figure (4.23): Pressure Sensor.	<b>73</b>
Figure (4.24): Arduino kit & screen.	<b>73</b>
Figure (4.25): Thermocouples used in test rig.	<b>75</b>
Figure (4.26): data logger used in test rig.	<b>75</b>
Figure (4.27): Adsorption bed flow meter.	<b>76</b>
Figure (4.28): Condenser & evaporator flow meter.	<b>76</b>
Figure (5.1): Effect of half cycle time on SDWP (numerical).	<b>82</b>
Figure (5.2): Effect of half cycle time on SCP (numerical).	<b>82</b>
Figure (5.3): Effect of bed hot water temperature on SDWP (numerical).	<b>83</b>
Figure (5.4): Effect of bed hot water temperature on SCP (numerical).	<b>84</b>
Figure (5.5): Silica-gel isotherms at 25°C.	<b>84</b>
Figure (5.6): Effect of condenser water temperature on SDWP (numerical)	<b>85</b>
Figure (5.7): Effect of condenser water temperature on SCP (numerical)	<b>85</b>
Figure (5.8): Effect of evaporator water temperature on SDWP (numerical)	<b>86</b>
Figure (5.9): Effect of evaporator water temperature on SCP (numerical)	<b>87</b>
Figure (5.10): Pictures of water condensation inside the condenser.	<b>88</b>
Figure (5.11): Effect of half cycle time on SDWP (Exp.).	<b>89</b>
Figure (5.12): Effect of half cycle time on SCP (Exp.).	<b>89</b>
Figure (5.13): Effect of bed hot water temperature on SDWP (Exp.).	<b>90</b>
Figure (5.14): Effect of bed hot water temperature on SCP (Exp.).	<b>91</b>
Figure (5.15): Effect of condenser water temperature on SDWP (Exp.)	<b>92</b>
Figure (5.16): Effect of condenser water temperature on SCP (Exp.).	<b>92</b>
Figure (5.17): Effect of evaporator water temperature on SDWP (Exp.).	<b>93</b>
Figure (5.18): Effect of evaporator water temperature on SCP (Exp.).	<b>93</b>

## List of Tables

Table (1.1): Silica-gel physical properties	<b>10</b>
Table (2.1): Summery of the researches.	<b>36</b>
Table (3.1): Operating conditions of the double bed validation test using Silica-gel.	<b>51</b>
Table (4.1): Heat exchanger characteristics.	<b>59</b>
Table (4.2): Specifications of temperature controller.	<b>67</b>
Table (5.1): Values of variables used in simulation.	<b>81</b>

## Nomenclature

A	Area	(m <sup>2</sup> )
c	Uptake	(kg <sub>water</sub> .kg <sub>ads</sub> <sup>-1</sup> )
c*	Equilibrium uptake	(kg <sub>water</sub> .kg <sub>ads</sub> <sup>-1</sup> )
c <sub>o</sub>	Maximum uptake	(kg <sub>water</sub> .kg <sub>ads</sub> <sup>-1</sup> )
c <sub>p</sub>	Specific heat at constant pressure	(kg. kg <sup>-1</sup> .K <sup>-1</sup> )
d	Diameter	(m)
E	Characteristic energy	(kJ.mol <sup>-1</sup> )
g	Gravitational acceleration	(m.s <sup>-2</sup> )
h <sub>fg</sub>	Latent heat	(kJ.kg <sup>-1</sup> )
k	Thermal conductivity	(W.m <sup>-1</sup> .K <sup>-1</sup> )
k <sub>o</sub>	Pre-exponential constant	(s <sup>-1</sup> )
L	Tube length	(m)
m	Mass	(kg)
<i>m</i>	Mass flow rate	(kg.s <sup>-1</sup> )
P	Pressure	(kPa)
PP	Electric pumping power	(kJ.s <sup>-1</sup> )
Q	Rate of heat transfer	(kJ.s <sup>-1</sup> )
Q <sub>st</sub>	Isosteric heat of adsorption	(kJ.kg <sup>-1</sup> )
R	Universal gas constant	(kJ.kmol <sup>-1</sup> .K <sup>-1</sup> )
SCP	Specific cooling power	(W.kg <sup>-1</sup> )
SDWP	Specific daily water production	(m <sup>3</sup> .tonne <sup>-1</sup> .day <sup>-1</sup> )
t	Time	(s)
T	Temperature	(K)
X	Salt concentration	(kgsalt.kgseawater <sup>-1</sup> )
z	Flag for adsorption/desorption processes	(-)
U	Overall heat transfer coefficient	(W.m <sup>-2</sup> .K <sup>-1</sup> )



### **Greek symbols**

$\theta$	Flag for seawater charging	(-)
$\gamma$	Flag for brine discharge	(-)
$\rho$	Density	(kg.m <sup>-3</sup> )

### **Subscripts**

a	Adsorbent material
abe	Adsorbed water vapor
ads	Adsorption
ads	adsorber bed
brine	Highly concentrated seawater
chilled	Water flowing in the evaporator coil
Cond.	Condenser
c <sub>w</sub>	Cooling Water
d	Distillate water
des	desorber bed
Des.	Desorption
Evap.	Evaporator
f	Liquid
g	Vapor
h <sub>w</sub>	Heating Water
HX	Heat exchanger
in	inlet
out	outlet
s	Seawater

### **Abbreviations**

AD	Adsorption desalination
BET	Burner emitted Taylor
COP	Coefficient of performance
ED	Electro-dialysis
FO	Forward osmosis
Frz	Freezing-desalination
G.Hyd	Gas-hydrate

HDH	Humidification - dehumidification
I.Ex	Ion-exchange
LLE	Liquid–liquid extraction
MED	Multi-effect distillation
MOFs	Metal organic frame works
MSF	Multi-stage flash
MVC	Mechanical vapor compression
NF	Nano-filtration
RO	Reverse osmosis
SD	Solar-distillation
TDS	Total dissolved solids (ppm)

# CHAPTER ONE

## Introduction

### 1.1 Background

Despite the fact that water covers (70%) of the earth, (98 %) of the water in the world supplies are saline, with just (2 %) being not salty. Seas, oceans, and some lakes store saline water, while (28 %) of drinkable water is kept underground and (70 %) is available as ice and snow in mountainous regions, in Antarctica, and the Arctic, with just (2 %) accessible by humans (see Figures 1.1 and 1.2), [1]. According to the World Health Organization (WHO), drinkable water is scarce for (2400) million people throughout the world, whereas (884) million people, on the other hand, do not have secure access [2, 3]. With the existing global population and limited supply of drinkable water, water desalination will help overcome the gap between limited drinkable water resources and the demands, ensuring a better existence for the entire world's population. Thermal, membrane, and chemical systems are one of the desalination technologies employed. However, disadvantages like increased electricity demand, high manufacturing costs, and pollution have resulted in the usage of desalination technology being restricted. For example, more than (60%) of the conventional desalination plants use reverse osmosis (RO), which to produce (1 m<sup>3</sup>) of drinkable water, and it normally takes around (4kW/h) of

electrical energy [4, 5]. As a result of such high energy demand, fossil fuel supplies are depleted, carbon dioxide levels rise, and the global warming trend worsens. Adsorption systems for water desalination have recently been studied, in which low-grade heat sources with temperature of (50–85°C) such as solar energy ,geothermal energy ,biomass energy and waste heat may be employed to generate drinkable water, lowering energy consumption, cost, and (CO<sub>2</sub>)emissions,[6, 7].

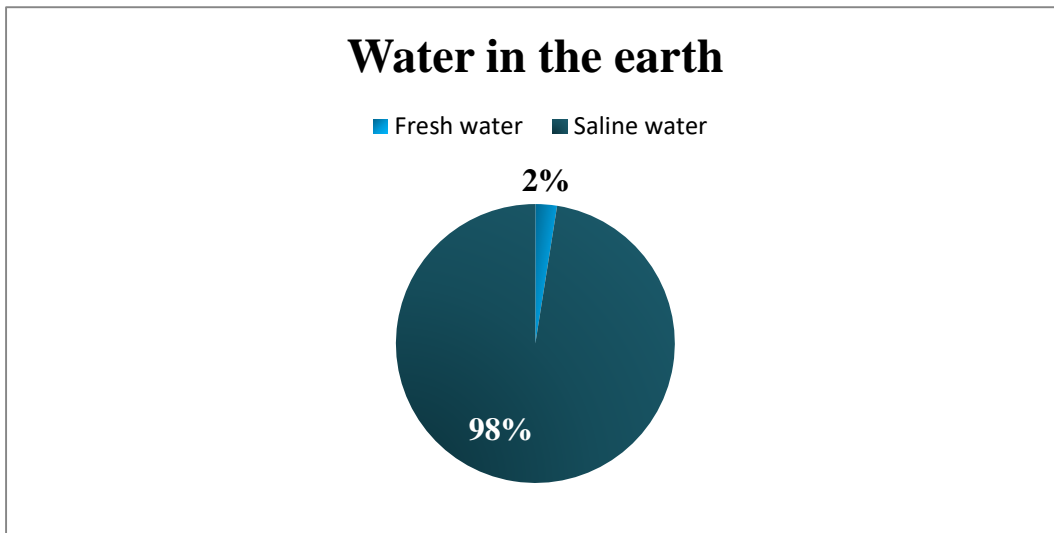


Figure (1.1): Water in the earth,[1]

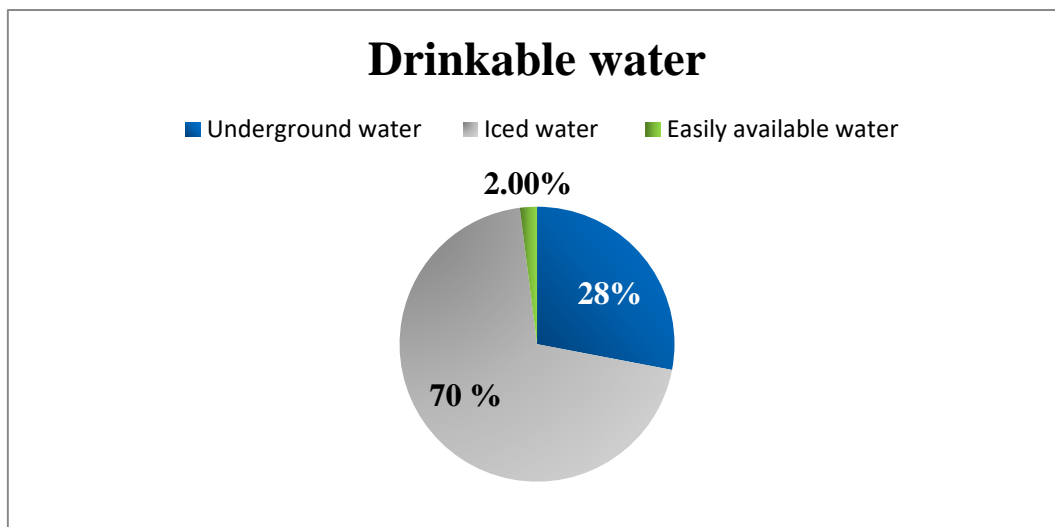


Figure (1.2): Availability of drinkable water around the world,[1]

## **1.2 Conventional desalination technologies**

Recently, many desalination technologies are used for generating drinkable water in many parts of the world[8]. Salt is extracted from seawater using thermally methods such as boiling (phase change; liquid to vapor) or freezing (phase change; liquid to solid). Salt is separated from saltwater using membrane-based techniques that apply an electric charge or pressure to the saline water, causing just pure drinkable water to flow over the membrane while impurities stay behind. Chemical desalination systems, unlike other desalination procedures, rely on chemical variations instead of pressure changes or phase change[5, 9].

There are many processes available in thermally-based desalination systems, like multi-stage flash (MSF), multi-effect distillation (MED), mechanical vapour compression (MVC), humidification - dehumidification (HDH), solar distillation (SD), and freezing desalination (Frz) as shown in (Figure 1.3).

For several years, multi stage flash (MSF) was usually used until it became one of the most widely used inventions in the world. To begin, the salty water suffers from successive evaporation processes until it reaches the last stage in which it is safe to drink.

Multi effect desalination (MED) is like to MSF in that it relies on salty water evaporation at various zones and collects and extracts the

residual condensed saline from the system. The evaporation technique and heat transfer methods, vary from system to another. However the blinking boxes, number of results (stages), and condenser are the main components of the MED plant [10-13]. The humidification-dehumidification (HDH) process is similar to the rain cycle that occurs in nature. Saline water is evaporated then air carries this pure water vapor (humidification process) which is condensed later to obtain distillate water (dehumidification process). The principle idea of these systems depends on the increasing ability of dry air to carry water vapor and heat energy with the elevation of its temperature.

Systems based on membrane employ porous polymer membranes that only let drinkable water particles to move through, leaving impurities as discarded. Membrane-based technologies include reverse osmosis (RO), forward osmosis (FO), nanofiltration (NF), and electro-dialysis (ED). Membrane- methods, unlike thermal processes, rely on electric charge or pressure variations between two membranes placed near to each other. Reverse osmosis, forward osmosis, and nanofiltration are pressure-based systems, whereas electro-dialysis is based on an electric charge difference. Once there is a difference in salt content over a membrane, the osmosis phenomenon occurs, and water continues to exit the low concentration region and flow across the membrane to the more saturated zone. This

method is repeated until the pressure differential equals the osmotic pressure, which happens when chemical equilibrium is reached. The reverse osmosis process (RO) is the polar reverse of natural osmosis, in which water is forced to move through a semipermeable membrane from a higher concentration area to a lower concentration region, leaving salts behind as waste.

Ion exchange (I.Ex), in an ion-exchange unit water enters a tank containing high capacity exchange beads (cation exchange resin). These beads are saturated with either sodium or potassium which are known as replacement ions. While water passes through this tank, an exchange occurs between contaminant ions and replacement ions which are released to the water. This type of desalination was found to be suitable for water treatment and for brackish water desalination. Liquid-Liquid Extraction (LLE), in the Liquid-liquid extraction system a specially tailored polymer solvent is used to extract fresh water in a desalination process at temperatures not more than 60°C. When seawater is contacted with these polymer solvents, two phases are produced; a polymer phase with dissolved water and another aqueous phase with insoluble polymer. Gas hydrates (G.Hyd), are crystalline solid structures that consist of water and other molecules like (N<sub>2</sub>), (CO<sub>2</sub>), (CH<sub>4</sub>), (H<sub>2</sub>) and others which are

employed for water desalination purposes and they are formed under low temperature and high pressures [5, 9, 14-18] (as shown in Figure 1.3).

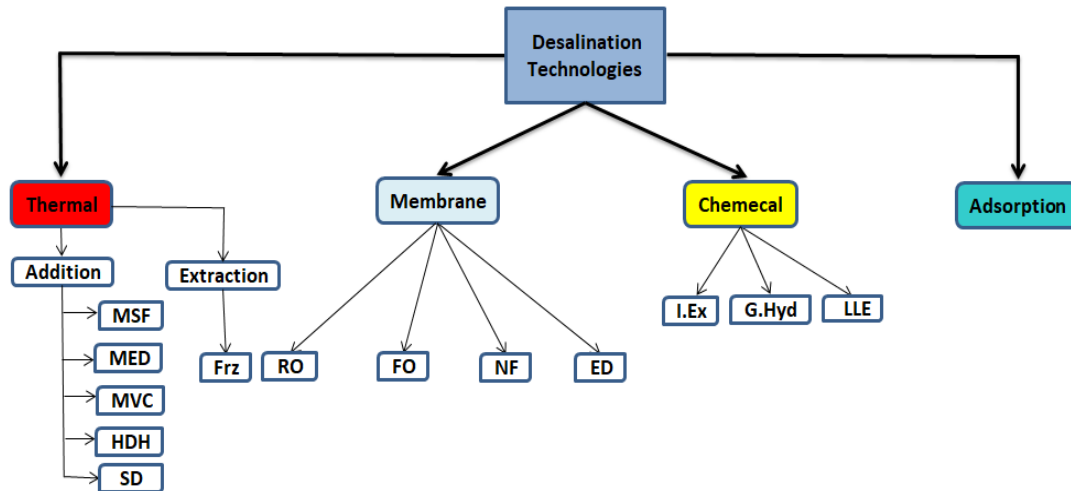


Figure (1.3): Classification of desalination technologies [1]

### 1.3 Adsorption technology

Adsorption is an ancient phenomenon, Scheele and Fontana, for example, recorded the adsorption of gases on charcoal and clays, respectively, in 1773 and 1777 AC. De Saussure further discovered that heat is generated during the process, and that the solid material's porosity is the primary cause of the adsorption process. Since then, adsorption has become a promising field with numerous scientific trials, as it can be used in a range of applications such as dehumidification, thermal batteries, electricity generation, cooling and freezing, and delivering drinking water to remote areas[19].



Adsorption is the process by which gas molecules adhere to a surface. This mechanism forms an adsorbate coating on the adsorbent's surface. It varies from absorption, which occurs when a liquid dissolves or permeates a solid for example Adsorption of water vapor on silica gel reduces humidity. Absorption is defined as the phenomenon in which a liquid substance, known as absorbent, gets soaked or absorbed completely into the surface of the absorbent for example absorption of water in a sponge and the absorption of oxygen in water is responsible for the survival of the aquatic ecosystem. while adsorption is a surface-based operation.

Adsorption may be categorized as either physical or chemical depending on the type of bond formed between the adsorbate (vapour molecules) and the adsorbent (solid), as well as the extent of the adsorption heat. As adsorption occurs due to contacts between a solid (adsorbent) and vapor molecules (adsorbate), it is important to differentiate between physical and chemical adsorption. In chemical adsorption, a straight chemical bond is formed. There is no direct chemical bond between the surface and the adsorbate in physical adsorption, and the adsorbate is kept in place by physical forces (i.e., van der Waals and electrostatic). As a result of the change in energy level of the adsorbate molecules between gaseous and adsorbed phases during physical adsorption, heat is released; hence, physical adsorption is an exothermic operation. Physical adsorption

contains weak bonds between molecules, as the heat needed to free adsorbate (i.e., adsorption heat) is like to the latent heat [20] as shown in Figure (1.4).

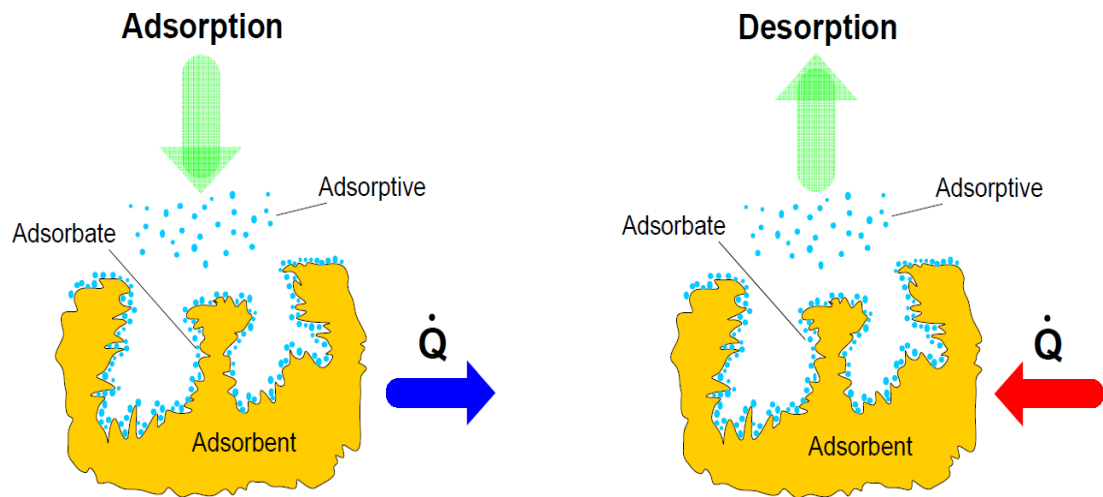


Figure (1.4): Adsorption – Desorption mechanism[4]

### 1.3.1 Adsorption materials

Each adsorption cycle requires an adsorber bed, which is filled with a solid adsorbent material such as Silica-gel to accomplish adsorbing and desorbing processes.

#### 1.3.1.1 Physical, chemical and compound adsorbent

Physical adsorbents are porous substances that adsorb using Van der Waals forces. They are steadier than chemical adsorbents and may keep their characteristics while desorbing the adsorbate. Different forms of

physical adsorbents include silicates, metal aluminophosphates, zeolites, activated carbons, and Metal Organic Frameworks (MOFs)[21].

The interaction between the adsorbate particles and the chemical adsorbent material is the basis of the adsorption and desorption mechanism in chemical adsorbents. Metal chloride salts besides metal hydrides, metal oxides, and composite adsorbents are all examples of chemical adsorbents (chemical and physical mixtures).

Since chemical adsorbents have a greater adsorption heat, as a result, a higher kinetics rate than traditional adsorbents, the primary reason of utilizing composite adsorbent is to increase the adsorption properties of physical adsorbent. They have resisted chemical adsorbent materials' disadvantages, such as agglomeration, and poor thermal conductivity. Addition of hygroscopic to Silica-gel, for example, will improve its adsorption properties and increase water absorption while avoiding the issue of chemical adsorbent materials[22].

### **1.3.1.2 Advanced physical adsorbent materials**

Advanced adsorbent materials with great adsorption abilities are needed to improve adsorption technology. Several scientists and companies carried out innovative adsorbent to improve the efficiency of adsorption devices over the last decade. Metal organic framework MOFs (Aluminum Fumarate, CPO-27Ni, MIL-100 (Al), etc....) are new

adsorbent materials with a high specific surface area and excellent water absorption. In addition, Mitsubishi Plastic's AQSAO-Z02 is an innovative adsorbent material that has attracted a lot of attention in recent years due to its high water absorption [23].

Silica gel and water has a poor uptake of around 0.21 kg/kg<sub>ads</sub>, but certain forms of Silica gel and water have a higher water uptake of 0.4466 kg/kg<sub>ads</sub> for type RD Silica gel and 0.3947 kg/kg<sub>ads</sub> for type A Silica gel. MOFs are great porosity, greater adsorption properties, equal pore size, and BET surface area (to 5500 m<sup>2</sup>/g) advanced adsorbents MIL101 (Cr), in particular, is an exceptional adsorbent substance with a water absorption of 1.47 kg/kg<sub>ads</sub>. Also, commercially available MOFs Al-Fumarate and CPO-27(Ni) have gross water uptakes of 0.531 kg/kg<sub>ads</sub> and 0.472 kg/kg<sub>ads</sub>, respectively[24],see Table (1.1).

\ Table (1.1): Silica-gel physical properties, [26]

<b>Property</b>	<b>Silica gel</b>
<b>BET surface area m<sup>2</sup>/g</b>	<b>841</b>
<b>Max uptake kg/kg ads</b>	<b>0.5092</b>
<b>Bulk density kg/m<sup>3</sup></b>	<b>820</b>
<b>Pore volume cm<sup>3</sup>/g</b>	<b>0.4478</b>
<b>Heat of adsorption (kJ/kg)</b>	<b>2431</b>
<b>Particle radius (m)</b>	<b>0.16 E<sup>-3</sup></b>

The reason for choosing silica gel in this study is due to its abundance in Iraq and the lack of other modern materials, in addition to the fact that silica gel is a standard material in the study of adsorption systems.

### **1.3.2 Adsorption cooling system**

The vast majority of global cooling and heating demands are met by traditional vapour compression systems, which use refrigerants with high Global Warming Potential (GWP) [25, 26]. Consuming promising green energy technology like adsorption and absorption, rich green energy supplies such as low-grade waste energy or solar energy can be converted into usable cooling and electricity. As a result, adsorption cooling, which has gotten a lot of attention recently, is a good alternative to traditional refrigeration and air conditioning systems because it transforms low-grade heat into usable cooling/heating and uses refrigerants with zero Ozone Depletion Potential (ODP) and Global Warming Potential (GWP) [27, 28]. Two adsorption beds, a condenser, and an evaporator make up basic adsorption cooling system. Adsorbent material, such as Silica-gel, is placed in the adsorber beds, and the device is filled with a working fluid, such as water.

### **1.3.3 Adsorption desalination system**

The adsorption desalination (AD) technique has the advantage of using low-grade heat source to generate drinking water using adsorbent material (See Figure 1.5). The AD device consists of major components (evaporator, adsorber bed and condenser. There are many benefits to the desalination method:

- 1~ It is a green technology since it can operate on limited heat sources below 100°C, lowering CO<sub>2</sub> emissions and lessen global warming.
- 2~ Lesser decay and pollution factors compared with rest low evaporating temperatures (<30°C) desalination systems.
- 3~ Limited moveable parts; resulting in lower cost and maintenance for the system.
- 4~ The adsorption desalination and cooling system presents the ability for manufacturing potable water and cooling to be provided using low grade heat sources.
- 5~ Usually uses environmentally sustainable materials[29].

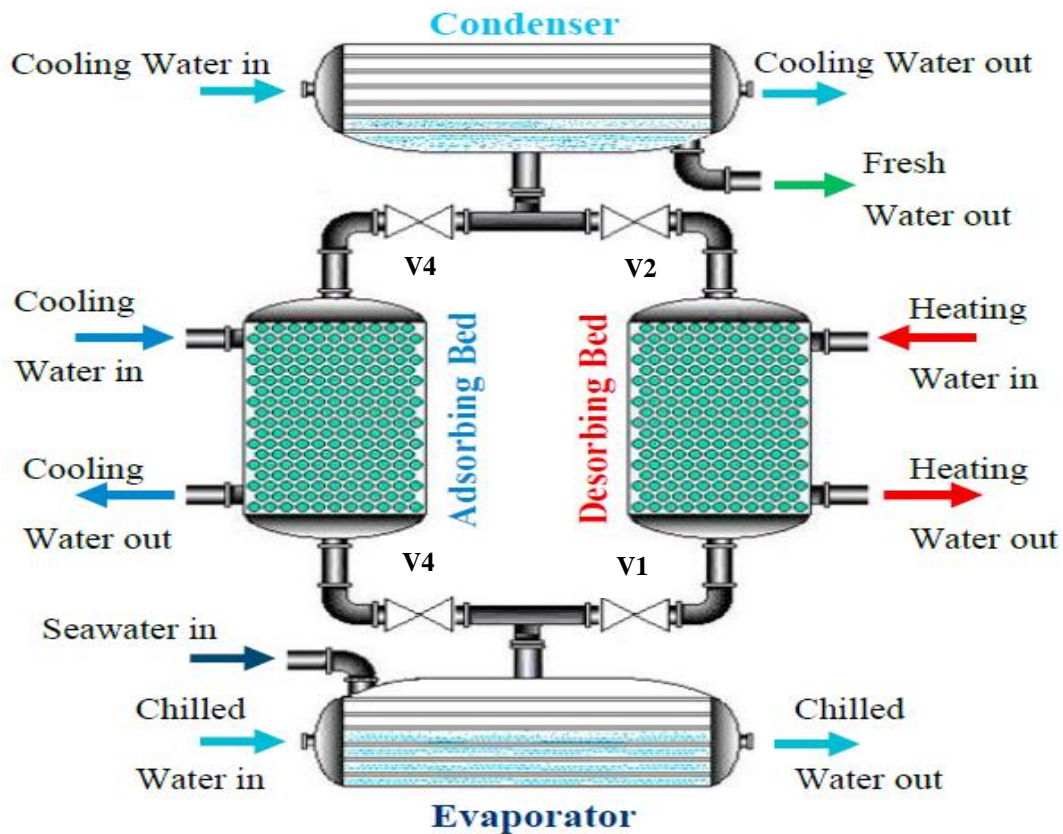


Figure (1.5): major components of AD system [1]

While the disadvantage of this system are large size of the system and high cost of modern adsorbents.

#### 1.4 Aims and Objectives of the Present Work

The goal of this research was to develop and investigate the feasibility of using heat driven adsorption-based desalination and cooling system. This work was accomplished by achieving the following task:

- 1- An experimental apparatus was built, which comprises Silica-gel one-bed adsorption desalination and cooling system using hot water as a heating sources.

- 2- A dynamic simulation model (MATLAB Simulink) that estimates the output of the adsorption desalination and cooling system introduced for this study.
- 3- The above-mentioned model is used to evaluate the impact of using different operating parameters on the adsorption desalination (AD) performance, and conclusions are drawn about the conditions under which (AD) is likely to be economically viable.

### **1.5 Research area**

The use of clean technologies such as adsorption techniques to produce potable water can help solving the problem of receding potable water, reduce energy consumption, and thus eliminate the polluting emissions to the atmosphere. Figure (1.6) summarizes the key technologies that employ low-grade heat sources and identifies research points. It should be noted that, there was no similar work on utilizing adsorption systems to generate drinking water in Iraq.



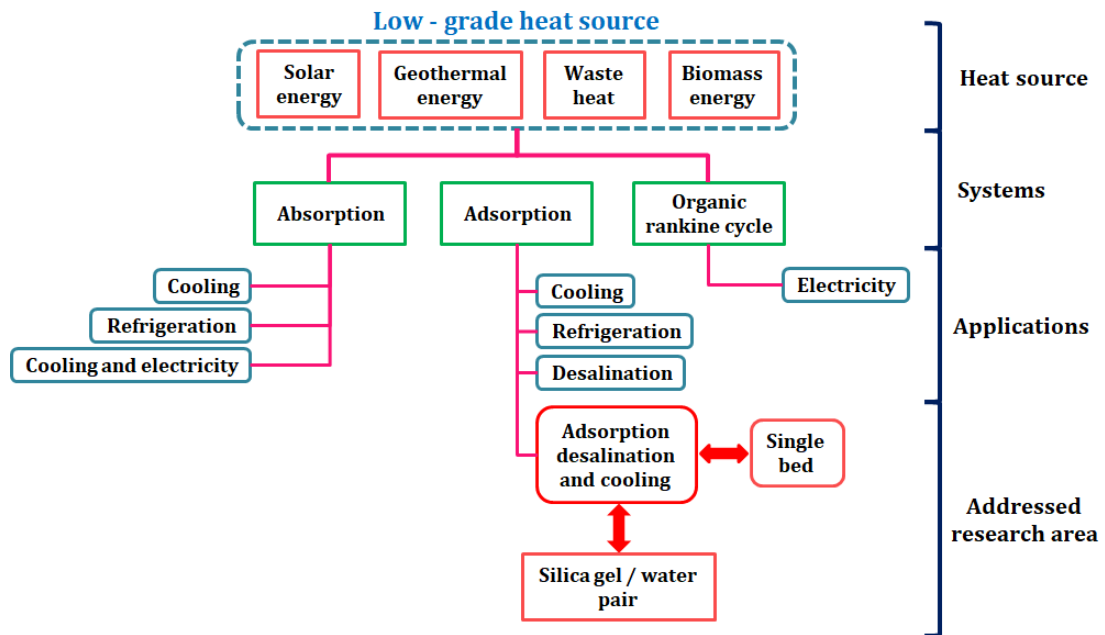


Figure (1.6): Research area of this study

# CHAPTER TWO

## Literatures review

### 2.1 Introduction

This chapter is related with a review of literature concerned with ...

### 2.2 Traditional desalination systems

#### 2.2.1 Reverse osmosis technology

**Namin, et. al, (2020),[30]**, had suggested a three innovative cascade systems based on ORC (Organic Rankine Cycle) and KC (Kalina cycle), with thermodynamic and thermoeconomic analyses performed on the future systems. The device is designed to have the highest net power, power efficiency, and exergy efficiency, as well as the lowest SUCP (sum unit cost of product) and overall exergy damage. According to the findings of the case study simulation for the Bushehr Port, owing to the low value of SUCP (72.42 \$/kWh) and the fact that more potable water was provided in June, the most cost-effective month for the planned power/desalination was June.

**Park, et. al, (2020),[31]**, have presented a batch (RO) system with two alternating phases that operates cyclically. To pass pressure from the feed fluid to the recirculating fluid, the mechanism employs a free piston installed in a pressure vessel. There is no full design

process for this configuration. They proposed a systematic model based on reasonable assumptions to fill this void. The model is implemented in a straight forward three-step method that only needs the solution of basic algebraic equations and does not require the use of specialised computational techniques. The findings show that the optimised batch (RO) can deliver potable water with low energy consumption at (80 %) recovery, with efficiency of (33.2 %) compare to (10–15 %) for traditional salty water (RO).

### **2.2.2 Solar distillation system**

**Singh, et.al, (2020),[32]**, discussed the changes that a solar distillation device undergoes to become active and have the best output in terms of produce and system productivity at a low distillate rate. The active device has the ability to connect to a wide range of similar elements and programmes, resulting in a significant increase in the system's overall performance. The installation of more collectors and concentrators increases the system's efficiency, allowing it to successfully support a vast population for a long time at a low cost. Furthermore, based on the results, it has been proposed that active solar distillation technology be used for the reliable and cost-effective processing of potable water in a sustainable manner.

**Chen, et. al, (2020),[33]**, had developed a CAPER (carbon black and air laid paper-based evaporator) which is a low-cost, robust, solar-driven evaporator for water desalination of (produced water) PW in the Permian Basin, United States. Solar distillation removed (99.97 %) salts and over (98 %) heavy metals from the PW, which had a gross dissolved solids content of (134 g/l). Ca, Na, Mg, Mn, Ni, Se and Sr all had a high removal performance of (99.99 %). Solar distillation extracted over (83 %) aromatic compounds, according to organic characterization. CAPER-based solar desalination is a low-cost, high-performance method for treating (PW) with high salinity and complex water chemistry for future fit-for-purpose beneficial applications.

## **2.3 Adsorption desalination**

### **2.3.1 Numerical studies**

**Thu, et. al, (2013),[34]**, have introduced a numerical simulation of an innovative adsorption desalination cycle with two beds to investigate an internal heat recovery between the evaporator and the condenser that used in this advanced adsorption desalination cycle, which uses an encapsulated evaporator–condenser device for efficient heat transfer (see Figure 2.1) . Values of the parameters used in the simulation program are hot water inlet temperature (65–85°C) from low temperature waste heat, cooling water inlet temperature (30°C) and Silica gel as adsorbent. To

determine the cycle's output, a mathematical model code runs on the platform of FORTRAN Power Station is used to call the numerical solver. The isotherm and kinetic properties of the Silica gel–water pair are used to estimate water vapour absorption by the Silica gels at different temperatures and pressures. The model is also evaluated using the mass and energy balances of the materials used in the cycle. The advantages of the advanced (AD) cycle are reduction in the parasitic electrical power consumption ( $1.38 \text{ kWh m}^{-3}$ ) with the elimination of pumps for chilled and cooling water circuits. The adsorption capacity of Silica gel getting better (40%) of the dry mass of the adsorbent) due to the pressurization effect of evaporator this achieved by increase in the evaporation temperature which is about ( $42^\circ\text{C}$ ) through heat recovery from condensation process thus specific water production yield improves remarkably: varying from (8100  $l$  to 26000  $l$ ).

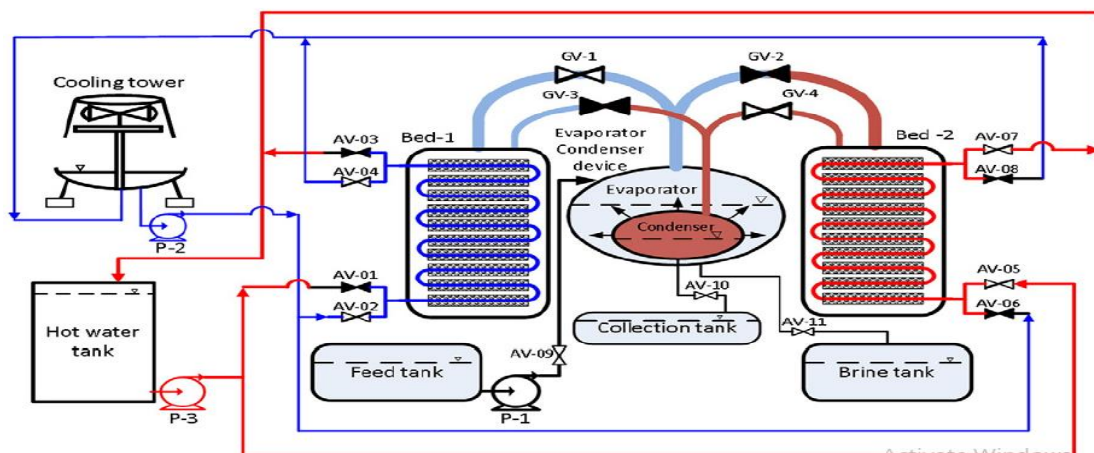


Figure (2.1): The advanced adsorption desalination (AD) cycle with an integrated evaporator–condenser device, [34]

**Mitra, et. al, (2014),[35]**, suggested a solar driven (AD) system. The system dynamics of a 4-bed single stage silica-gel + water-based AD system was investigated in this report. A lumped model produced by combining energy and mass conservation with the kinetics of the adsorption/desorption process. The governor equations for the system parts, namely the evaporator, adsorber, and condenser, are solved, and the efficiency of the system is evaluated for a single stage (AD) system at different condenser temperatures and cycle times to decide the best operating conditions needed for desalination and cooling. The hot and cold-water temperatures and half cycle time used in simulation were (85°C), (30°C) and (1200s) respectively. The simulation study shows that the single-stage AD system has an optimum half cycle time in the range of (600-900s) and condenser temperature of (25°C) for maximizing desalination about (2.4 l/kg<sub>ads</sub> per day).

**Youssef, et. al, (2016),[36]**, carried out a numerical simulation of combined adsorption desalination cycle with combined evaporator/condenser utilizing AQSOA-Z02 as adsorbent. It consists of two cycles of 2-adsorber beds connected by an integrated evaporator/condenser; one cycle uses the built-in evaporator/condenser as a condenser and the next as an evaporator (lower) (see Figure 2.1). Depending on the desalinated water and cooling requirements, this machine can work in three modes, a full scale adsorption machine with

the configuration presented is simulated by Simulink. The specific daily water production varies from (6.64 to 15.4 l/kg<sub>ads</sub> per day) at evaporator temperature of (10°C).

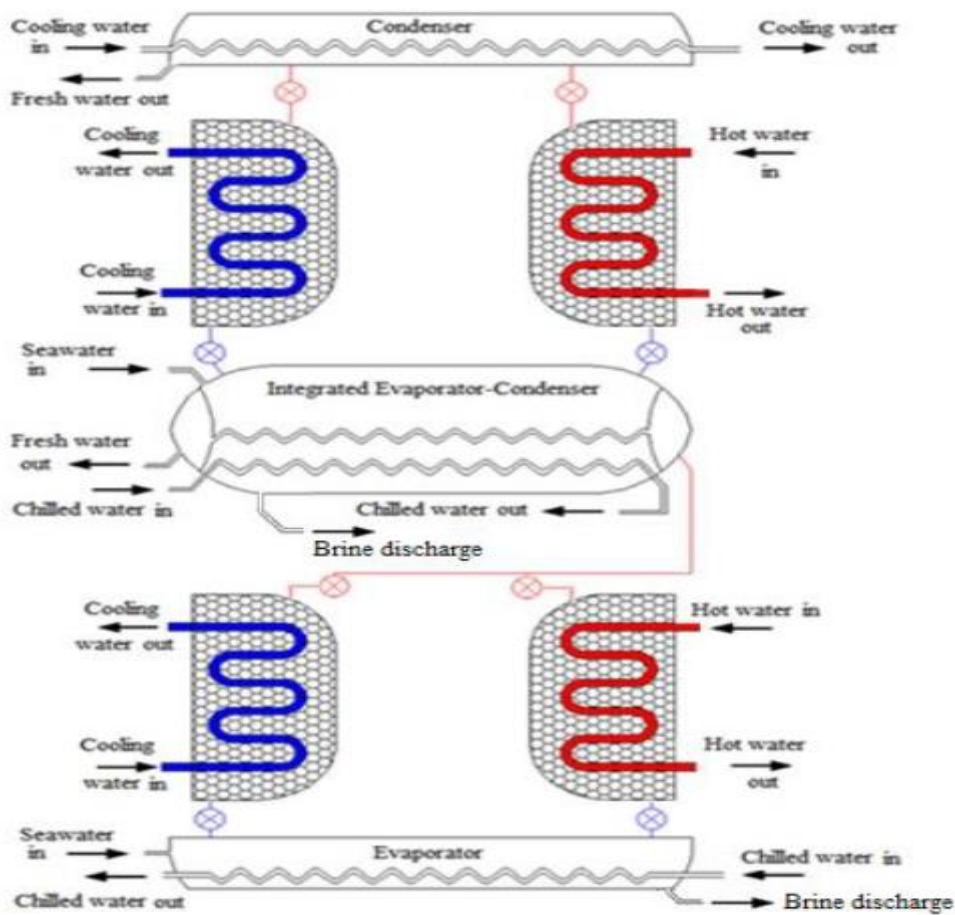


Figure (2.2): The integrated adsorption desalination and cooling cycle, [36]

Ali and Chakraborty, (2016),[37], had offered adsorption-assisted cooling and desalination system using zeolites and Silica gel as adsorbents and water as an adsorbate for effective cooling and desalination effects at the evaporator and condenser. They proposed a cooling cum desalination system that combines the adsorption cooling system (stage-1) with the adsorption desalination system (stage-2). As a result, heat recovery between the condensers and evaporators in both cycles improves overall

efficiency. Specific cooling power (SCP), specific daily water production (SDWP), coefficient of performance (COP), performance ratio (PR), and overall conversion ratio (OCR) are all used to define the simulation effects by using MATLAB. In addition, these results are compared with experimental data. The results show that the proposed system's cooling power and SDWP are (44 % and 45%) higher, respectively, than a traditional two-bed adsorption cooling cum desalination system, the proposed system generates (26%) more water and (45%) more cooling than a similar traditional adsorption cooling and desalination system of the same scale. The best performances in terms of cooling capacity and SDWP was obtained for (85°C) hot water inlet temperature and (1.5 kg/s) of hot and cooling water flow rate.

Numerical studies have investigated by **Thu, et. al, (2016),[38]**, in which they discussed a performance of a waste heat-driven 3-bed 2-evaporator adsorption cycle for cooling and desalination at two temperature stages for both dehumidification and sensible cooling. (A++) Silica gel type has used as adsorbent substance. A detailed numerical model for such an (AD) cycle is carried out, and performance results are offered using various hot water and cooling water inlet temperatures. The hot water temperature ranged between (65 - 85°C) that gained from process waste heat or solar energy, while cold water temperature was (30°C), mass flow of cooling water to adsorber bed is (1.54 kg/s) and mass flow rate of



hot water to the desorber bed is (1.83 kg/s). The results display that the cycle produces high-grade potable water at a rate of (6.5 l/kg<sub>ads</sub> per day).

**Elsayed, et. al,(2017),[39]**, had presented a thermodynamic cycle performance of a two-bed adsorption device using MATLAB Simulink software to determine the suitability of such (MOFs) for adsorption desalination and their performance under various operating conditions. The CPO-27(Ni) was found to be more suitable when low evaporation temperature (5°C) and high regeneration temperature (110°C) are available, resulting in an SDWP of (4.6 m<sup>3</sup>). (ton. day)<sup>-1</sup>. The aluminium fumarate performed well at high evaporator temperatures (20°C), with an SDWP of (6.3 l/kg<sub>ads</sub> per day). Aluminium fumarate also discovered to have a poor regeneration temperature (70°C). MIL-101(Cr) performed extremely well, yielding (11 l/kg<sub>ads</sub> per day), outperforming all other adsorbent.

Numerical studies have carried out by **Youssef, et. al, (2017),[40]**A substance called Aluminum fumarate Metal Organic Framework (MOFs) working material is numerically examined and compared with silica-gel and (AQSOA-Z02) for adsorption desalinating/cooling applications in a 2-bed device. The impact on the specific daily water output and cooling capability of evaporator and desorbed water temperature has been analyzed. The water temperatures for the evaporator are (10-30°C) and for

the desorbent bed were (65-85°C). Results revealed that the water productivity and cooling capability of all products are increasing with the evaporator water temperature. Al-fumarate produce (11.3 l/kg<sub>ads</sub> per day) water and the cooling temperature (0.319 kW/kg<sub>ads</sub>) with hot water temperature of (85°C) and cooling temperature (30°C) for evaporator and bed cooling, while AQSOA-Z02 produces (6.4 l/kg<sub>ads</sub> per day) and Silica gel produces (8.4 l/kg<sub>ads</sub> per day) and (0.21 kW /kg<sub>ads</sub>) of cooling, respectively. As a result, desalination-cooling adsorption of al-Fumarate is feasible particularly at low desorption temperatures.

**Ali, et. al, (2017),[41]**, have introduced a theoretical simulation to investigate the effect of the reverse osmosis brine recycling system employing adsorption desalination on overall system desalinated water recovery (see Figure 2.3). Reverse osmosis desalination is simulated by engineering equation solver (EES), while the adsorption desalination system has been simulated by MATLAB and using Silica gel as an adsorbent. The adsorption desalination system receives the brine from the reverse osmosis system. The results show that, when compared to a single stage RO system, the (RO-AD) findings show that system recovery improved by around (25%) that is, the maximum achieved water productivity (7.8 l/kg<sub>ads</sub> per day), specific cooling power (100 W/kg<sub>ads</sub>) and COP of (0.46).

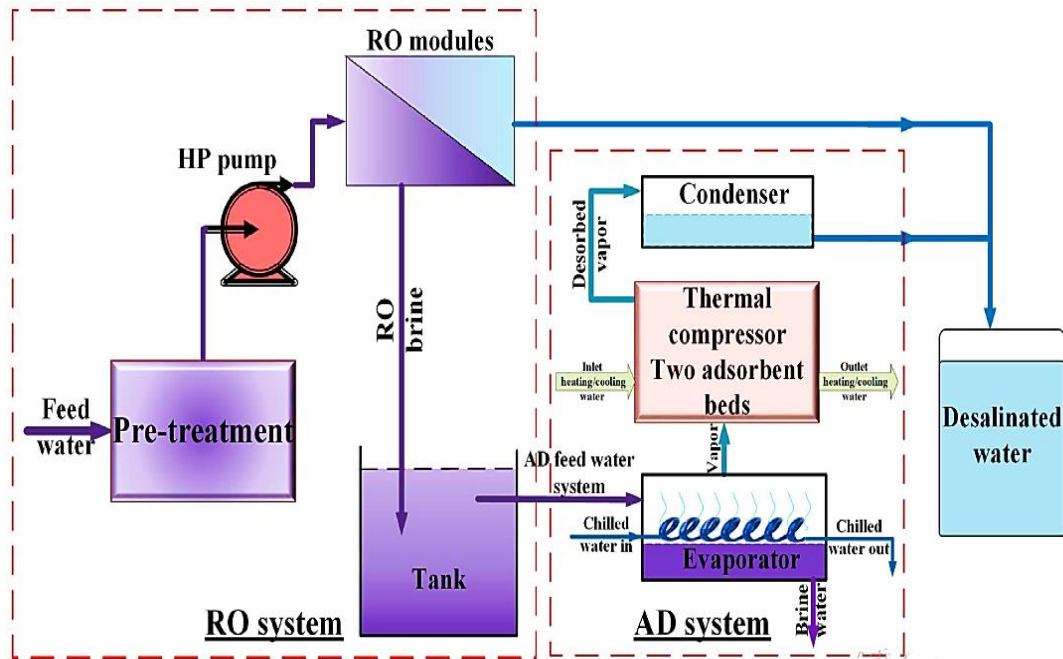


Figure (2.3): Schematic of the investigated RO-AD [45]

**Rezk, et. al, (2019),[42]**, introduced a numerical study to optimize the efficiency of a solar-driven adsorption desalination cooling (SADC) system by determining the best operating conditions using a new optimization algorithm, for deciding the best operating parameters of the (SADC) process, a stable, simple, and fast optimization algorithm known as radial movement optimizer is used . The parameters that were relied upon in the study are cycle time (250-1200s), hot water inlet temperature (55-95°C), and cold-water inlet temperature (20-40°C) and flow rate (0.002-0.4 kg/s). The performance of the system is evaluated by calculating the system outputs, which are the specified daily water production (SDWP), specific cooling power (SCP) and coefficient of performance (COP). The use of optimum working conditions results in a (70%) improvement in SDWP and SCP with no changes to the system

design or materials used. The proposed (SADC) system's potential outputs include (6.9 l/kg<sub>ads</sub> per day) desalinated water, cooling capacity of (191 W/kg), and COP of (0.961).

**Amirfakhraei, et. al, (2020),[43]**, explained a modern two-bed ADS operating cycle of heat / mass recovery between the beds, condenser, and evaporator using Silica gel as adsorbent. In the recovery, cold water used to remove heat from the beds and condenser and transfer it to the evaporator, and two beds were joined together using control valves to maintain pressure equilibrium. At a hot water temperature of (95°C) and a cold-water temperature of (30°C), the specific daily water production (SDWP) for these 2-bed ADS is (9.58 l/kg<sub>ads</sub> per day). As a result, the advanced 2-bed ADS has a (66 %) higher SDWP than the traditional 2-beds system.

**Askalany, et. al, (2020),[44]**, provided a novel hybridization of an adsorption desalination cycle and two ejectors. Potable water productivity can be increased by many folds. For this integration, a working pair of Silica gel and water is used. Two sorption beds, two evaporators, two condensers, and two ejectors are used in the planned hybrid design, called (AD2EJ). The hybrid cycle's efficiency had measured in terms of specific daily water production (SDWP) and Coefficient of Performance (COP). The optimum half-cycle time for the

(AD2EJ) method is about (400 s), with an SDWP of (23.0 l/kg<sub>ads</sub> per day) at a COP of (1.64) and a regeneration temperature of (85°C), according to the empirical data. This volume of potable water is three times higher than that of a normal adsorption desalination device (ADS). At a COP of (2.22) at regeneration of (95°C) and (400s) half cycle time, the SDWP of the device (AD2EJ-HR) is (79.4 l/kg<sub>ads</sub> per day).

**Elbassoussi, et. al, (2020),[45]**, suggested a novel hybrid AD based on Silica gel -(water-heated) humidification-dehumidification desalination unit (HDH) device that concurrently generates potable water and cooling power. The system is operated primarily by a low-grade energy supply (natural gas) (65– 80°C), with photovoltaic (PV) panels used to power auxiliary components including pumps and blowers. To investigate the influence of various parameters on device efficiency and product cost, a comprehensive thermoeconomic model is developed and used MATLAB software to solve it. The results show that the potable water (522 l/day) and the cooling capacity is (2.53 kW).

**Naeimi, et.al, (2020),[19]**, suggested a conceptual theoretical framework based on innovative advanced adsorption desalination and cooling system configured of double-cycle multi-bed dual-evaporator with internal heat recovery and using Silica gel as adsorbent material. The hot

water bed (80°C), cold water bed (30°C), condenser water temperature (25-35°C), low pressure evaporator temperature (10-30°C) and high pressure evaporator temperature (20-30°C). The reliability of the device is calculated in terms of specific daily water production (SDWP), low and high-pressure cooling capacities (SCPLP and SCPHP), and overall conversion ratio (OCR). It has shown that not only does the proposed configuration's SDWP improve by (20%) as compared to a single-cycle multi-bed dual evaporator system, but it can also provide significant amounts of two different types of cooling water. The planned design, which involves (9600 l) of SDWP and high and low-grade cooling capacities of (0.08 kW/kg<sub>ads</sub>), may be a good alternative to standard adsorption desalination setups.

**Ghenai, et. al, (2021),[46]**, presented a performance analysis, parametric study based optimization of hybrid Multi-Effect Distillation Adsorption Desalination (MEDAD) system powered with solar. Four input factors had chosen: heat transfer fluid temperature (80°C) and Reynolds number (7000-214000), as well as seawater temperature and total dissolved solids TDS (20000-50000). The results show that adding the adsorption desalination step increased the rate of potable water production by (2.68 times), resulting in a (57.78 %) lower specific energy usage. The potable water output rate and efficiency ratio improved by (14.73 % and 12.86 %),

respectively, for heat recovery from residual brine, while the real energy consumption declined by (11.34 %).

### **2.3.2 Experimental Studies**

**Thu, et. al,(2011),[47]**, studied experimentally the efficiency of a silica gel–water advanced adsorption desalination (AD) cycle with internal heat recovery between the condenser and evaporator. A mathematical model of the (AD) cycle was created, and performance data were compared to experimental results. At 70°C hot water inlet temperature, the advanced (AD) cycle will achieve a specific daily water production (SDWP) of (9.24 l/kg<sub>ads</sub> per day), whereas the corresponding performance ratio (PR) is comparatively high at (0.77). The cycle observed to be operational at (50°C) hot water temperature with (SDWP) of (4.3 l/kg<sub>ads</sub> per day). The advanced cycle's (SDWP) is almost double that of the traditional (AD) cycle.

**Ng, et. al,(2012),[6]**, explained the efficiency of a waste heat-driven adsorption cycle. The mechanism provides cooling energy and high-quality potable water at the same time when adsorption/desorption phenomena are used. The isotherm properties of the adsorbent/adsorbate pair (Silica gel / water), as well as energy /mass balances for each part of the cycle, are used to create a mathematical model. The cycle's efficiency is evaluated using four main output parameters: (i) specific cooling power (SCP), (ii) specific

daily water production (SDWP), (iii) coefficient of performance (COP), and (iv) overall conversion ratio (OCR). Experimental data is used to verify the adsorption cycle's numerical performance. The results of a parametric study of various hot and chilled water temperatures are presented. The cycle produces (3600 l) of potable water and (80.8 kW) of cooling at a produced chilled water temperature of (10° C) at an inlet temperature of (85° C).

**Youssef, et. al, (2017),[48]**, suggested an experimental and numerical analysis to investigate the use of a one bed adsorption system for potable water processing and cooling purposes use CPO-27(Ni) as adsorbent. Effects on cycle water output and cooling were studied for the effects of operating parameters such as changing time, half a cycle time and the intake temperature on evaporators and condensers. A mathematical model of simulation is also developed, validated and used to predict cycle performance under various operating conditions. With a (40°C) evaporator temperature, a (5°C) condenser temperature, and a (95°C) desorption temperature, a water yield of (22.8 l/kg<sub>ads</sub>/day) was achieved. With a condensing temperature of (30°C) and a desorption temperature of (120°C), similar water output can be achieved. Cycle cooling produced found to be (2.28 kW/kg<sub>ads</sub>) for space cooling applications ( $T_{\text{evap}} < 20 \text{ }^{\circ}\text{C}$ ).



**Dakkama, et. al, (2017),[49]**, presented experimentally the using of a nickel-based polymer with (MOFs) / sea water as a working pair, the invention of MOFs - based adsorption method for producing ice, freezing, and drinking water. The impact of the number of cycles, switching time, adsorption/desorption time, and salinity of saline water on the adsorption system's efficiency in terms of coefficient of performance, specific daily production of ice, slurry mixture, and potable water was studied. The maximum ice productivity (8.9 ton/day/ton<sub>ads</sub>) at generation, chilled antifreeze, and ambient temperature of (95 C, -1C, and 24 C), respectively, were observed with the number of cycles, switching time, adsorption/desorption time, and salinity as up to (3 cycles, 3 min, 15 min), and (35,000 ppm).

**Thu, et. al,(2017),[50]**, introduced an investigation on a multi-bed adsorption desalination cycle with internal heat recovery between the condenser and the evaporator. For a 4-bed adsorption cycle with the master-slave configuration and the aforementioned internal heat recovery scheme, a numerical model created. The adsorbent and adsorbate pair is made up of mesoporous Silica gel and water vapour generated by seawater evaporation. Heat source temperatures ranging from (50 to 70°C). The numerical model is tested, and a parametric analysis is carried out for the cycle's output under different operating conditions, such as hot and cooling water inlet temperatures, and cycle times. For the heat source temperature

of (70 °C), the specific daily water output (SDWP) of the current cycle found to be about (10 l/kgads per day) of Silica gel.

Zhan,et.al,(2020),[51],presented a developed pilot-scale adsorption desalination system with water output of (2400 l/day). Under steady-state conditions, the system's seawater evaporation and water efficiency were studied experimentally (see Figure 2.4). When the temperature of the hot water entering the desorber bed was (55 °C) and the flow rate was (28 m<sup>3</sup>/h), the rate of water output was (>100 kg/h). The water output rate improved as the hot-water temperature and flow rate increased, reaching (191.3 kg/h) while the hot-water temperature was (80 °C).

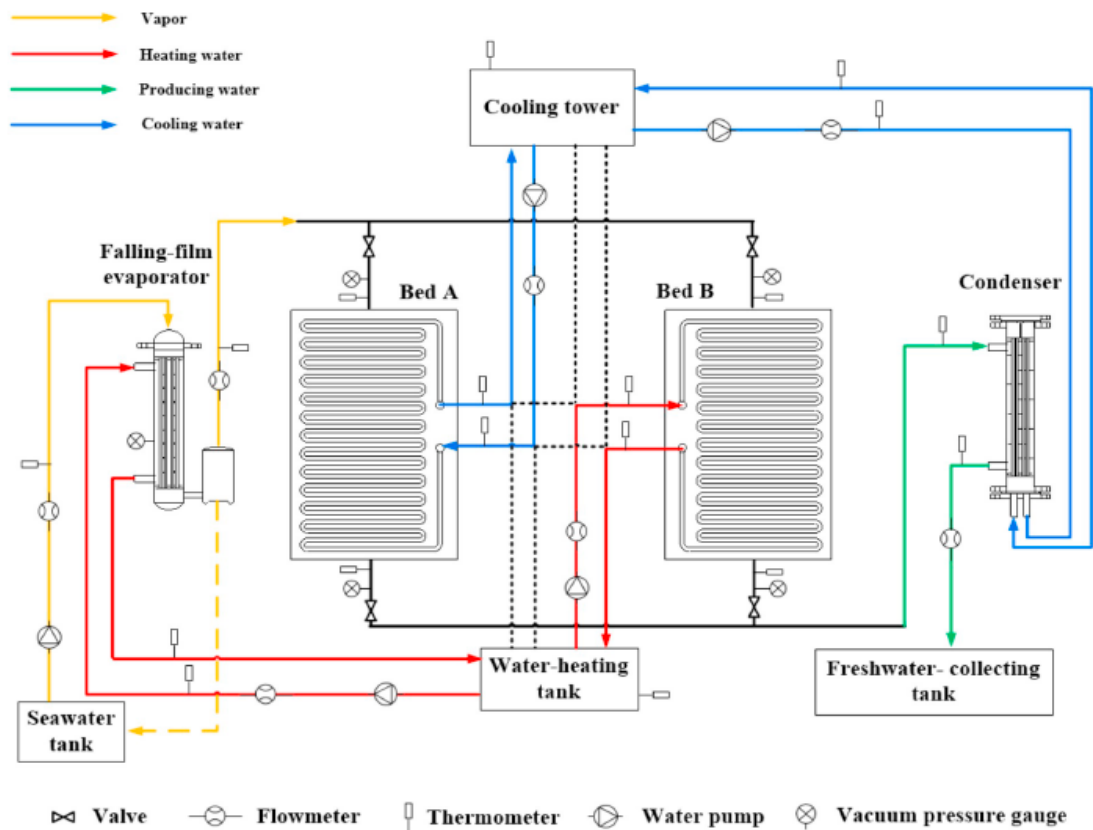


Figure (2.4): Schematic diagram and instruments location of the AD system, [47]

**Bai, et. al, (2020),[52]**, Carried out a study to find the correlation between saltwater salinity and the cooling / desalination performance, and to build up a comprehensive numerical model that can exactly expect the cooling / desalination performance of an adsorption desalination cycle. The results showed that, the specific cooling capacity and specific daily water output values for seawater are 490 W/kg and 18 l/ kgads per day, respectively, under operating conditions with the desorption temperature at 85 °C and the evaporation temperature at 14°C. both experiment and simulation results demonstrate that the adsorption cooling cum desalination system adopting the composite adsorbent has a great potential to sustainably provide fresh water and cooling effect.

**Elsayed, et. al, (2020),[53]**, provided an experimental research of a (MOF) element, aluminium fumarate, and how it can improve the efficiency of adsorption desalination systems for the first time. A parametric analysis performed to investigate the impact of various parameters on the efficiency of the adsorption device, including chilled water, adsorption-cooling water, and condensation cooling water, desorption heating water temperatures, and half cycle time. The efficiency of aluminium fumarate compared with traditional adsorbents like Silica gel. According to the findings, aluminium fumarate needs desorption temperature as low as 70 °C or even lower. At a chiller water temperature greater than 10 °C, aluminium fumarate beat standard Silica gel while

operating at an adsorption temperature of 30 °C, where SDWP (1.4-12.5 m<sup>3</sup>/ton per day) and SCP (20 – 410 W/kg<sub>ads</sub>).

**Son, et. al, (2020),[54]**, studied the hybrid cycle - desalination method of multi-effect distillation (MED) and adsorption desalination (AD) to optimize the utilization of energy input in desalination. Two separate thermal desalination systems were combined, and the hybrid system's efficiency was improved due to the synergetic effect of using steam. This study established a synergetic thermodynamic model, and experimental findings from a pilot unit with a nominal output volume of (10000 l/day) installed at KAUST, KSA, backed up the proposed model. In different quality of the heat source (40–60°C), both the water production and the uniform output ratio (UPR) to the (MED) have increased (2–5 times). Furthermore, the (MED-AD) hybrid method will scavenge energy for desalination from ambient temperatures below (30°C). To analyses, the thermodynamic synergy of the hybridization, the used energy of both thermal and flash evaporation under all operating environments, as well as individual results, has been inventoried. The energy input in the first effect is transferred forward to the subsequent results of single (MED) activities, and part of it is used for thermal evaporation.

## **2.4 Summery of Literature Review**

The following table presents a summary of previous studies in the field of adsorption desalination systems (Table 2.1). The table shows the titles of the study, the name of the researcher, the year of publication, the type of study, theoretical or experimental, the number of beds used, the type of heat source used, its temperature, the type of adsorption material used in the system, and finally the outputs of the system.

Table (2.1): Summary of the researches

Reference No.	Author	Year	Numerical/ Experimental	Materials	Temperature range °C	System arrangement	Heat source	Main Findings
[48]	G. Youssef and et al.	2017	Experimental and numerical	CPO-27Ni MOF	95	1 bed	low-grade	water production 22.8 l/kg.ads/day and Cooling capacity 65 Rton/tonne.ads
[36]	G. Youssef and et al	2016	Numerical	AQSOA-Z02	85	4 beds	waste heat	Daily water production ranges from 6.64 to 15.4 l/kgads/day and cooling capacity reaches up 1.63 kW/kg
[40]	Peter Youssef and et al.	2017	Numerical	Aluminium Fumarate Silica gel AQSOA-Z02.	65 -85	2 beds	-----	Al-Fumarate can produce 11.3M'/tonne.ads/day of water and 90.9rton/tonne.ads of cooling while aqsoa-z02 and silica-gel produce 6.4 and 8.4M' of water/day and cooling of 50.5 and 62.4rton per tonne.
[50]	Kyaw Thu and et al.	2017	Experimental	Silica gel	50 – 70	4 beds	-----	Water production 10 m3/t-day
[47]	Kyaw Thu and et al.	2011	Experimental	Silica gel	50 – 70	4 bed	Waste heat	Water production 5.5 to 9.34 m3/tonne per day
[6]	Kim Choon Ng and et al.	2012	Experimental and Numerical	Silica gel	85	4 bed	Waste heat	Water production and cooling capacity 8 m3 and 51.6 Rton per tonne of Silica gel.
[34]	Kyaw Thu and et al.	2013	Numerical	Silica gel	50 - 85	2 beds	Waste heat recovery	Water production yield improves varying: From 8.1 m3 to 26 m3
[41]	Ehab s. Ali and et al.	2017	Numerical	Silica gel	55 -95	2 beds	low- heat source	Water production 7.6 m3/t-day
[42]	Hegazy Rezkand et al.	2019	Numerical	Silica gel	75- 95	2 bed	Solar energy	Water production 6.9m3/day/ton and 191 W/kg cooling capacity
[38]	Kyaw Thu and et al.	2016	Numerical	Silica gel	55 – 85	3 bed	low-temperature heat source	Water production 6.1 m3/day/ton

[39]	Eman Elsayed and et al.	2017	Numerical	CPO-27(Ni) aluminium Fumarate MIL-101(Cr) MOF	90-150	2 bed	-----	4.31 m <sup>3</sup> · (ton·day) <sup>-1</sup> 6 m <sup>3</sup> · (ton·day) <sup>-1</sup> 11 m <sup>3</sup> · (ton·day) <sup>-1</sup>
[35]	S. Mitra and et al.	2014	Numerical	Silica gel	85	4 bed	Solar energy	Water production 2.4 m <sup>3</sup> per ton and cooling capacity Rton\ton
[49]	Hassan J. Dakkama and et al.	2017	Experimental	CPO-27 (Ni) MOF	20 - 95	1 bed	Low-grade heat source.	water production 1.8 ton/day/ton
[37]	Ali and Chakraborty	2016	Numerical	Silica gel-AQSOA-Z02	85	2-bed 2-stages	Low-grade heat source.	47.82 Rton/ton <sub>ads</sub> SCP 10.14 m <sup>3</sup> /ton <sub>ads</sub> SDWP
[43]	Amirfakhraei, et. al	2020	Numerical	Silica gel	30-95	2-bed	Low-grade heat source.	9.58 l/kg <sub>ads</sub> per day SDWP
[44]	Askalany, et. al	2020	Numerical	Silica gel	85-95	2-bed	Low-grade heat source.	79.4 l/kg <sub>ads</sub> per day SDWP
[45]	Elbassoussi, et. al,	2020	Numerical	Silica gel	65-80	2-bed	natural gas	potable water (522 l/day) , cooling capacity is (2.53 kW
[19]	Naeimi, et.al	2020	Numerical	Silica gel	30-80	2-bed 2-evaporator	Low-grade heat source.	(9600 l) of SDWP (0.08 kW/kg <sub>ads</sub> )
[51]	Zhan,et.al	2020	Experimental	Silica gel	80	2-bed	Low-grade heat source.	(191.3 kg/h) SDWP
[52]	Bai, et. al	2020	Experimental	multi-walled carbon-zeolite 13X/CaCl <sub>2</sub> .	85	2-bed	Low-grade heat source.	18 l/kg <sub>ads</sub> /day 490 W/kg <sub>ads</sub>
[53]	Elsayed, et. al	2020	Experimental	aluminium fumarate	70	2-bed	Low-grade heat source.	SDWP(1.4-12.5 m <sup>3</sup> /ton per day) and SCP (20 – 410 W/kg <sub>ads</sub> ).

[54]	Son, et. al	2020	Experimental	Silica gel	40-60	4-bed	Low-grade heat source.	(10000 l/day) SDWP
<b>Present study</b>	Esraa A. et al.	2022	Experimental and Numerical	Silica gel	70-90	1 bed 2 bed	Low-grade heat sources.	



## **2.5 Scope of the Present Work**

Previous experimental and numerical studies have provided sufficient information about the possibility of establishing adsorption systems to desalinate water and generate cooling by exploiting low-grade heat sources. However, the works deal with this problem are still limited.

However, it is a good starting point for the study of adsorption systems and the modernizations that have occurred on them.

The present study will focus on:

- Establishment of a one-bed adsorption system that exploits silica gel as an adsorbent and low energy sources as a driving force for water desalination and cooling energy production.
- Create a simulation model using Matlab Simulink to simulate a standard two-bed adsorption system.
- Examination of the effect of hot water temperature of the adsorption bed, condenser water temperature, evaporator water temperature and half-cycle time on the system products experimentally numerically.

# CHAPTER THREE

## Mathematical Modelling and Numerical Analysis

### 3.1 Introduction

Modeling is one of the most important and powerful methods for developing and analyzing any thermal system. Basic 2-bed adsorption desalination and cooling cycle utilizing Silica gel is simulated (utilizing MATLAB Simulink) under steady state condition in this chapter. The system comprises mainly adsorption bed, evaporator and condenser in addition to control valves as shown in Figure (3.1).

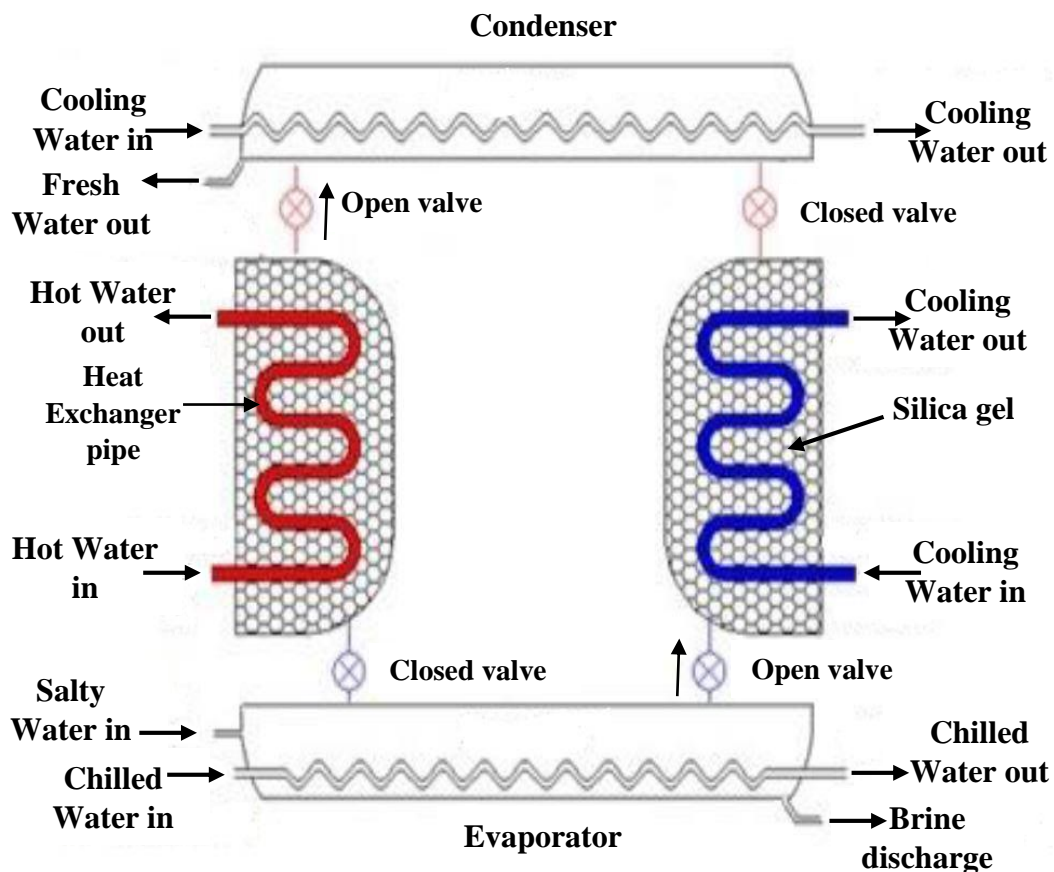


Figure (3.1): Adsorption desalination and cooling system.

### 3.2 System modeling

To define the adsorption desalination and cooling system, energy balance for the adsorber bed, evaporator, and condenser are carried out using both energy and mass conservation equations[1].

The two famous concepts "isotherms" and "kinetics" are used to describe the efficiency of adsorbent materials. Adsorption isotherms show how much adsorbate (working fluid) can be adsorbed per dry kilogram of adsorbent, whereas kinetics shows how fast the adsorbent can adsorb or desorb the adsorbate at a given partial pressure. Because silica gel is a member of the mesoporous silicate family, it is the only sorbent material that was used for adsorption desalination and cooling applications at the beginning of the discovery of adsorption technology.

With the progress of research in the field of adsorption techniques, new adsorption materials with very high efficiency were used or manufactured. An example of these modern materials are AQSOA-Z02, AL-Fumarate, CPO-27Ni and MIL-101Cr.

At pressure ratios less than 0.1, AQSOA-Z02 belongs to the Zeolites group and has a different isotherm shape than silica-gel, with adsorption uptake rising very quickly. AL-Fumarate, CPO-27Ni, and MIL-101Cr are all metal organic framework adsorbent materials having higher surface area and uptake than silica-gel, as well as differing isotherm shapes,

allowing them to act differently. Furthermore, all of these materials are commercially accessible, with the exception of MIL-101Cr, which has a high absorption value of  $1.4 \text{ kg}_{\text{water}}/\text{kg}_{\text{ads}}$ . A DVS (Dynamic Vapour Sorption) analyzer from Surface Measurement System Ltd is utilised to test the adsorption characteristics of adsorbent materials, [26].

Equilibrium uptake,  $C$  ( $\text{kg}_w/\text{kg}_{\text{ads}}$ ), is the mass of vapour adsorbed per kg of adsorbent material in this state, and it is dependent on equilibrium pressure, adsorbent temperature, and characteristics of the adsorbent/adsorbate working pair. Because achieving equilibrium takes a long time, the adsorption cycle time must be estimated, which is referred to as adsorption kinetics, "Langmuir, Freundlich, Modified Freundlich, Dubinin-Astakhov, Toth and Sips" [1]. One of the mostly used adsorption equilibrium models is the Dubinin–Astakhov (D–A) equation. This equation was introduced in (1971). The (D–A) equation has been developed mainly to describe adsorption of gases in microporous adsorbents particularly appropriate for activated carbon with a large pores heterogeneousness. This model is known to be better than other models due to its thermodynamic character, [55]. According to the (D–A) model, the amount of uptake ( $C$ ) is expressed as follows: -

$$C^* = C_o \exp \left[ - \left( \frac{RT}{E} \ln \left( \frac{p}{p_o} \right)^n \right) \right] \quad (3.1)$$

where ( $C^*$ ) represents the equilibrium uptake ( $\text{kg}/\text{kg}_{\text{ ads}}$ ), ( $C_o$ ) represents the highest adsorbed volume,  $R$  represents the universal gas constant ( $\text{kJ}\cdot\text{mol}^{-1}\cdot\text{K}^{-1}$ ), ( $T$ ) represents the adsorbent temperature ( $\text{K}$ ), ( $E$ ) represents the characteristic energy ( $\text{kJ}\cdot\text{mol}^{-1}$ ),  $n$  represents the (D-A) constant, and  $P$  and  $P_o$  represent the saturation pressures at refrigerant and adsorbent temperatures, respectively.

As discussed earlier, equilibrium uptake alone cannot predict the capability complex adsorption of the cycle and hence adsorption kinetics models are required. Several models exist to predict adsorption kinetics like Fickian Diffusion (FD), Linear Driving Force (LDF) and Quadratic Driving Force (QDF). The (LDF) kinetics model improved by Glueckauf, as seen in equations (3.2) and (3.3), is the most basic, commonly used, [1,26,51]

$$\frac{dc}{dt} = k(C^* - C) \quad (3.2)$$

$$k = k_o e^{\left(\frac{-E_a}{RT}\right)} \quad (3.3)$$

where " $C$ " represents the instantaneous uptake at a given time " $t$ ," " $k_o$ " represents a pre-exponential constant, and " $E_a$ " represents the activation energy constant.

### 3.2.1 Adsorber /Desorber Bed Energy Balance Equation [1]

Water vapour enters the bed throughout the adsorption process or exits throughout desorption to be adsorbed and desorbed by the adsorber grains, as seen in Figure (3.2). At the same time, during the adsorption or desorption procedures, a coil circulates cooling or heating fluid through the adsorber bed. Since adsorbent material grains have varying temperatures based on the location of the cooling / heating coil and the proximity to water vapour, it is thought that the adsorber bed has the same temperature at all points to optimise modelling.

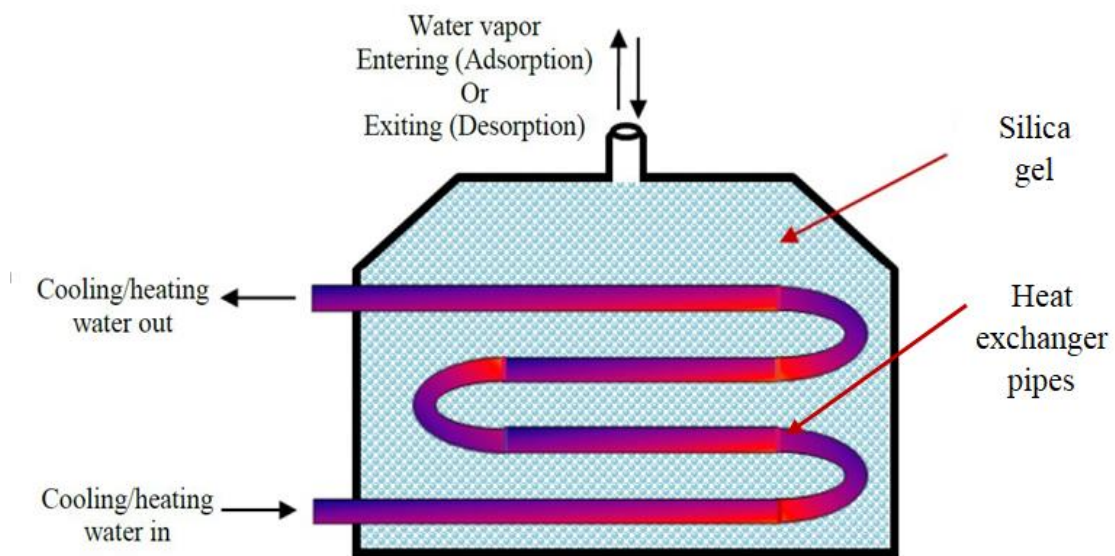


Figure (3.2): adsorber bed schematic diagram [1]

The energy balance applied according to the inlet and exit fluid sources.

$$\begin{aligned}
 &\text{heat required to be either extracted / added to the adsorbent granules} + \text{heat required to be either extracted / added to heat exchanger metal parts} + \text{heat required to be either extracted/added to the adsorbed water vapour inside adsorbent pores during adsorption/desorption processes} \\
 = &\text{rate of heat generated or extracted during adsorption / desorption processes} + \text{the heat transferred to or from the secondary fluid in adsorption or desorption processes}
 \end{aligned}$$

The expressions of the equation (3.4) are: -

$$\begin{aligned}
 & \left[ M_a C_{p,a} + M_{HX} C_{p,HX} + M_{abe} C_{p,abc} \right] \frac{dT_{ads/des}}{dt} \\
 & = z Q_{st} M_a \frac{dc_{ads/des}}{dt} \\
 & + m'_{cw/hw} C_p (T_{cw/hw,in} - T_{cw/hw,out})
 \end{aligned}
 \tag{3.4}$$

where  $z$  is a flag that is always 1 except during the heat recovery process, when it is 0, [1,26,51].

### 3.2.2 Evaporator Energy Balance Equation[1]

As seen in Figure (3.3), several fluid branches enter and leave the evaporator. The fluids are saline and chilled water which act as the heat load, while the fluids discharging are the vaporize water vapour, the condensed saline and chilled water. The energy balance is applied as in the equation (3.5) according to the inlet and exit fluid sources.

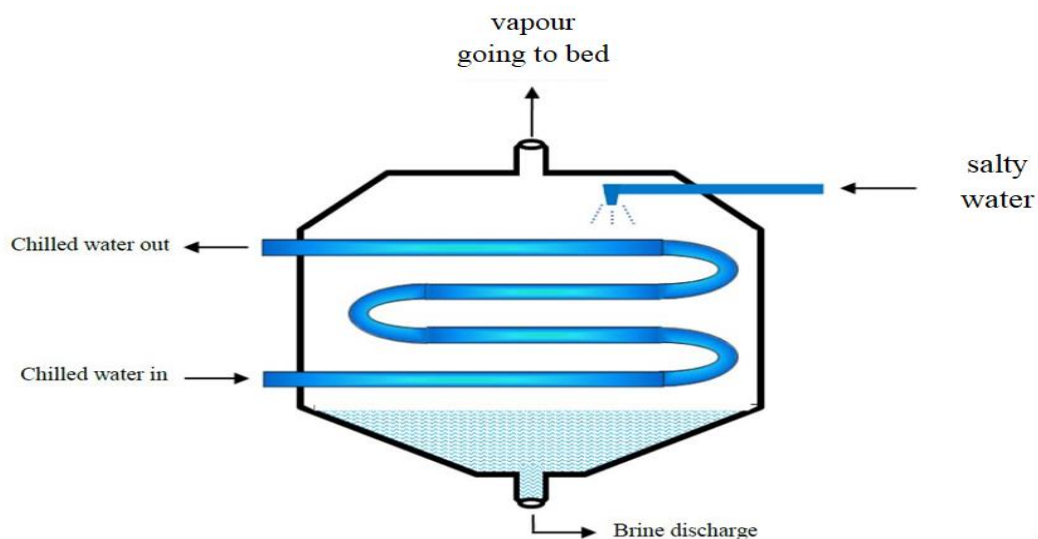


Figure (3.3): schematic diagram of the evaporator [1].

The energy balance applied according to the inlet and exit fluid sources.

$$\begin{array}{l}
 \text{rate of heat extracted} \\
 \text{from salty water in} \\
 \text{evaporator}
 \end{array}
 +
 \begin{array}{l}
 \text{rate of heat removed} \\
 \text{from evaporator fins and tubes}
 \end{array}
 =
 \begin{array}{l}
 \text{rate of heat added} \\
 \text{by the fed salty water}
 \end{array}$$
  

$$\begin{array}{l}
 \text{rate of heat extracted} \\
 \text{from salty water due to} \\
 \text{the evaporation effect}
 \end{array}
 +
 \begin{array}{l}
 \text{rate of heat removed} \\
 \text{by discharged brine} \\
 \text{out of the evaporator}
 \end{array}
 +
 \begin{array}{l}
 \text{rate of heat extracted from} \\
 \text{chilled water passing} \\
 \text{through evaporator coil}
 \end{array}$$

The expressions of the equation (3.5) are: -

$$\begin{aligned}
 & \left[ M_{s, \text{evap}} C_{p,s}(T_{\text{evap}}, X_{s, \text{evap}}) + M_{HX, \text{Evap}} C_{p, HX} \right] \frac{dT_{\text{evap}}}{dt} \\
 & = \theta \cdot h_f(T_{\text{evap}}, X_{s, \text{evap}}) m'_{s, \text{in}} \\
 & - z \cdot h_{fg}(T_{\text{evap}}) \frac{dc_{\text{ads}}}{dt} M_a \\
 & - \gamma h_f(T_{\text{evap}}, X_{s, \text{evap}}) m'_{\text{brine}} \\
 & + m'_{\text{chilled}} C_p(T_{\text{evap}}) (T_{\text{chilled, in}} - T_{\text{chilled, out}})
 \end{aligned} \tag{3.5}$$

where  $\theta$  a flag equals 1 in the evaporator during saline water feed and zero in every other case. The parameter  $\gamma$  a flag equals 1 in the evaporator with saline discharge and in all other situations zero, [1,26,51].

### 3.2.3 Condenser Energy Balance Equation [1,26,51]

As seen in Figure (3.4), during desorption, the condenser takes the water vapour which is discharged from the desorber bed. The latter loses the latent heat and then cools down by cooling effect. For these three types of fluids, the equation of the energy balance is taken as in the equation (3.6).



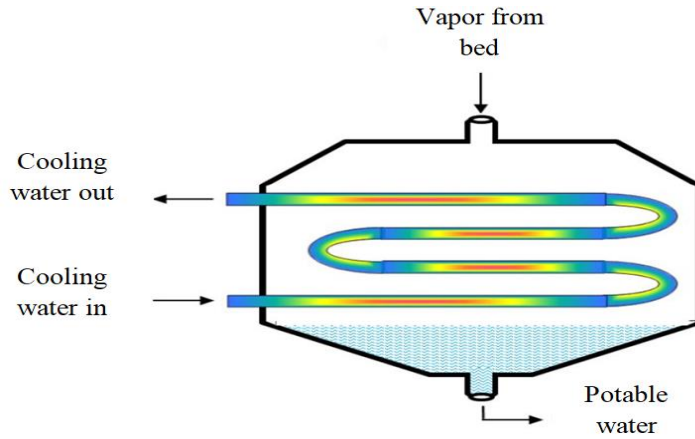


Figure (3.4): condenser schematic diagram [1].

The energy balance applied according to the inlet and exit fluid sources.

$$\begin{aligned}
 &\text{rate of heat extracted from condenser fresh water in the condenser} + \text{heat extracted from condenser fins and tubes} = \text{rate of heat transfers due to condensation of water vapour coming from desorbing bed} \\
 &\text{rate of heat removed by fresh water leaving the condenser} + \text{rate of heat transfers condenser cooling water}
 \end{aligned}$$

The expressions of the equation (3.6) are: -

$$\begin{aligned}
 &\left[ M_{cond} C_p (T_{cond}) + M_{HX,cond} C_{p,HX} \right] \frac{dT_{cond}}{dt} \\
 &= z \cdot h_{fg} (T_{cond}) M_a \cdot \frac{dc_{des}}{dt} - h_f (T_{cond}) \frac{dM_d}{dt} \\
 &+ m'_{cond} C_p (T_{cond}) (T_{cond,in} - T_{cond,out})
 \end{aligned} \tag{3.6}$$

### 3.2.4 Mass Balance Equations

As seen in Figure (3.3), the saline water is delivered to the evaporator and then the evaporated water vapour is discharged into the adsorber bed. The residual dissolved saline water (brine) is also discharged, [1]. To calculate the instantaneous volume of saline water inside the evaporator, a mass balance is used as follows:

$$\boxed{\frac{dM_{s,evap}}{dt} = \theta m'_{s,in} - \gamma m'_{brine} - M_a \frac{dc_{ads}}{dt}} \quad (3.7)$$

The left hand side of the equation (3.7) is the rate of salty water mass changing in the evaporator whereas the right hand side expressions are the rate of salty water feed, saline discharge, and evaporated salty water.

The salt concentration in the evaporator is essential for the application and modeling of both the adsorption desalination and cooling systems because it involves when the brine should be emptied and the salty water should be pumped. The equation (3.8) is then used to calculate the salt equilibrium in the evaporator, where X is the mass fraction of salts in the salty water of unit kg salt / kg salty water [1,26,51].

$$\boxed{M_{s,evap} \frac{dX_{s,evap}}{dt} = \theta X_{s,in} m'_{s,in} - \gamma X_{s,evap} m'_{brine} - X_g \frac{dc_{ads}}{dt} M_a} \quad (3.8)$$

The left-hand side of the equation (3.8) is the change rate in the evaporator saline water concentration, while the right-hand side is the increased concentration of salt due to saline water feed, the reduced concentration of salt owing to the brine evacuating, and the evaporated saline water leaving the evaporator.

### 3.2.5 Cycle Performance Formula

Specific daily water production (SDWP) and specific cooling power (SCP) are used to evaluate the performance of the adsorption desalination and cooling system. The volume of water collected daily in cubic metres per tonne of packed adsorbent is known as specific daily water production. Equation (3.9) is used to measure SDWP. The specific cooling power gained from the system in watts per kilogram of adsorbent is calculated from equation (3.11), [1,26,51].

$$SDWP = \int_0^{t_{cycle}} \frac{Q_{cond}}{h_{fg}M_a} dt \quad (3.9)$$

$$Q_{cond} = \dot{m}_{cond} C_p (T_{cond,out} - T_{cond,in}) \quad (3.10)$$

$$SCP = \int_0^{t_{cycle}} \frac{Q_{evap}}{M_a} dt \quad (3.11)$$

$$Q_{evap} = \dot{m}_{evap} C_p (T_{evap,in} - T_{evap,out}) \quad (3.12)$$

### 3.3 MATLAB SIMULINK Model

Simulink is visual interface software that uses blocks and embedded functions to perform computational simulations. It allows fast model creation as well as versatility in changing the blocks.

Figure (3.6) shows the model's flow diagram. The Double adsorber/desorber beds, evaporator, and condenser are the major heat-exchanging equipment in the system. There are also a variety of auxiliary blocks that route inputs to the main blocks based on the operational process, as well as other blocks that yield main cycle effects. Other subsystem blocks and Matlab functions exist under each main block to solve the energy balance and the heat transfer equations. There are additional blockages that exist to model adsorbent matter output in the case of adsorber /desorbent bed blocks. Furthermore, there are supplementary blocks under the evaporator main block that model mass and salinity equilibrium equations as well as monitor saline water feeding and brine discharges signals. With a variable time step and relative tolerance of  $10^{-3}$ , this Simulink model contains a numerical integration utilizing an ordinary equation solver (ODE45) which is the explicit Runge-Kutta method created by Dormand and Prince.

### **3.4 SIMULINK Model Validation**

The fundamental two-bed adsorption cycle illustrated in Figure (3.1) has been validated using experimental data from a two-bed desorption system. The predicted output temperature profile shows a less than (12%) divergence from the experimental data of the bed, condenser, and

evaporator. Table (3.2) shows operating conditions of the 2- bed validation test utilizing Silica-gel.

Table (3.1): Operating conditions of the 2- bed validation test utilizing Silica-gel.

Parameter	Average deviation
Heating water temperature	120°C
Cooling water temperature	26°C
Condenser cooling water inlet temperature	26°C
Evaporator chilled water inlet temperature	18°C
Half cycle time	300 sec

Figure (3.5), shows a comparison between numerical results and experimentally measured results for the main components of the basic adsorption system namely; adsorber/desorber beds, evaporator and the condenser.

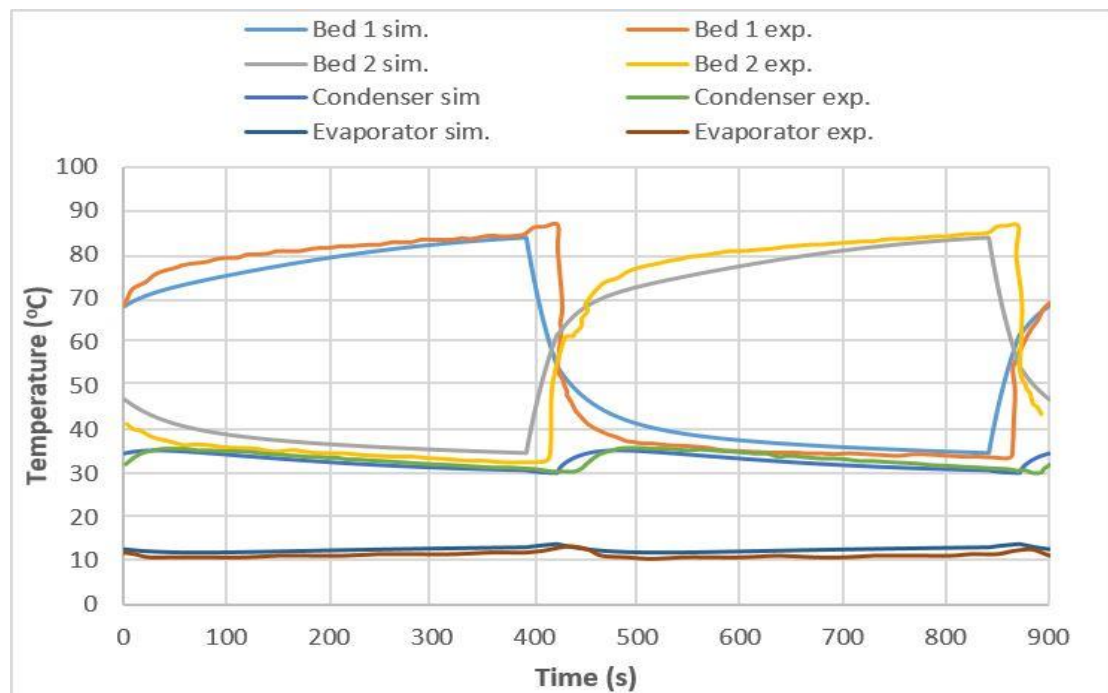


Figure (3.5): Validation of Simulink, temperature profiles of adsorber beds, evaporator and condenser.

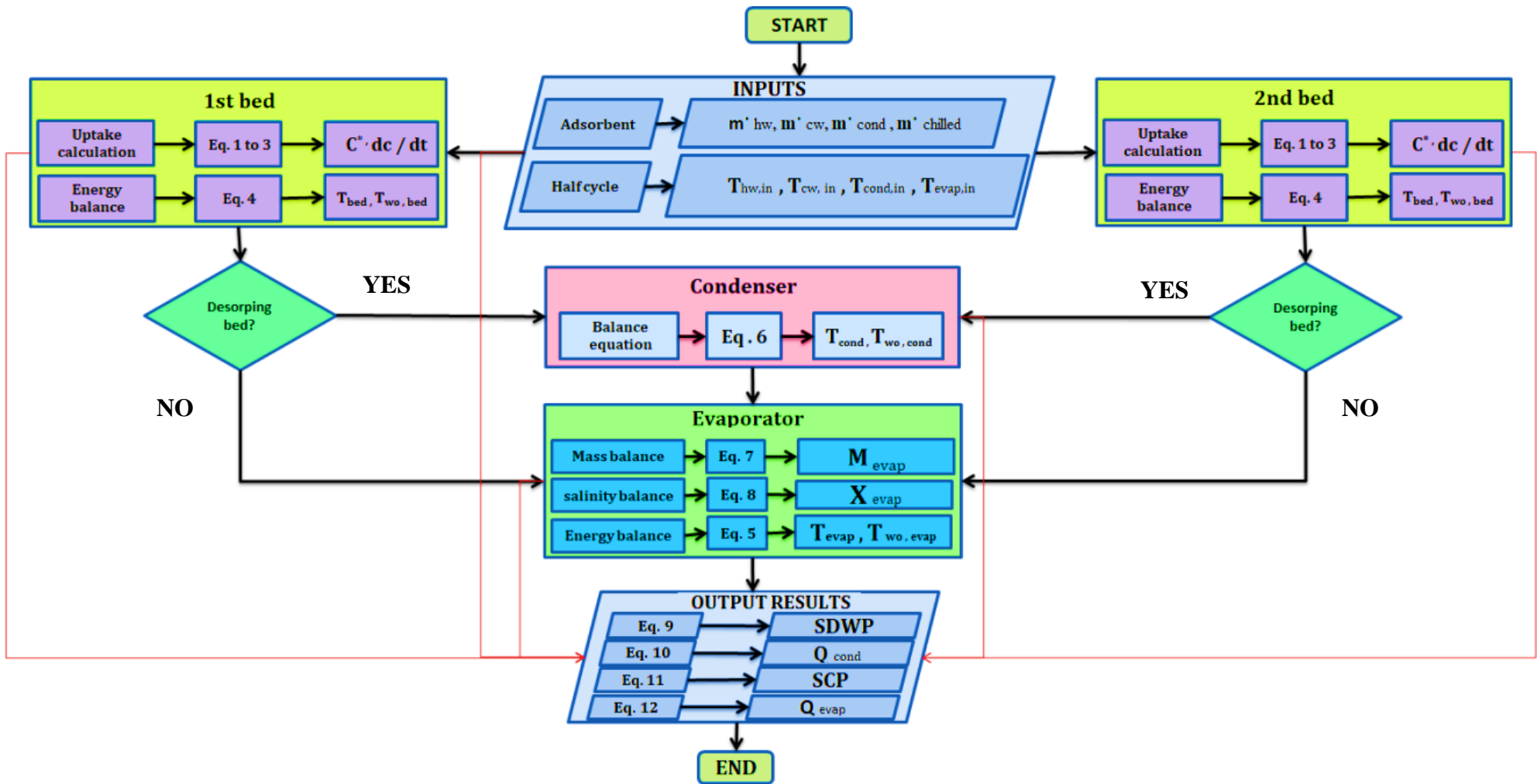


Figure (3.6): Flow chart for the Simulink model

### **3.5 Summary**

In this chapter, the physical properties of adsorbents are reviewed. A mathematical model was performed using Matlab Simulink for a two bed adsorption system that uses a pair of Silica gel and water. The numerical model dealt with all the governing equations for this system, and solved them and analysed the system performance by two products, namely SDWP and SCP. The numerical model was validated against those of published experimental researches.

## **CHAPTER FOUR**

### **Experimental Work**

#### **4.1 Introduction**

This chapter provide a set up and operate the one- bed adsorption desalination and cooling system at various working conditions utilizing Silica gel as adsorbent. The system performance is experimentally investigated by reading and analyzing the main input parameters like heating temperature, cooling temperature, cycle half time, switching time and output parameters like SCP and SDWP.

#### **4.2 System Description**

The system consists of three main parts adsorber bed, evaporator and condenser. The adsorber bed is an iron cuboid made from 6 mm thick plate it contains two heat exchangers, where the adsorbent (Silica gel) is filled between the fins of heat exchangers. The evaporator and condenser are cylindrical shape made from 6 mm thick iron plate. Copper coils are used as heat exchangers in the evaporator and condenser. An electric water boiler, cold water tank, heating-chiller unit in addition to a number of water pumps and valves are used in this study to meet the requirements of adsorption and desorption processes. Dry vacuum pump is used to get the



necessary vacuumed pressure level in the adsorber bed, evaporator and condenser.

To measure the temperature, pressure and flow rate measurement, sensors such as pressure transducers are used at different locations within the system in addition to thermocouples and flow meters. The following section explain in detail every part of the system, showing the adsorber bed, evaporator, condenser, water circuit, measurement equipment, solenoid flow control, and manual valves, as well as data collection devices as shown in Figure (4.1). The test rig located in the laboratory building of Mechanical Engineering Department in Kerbalaa University as shown in Figure (4.2).

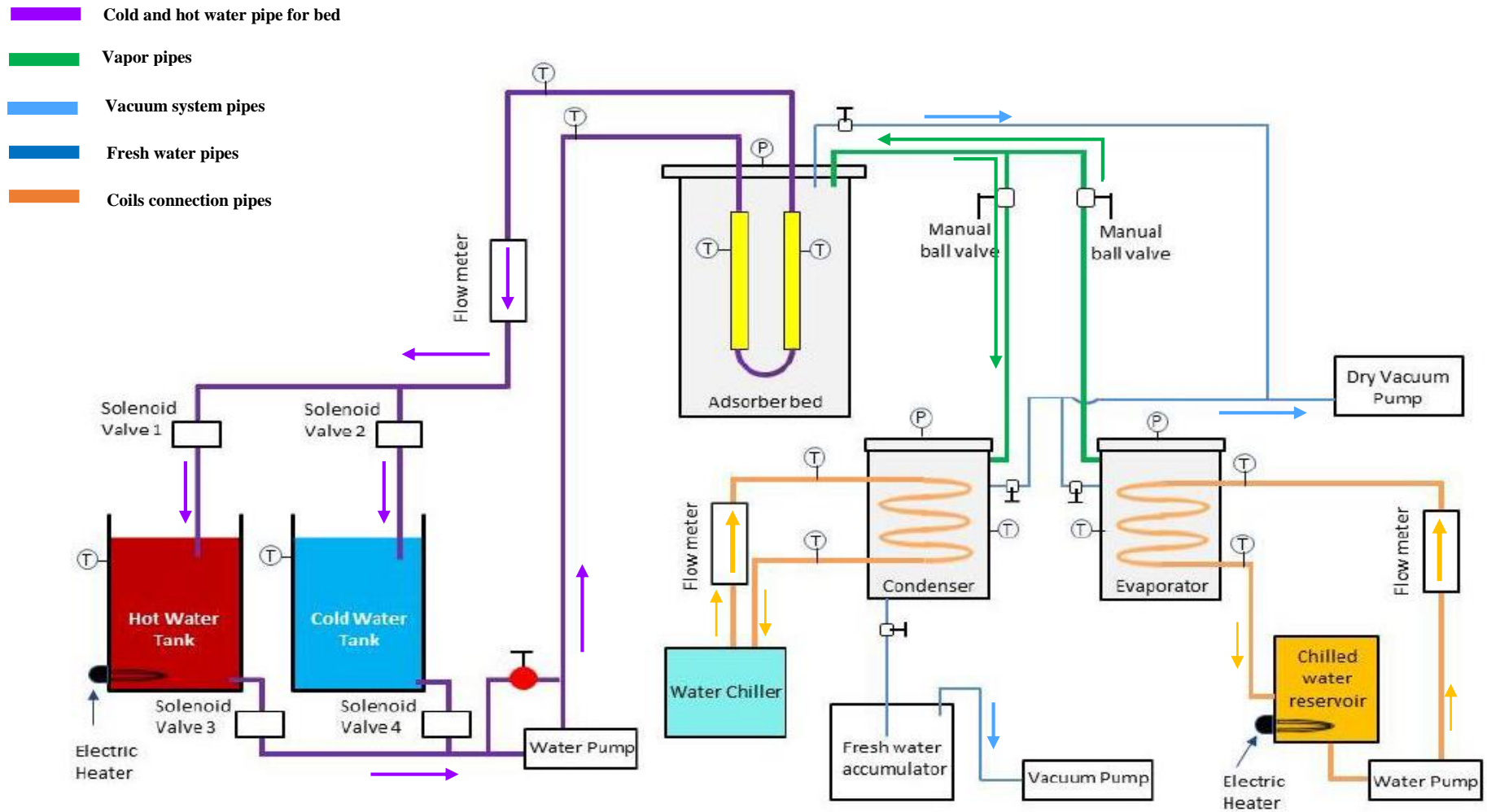


Figure (4.1): Schematic scheme for the test facility of the single bed

- 1- Adsorption bed
- 2- Condenser
- 3- Evaporator
- 4- Chiller unite
- 5- Hot water tank
- 6- Cold water tank
- 7- Vacuum pump
- 8- Bed pump
- 9- System control
- 10- Evaporator pump
- 11- Bed flowmeter
- 12- Evap. flowmeter
- 13- Pressure sensor
- 14- thermocouple

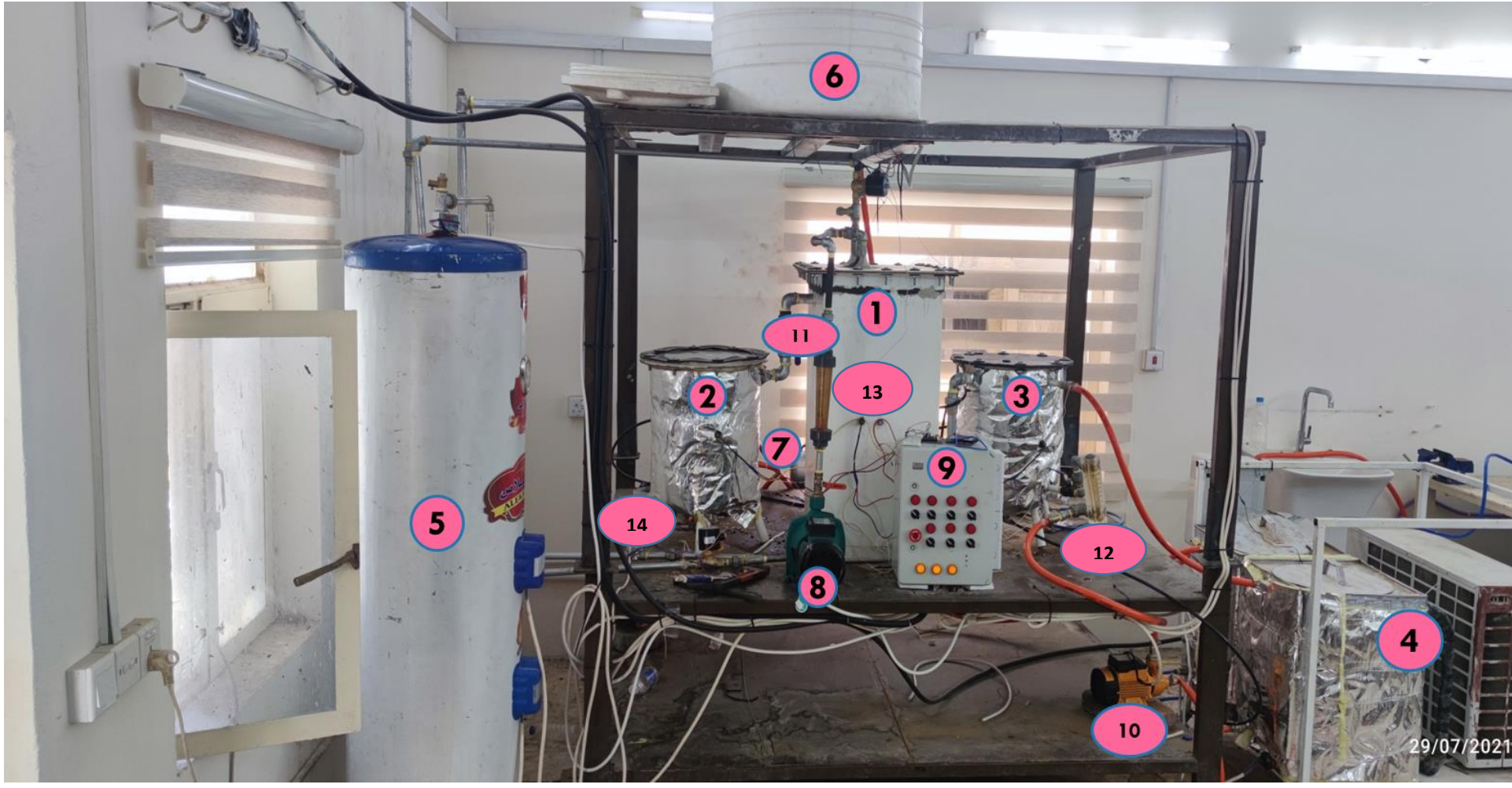


Figure (4.2): An image of the single-bed testing facility

### 4.2.1 Adsorber Bed

The adsorbent is placed in an adsorption bed that contains two parallel heat exchangers as shown in Figure (4.3), where the adsorbent material is placed between the fins of the heat exchanger to enhance the adsorption and desorption process of water vapor. Table (4.1) presents the dimensions of heat exchanger.



Figure (4.3): Heat exchanger module

Table (4.1): Heat exchanger characteristics

Parameter	Value (mm)
Heat exchanger length	590
Fin width	330
Fin pitch	1.25
Fin thickness	0.5
Tube dimension	25 x 2.5
Tube thickness	1.5

The adsorbent bed shall be in the form of a tank of rectangular cuboids made of iron with a thickness of (6 mm) and containing five holes: two for entering and exiting water vapor, and other three for entering the measuring devices and for discharging the air as shown in Figure (4.4). The adsorbent bed contains a cover made of the same metal and is supplied with four tubes to provide the heat exchangers with the hot and cold water necessary for the adsorption and desorption process (see Appendix A).





a



b



c

Figure (4.4): Manufacturing of the adsorbent bed

(a) 6mm iron plate. (b) Heat exchanger carriers. (c) Adsorbed bed.

Silica gel was utilized as an adsorbent in the system which was prepared after laboratory testing and grinding to fit the distances between the fins of the heat exchanger. The heat exchanger was completely filled with 3.2 kg of adsorbent material distributed on two heat exchangers inside the adsorption bed, and both sides of the heat exchanger were covered by a mesh made of stainless steel in order to keep the adsorbent in its desired place (see Figure 4.5).

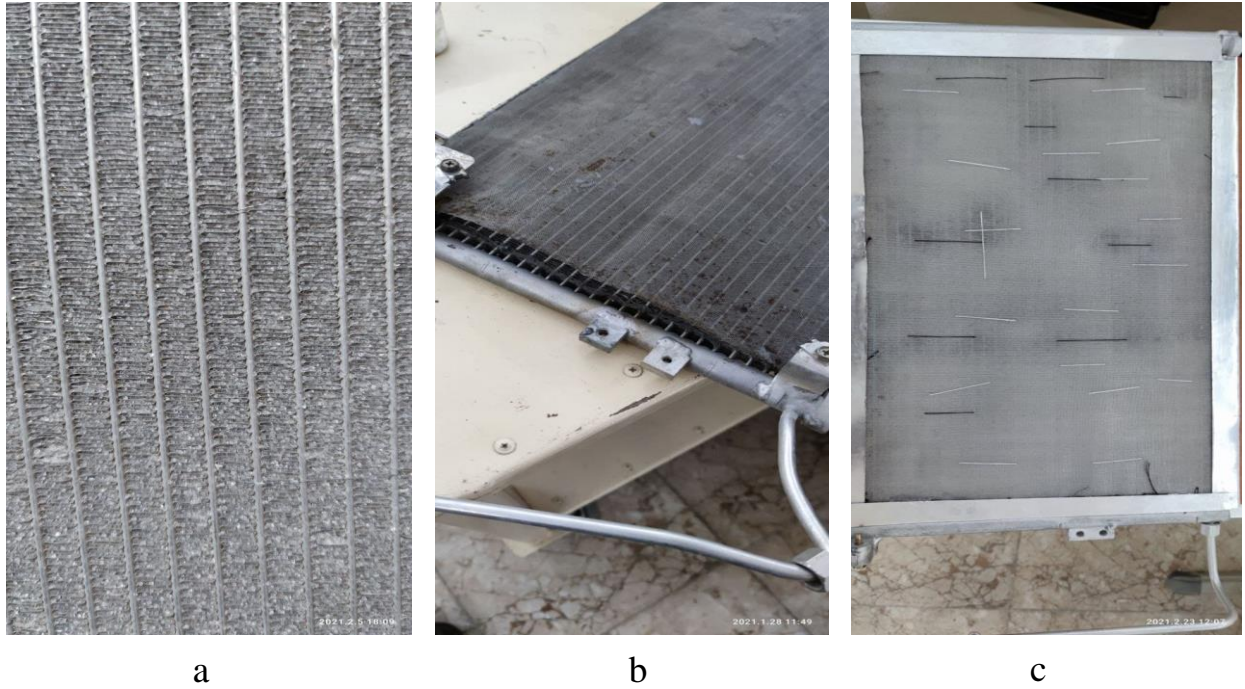


Figure (4.5): Adsorbent bed heat exchanger  
 (a) Silica gel granules between exchanger fins. (b) Stainless steel mesh. (c) Mesh cover the exchanger.

The tests were performed on the adsorption material to examine the physical properties. The tests were taken place in the laboratories of the University of Babylon, and XRD-6000 X-ray Diffractometer shown in Figure (4.6) were used. The properties of the tested material are shown in Table (4.2).

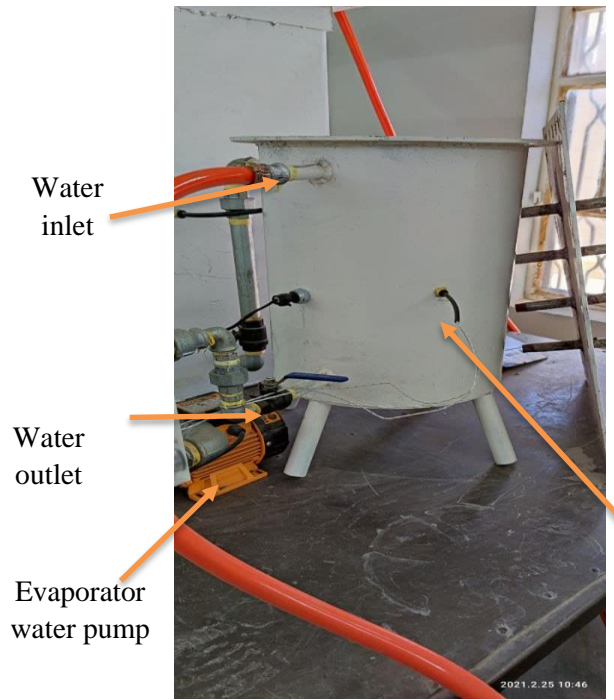


Figure (4.6): XRD-6000 X-ray Diffractometer  
 (a) Front view. (b) Side view

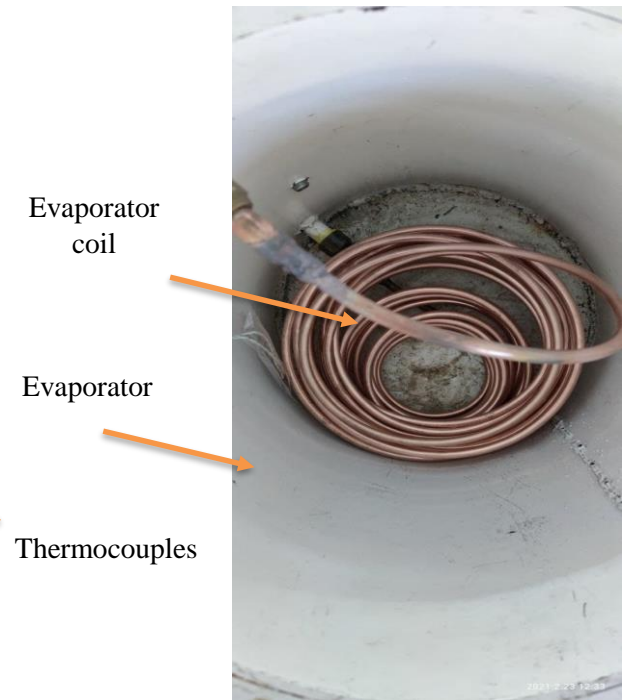
### 4.2.2 Evaporator

It is a cylindrical device made of iron with a thickness of (6 mm), height (45 cm) and diameter of (34.6 cm). It is coated with a greasy coating and contains a copper coil to be used as a heat exchanger. The evaporator has four terminals for the water inlet and outlet. The evaporator is covered with a tempered glass lid containing (8 holes) to be attached to the evaporator base by screws. A rubber gasket is placed between the piece of tempered glass and the base of the evaporator to seal the evaporator and maintain a tight vacuum pressure. The coil of the evaporator is made of a copper tube with an outer diameter of (9.525 mm), a thickness of (1.5 mm) and (6.56 m) long as shown in Figure (4.7). The copper coil acts as the heat source which is used to evaporate the salt water in the evaporator (see Appendix A).





a



b



c



d

Figure (4.7): Evaporator used in the test rig  
 (a) Front view. (b) Top view. (c) Gasket. (d) Tempered glass

### 4.2.3 Condenser

The condenser consists of a cylinder and cooling coil in the form of spiral cone, which is a copper tube with an outer diameter of (15.875 mm), thickness of (1.5 mm), and length of (7.1 m) as shown in Figure (4.8). It is similar to the evaporator in size, shape and number of holes. The cooling coil is wrapped inside the condenser to take the latent heat from the working fluid (water) (see Appendix A).

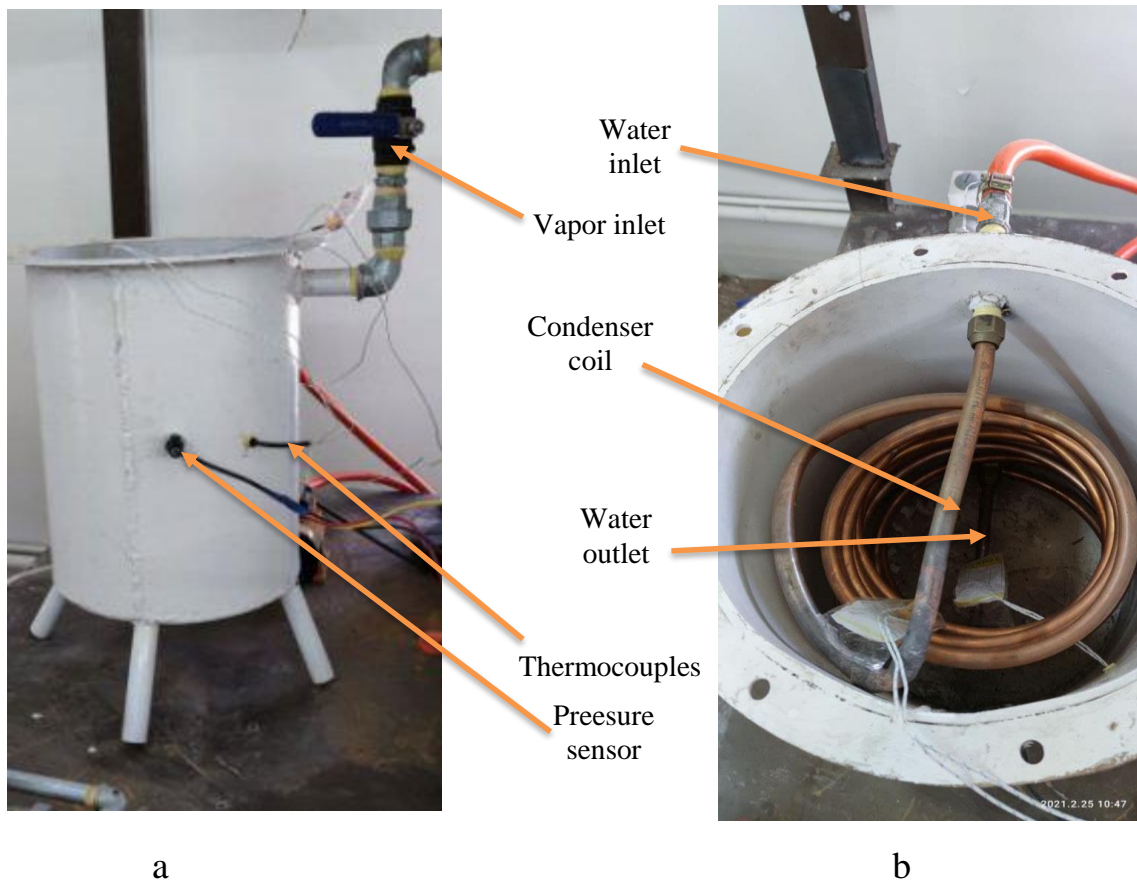


Figure (4.8): Condenser used in the test rig  
(a) Front view. (b) Top view.

#### **4.2.4 Chiller/Heater Unit**

This unit consists of two thermally isolated tanks with a condensation unit that supplies the tanks with cooling water. The two tanks are made of 2 mm thick stainless steel plate with total storage capacity of (200 liters) and in addition to the cooling coil which is a (4- kW) power heater to heat the water in the tanks. One of the tanks is connected to the evaporator cooling coil, and the second tank is connected to the condenser cooling coil. The temperature of the cooling water is controlled by a two-load controller connected to the thermal resistance on one side and to the external part of the air conditioner on the other side as shown in Figure (4.9). The advanced temperature controller can measure and monitor temperatures between (-50 and 90 °C), switch modes between cooling and heating, and temperature level by setting the value of the temperature and the difference value. Also, it can calibrate the temperature, of the cooling /heating performance by delaying if the temperature is greater than the maximum predicting by the sensor, as presented in Figure (4.10) and Table (4.3).

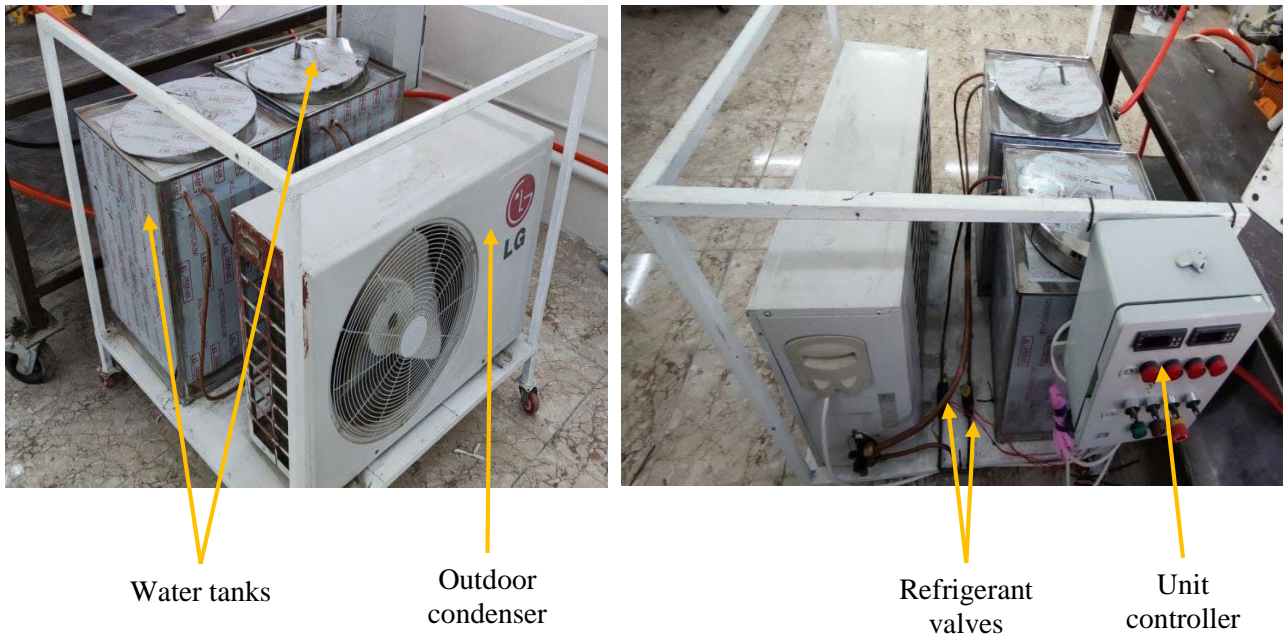


Figure (4.9): Chiller/heater unit utilized in experimental work



Figure (4.10) temperature controller used in the chiller/heater unit

(a) Side view. (b) Front view.

Table (4.2): Specifications of the temperature controller used in the chiller/heater unit

Parameter	Value
Temperature measuring range	-50° to 90° C
Control temperature difference	0.3° to 10° C
Resolution	0.1° C
Accuracy	±1°C
Power consumption	3 W
Power supply	110~220V AC ±10% , 50/60Hz
Sensor	NTC sensor

#### 4.2.5 Water Pumps

There are two types of water pumps used in the system, the first type is used to provide the adsorption bed with water required for the adsorption and desorption process, and the second type is used to provide the evaporator and condenser coils with water. The pump of bed is used to pump hot / cold water, so it is designed for delivering hot water with a flowrate of (120 l/min) and a maximum pumping head of (32 mH<sub>2</sub>O), made by the SHIMGE with model no. of (“CPm 158”), as shown in Figure (4.11). The water supply pumps for condenser and evaporator are manufactured by INGCO, with a highest flow rate of (35 l/min), pumping head of (35



mH<sub>2</sub>O), and liquid temperature of (45° C) with a model number of “VPM3708” as shown in Figure (4.12).



Figure (4.11): adsorbent bed pump



Figure (4.12): evaporator & condenser pump

#### 4.2.6 Flow Control Valves

Two kinds of flow valve are used: manual type used in the steam pipelines between the adsorbent bed and condenser from one side and the adsorbent bed and evaporator from the other side, and the automatic type used to control the stream of hot and cold water entering the bed. The manual valve is a ball valve made of carbon steel to withstand high pressures and temperatures, and it has a diameter of (1 inch) as shown in Figure (4.13). The automatic valve has two types, one of which is to control the entry and exit of hot water into the bed. It is made of brass material and can withstand

high temperatures of up to (180°C) and maximum pressure (14.15 bar) with port size (1/2") as shown in Figure (4.14). The second type is used to control the course of cold water, and it is made of stainless steel bearing temperatures of up to (80 ° C) and maximum pressure of (10 bar) with port size (1/2" ) as shown in Figure (4.15). The initial set of the automatic valves is closed, and it is opened after the valves signalled with an electric voltage via a double electric timer, see Figure (4.16).



Figure (4.13):  
Manual valve



Figure (4.14): Hot water  
automatic valve



Figure (4.15): Cold  
water automatic  
valve



Figure (4.16): Double electric timer  
(a) Front view. (b) Side view.

#### 4.2.7 Hot and Cold-Water Tanks

To provide the adsorbent bed with cold water, a (250-liter), three-layer plastic insulated tank is used as shown in Figure (4.17). It is filled with the tap water and, the water returning from the bed is drained out to ensure a constant temperature for the cold water entering the bed. In order to supply the bed with hot water, a hot tank (electric boiler) (see Figure 4.18) with a capacity of (200 L) is used. It is made of stainless steel, insulated from the outside, and equipped with three electric heaters that are controlled by a sensitive temperature controller of model number “xh-w3001” operating from (-50° to 110° C), with accuracy of ( $\pm 0.2^{\circ}\text{C}$ ) and precision temperature control of ( $\pm 0.1^{\circ}\text{C}$ ) as shown in Figure (4.19).



Figure (4.17): Cold water tank utilised in the test facility



Figure (4.18): Hot water tank (electric boiler) utilised in the test facility





Figure (4.19): Electric boiler temperature controller

#### 4.2.8 Vacuum System

The system operates at a very low pressure about (0.007 bar), so a vacuum system must be provided to draw air from the adsorption bed and both the evaporator and condenser. The vacuum system consists of a pump with a capacity of (1 *hp*) as shown in Figure (4.20). Flexible plastic tubes and special iron fittings are used for the same purpose as shown in Figure (4.21). Also, a steel manifold is utilized to distribute the flow of vacuum pump to the required parts, see Figure (4.22).



Figure (4.20): Vacuum pump used in this test facility



Figure (4.21): Vacuum system accessories



Figure (4.22): Vacuum system manifold

### 4.3 Measuring Devices

Several types of measuring devices are used in the system to measure the temperature, pressure, and flow rate of bed water, condenser, and evaporator.

### 4.3.1 Pressure Measurements

Three pressure sensors are used in the bed, condenser and evaporator with model number of “HK1100C”. The pressure range is(0-1.2MPa), while the temperature range is (0°-85° C), and the accuracy is of ( $\pm 1\%$  FS) as shown in Figure (4.23).



Figure (4.23): Pressure sensor

The output current signal is connected to Arduino kit with screen to view the results as shown in Figure (4.24).

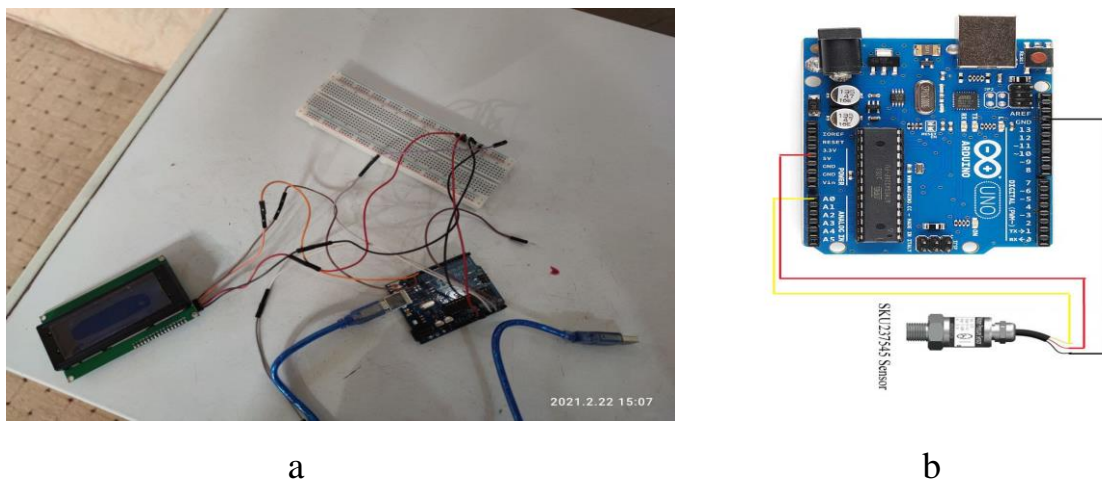


Figure (4.24) :(a) Connect Arduino (b) Arduino kit

### 4.3.2 Temperature Measurements

There are two kinds of thermocouples utilized: "K" thermocouples and "RTD" thermocouples as shown in Figure (4.25). Two of types K are used in both the evaporator and condenser to read the temperature of vapour and water. In the bed, five K-type thermal terminals are used to measure the temperature of the steam inside the bed, and to measure the temperature in the adsorbent material, where the remaining four are distributed on the base and middle of each heat exchanger. eight RTD thermocouples are utilized to read the water temperature at the inlet and outlet of the water pipes prepared for the adsorption bed, the condenser and the evaporator. Type "K" thermocouple can measure temperature from (-50 ~700°C), with accuracy of ( $\pm 2.5$ ) and a wire length of (100 cm), and it has a sensor bulb with a diameter of (2.5 mm). RTD thermocouple is for recording temperature in the range of (-50 to 300°C) with a wire long (100 cm). The reading of the thermocouples was recorded by a data logger which is shown in Figure (4.26). Calibration, uncertainty and error were made for each of the thermocouples and the data logger in the Ministry of Planning / Central Organization for Standardization and Quality Control (COSQC), (see Appendix B).

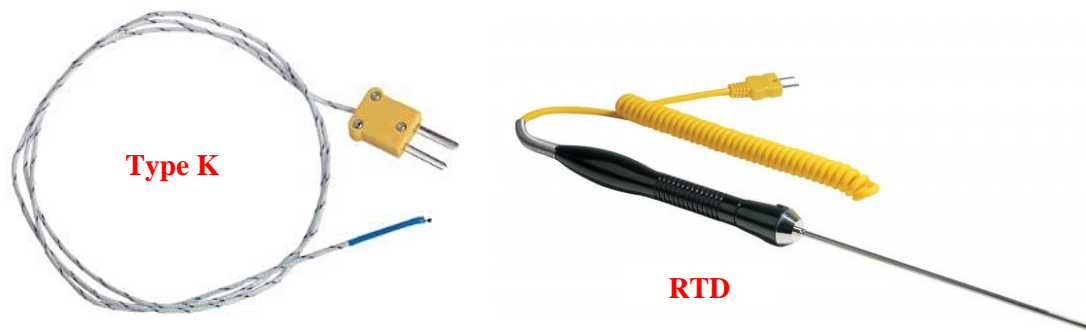


Figure (4.25): Thermocouples used in used in the test rig



Figure (4.26): data logger used in the test rig

### 4.3.3 Flow Rate Measurements

There are three flow meters used to monitor the flowrate of water entering the evaporator, condenser and adsorption bed. Two types of flowmeters are used one for adsorption bed and the other to condenser and evaporator. The first one is” LZS-32-400-4000LPH” with a range of (400 to 4000 l/h) with fluid temperature up to (70° C). The second type is “ZYIA flow meter” with a range of (300 -2100 L/h), see Figures (4.27) and (4.28).



Figure (4.27): Adsorption bed flow meter



Figure (4.28): Condenser & evaporator flow meter

#### 4.4 Test Rig Checking

It is necessary to conduct checks on the parts of the system after assembling it as shown in the Figure (3.1). The purpose of these checks is to detect any leakage locations (water connections and pumps) and air leakage locations (evacuated parts of the air).

1- In order to check the water connections, the water pumps are operated at the maximum flow rate.

2- The leakage of air connections is checked by using a paste material such as toothpaste, for example, after operating the vacuum pump on the parts to be examined.

3- The connections mounted on the walls of the evaporator and condenser are tested by filling the evaporator and condenser with water after they are

evacuated from the air. The bubbles generated inside these devices result from the air flowing through the wall connections.

4- Finally, in order to check the leakage in the lids of both the evaporator and the condenser, soap bubbles are poured, while for checking the leakage between the bed cover for adsorption and its gasket, soap bubbles are utilized too.

## **4.5 Experimental Procedure**

### **4.5.1 Initial Preparations**

1- First, the thermocouples are attached to the data logger, and the pressure sensors are connected to its Arduino board.

2- The cold and hot water tanks are filled and their temperature is adjusted to the required degree. Also, the chiller/heater unit is prepared in the same way above.

3- The timer is set for operating the automatic valves and opening the hot water inlet and outlet valves to the adsorption bed, in order to dry the adsorbent material, while keeping the other valves closed.

4- The adsorption bed pump is turned on to provide hot water to the bed while keeping the vacuum pump running and connected to the adsorption bed line until the pressure and temperature in the bed reach (0.008 bar) and (80° C), respectively.



5- Water is placed in the evaporator, estimated at (2 liters). The evaporator pump is operated to pump water through the evaporator coil.

#### **4.5.2 Starting the Test**

1- Before the adsorption process begins, switching key is used to pre-cool the adsorber bed for a certain amount of time. As a result, the cold water solenoid valves are opened while the hot water solenoid valves are sealed, allowing the adsorber bed to cool down while the manual valves remain sealed.

2- The adsorption process began when the manual valve between the evaporator and the adsorber bed is opened. Water vapor travels to the adsorber bed while salty water evaporates, leaving brine in the evaporator.

3- Both manual valves are sealed while the automated solenoid valves for hot water are opened, and valves for cold water are closed to heat the adsorber bed before the desorption process begins.

4- Desorption began when the manual valve connecting the condenser to the adsorber bed is opened. Desorbed water vapor travels to the condenser, where it condenses and produces potable water.

5- At this point, one full cycle has been completed; therefore, steps "1" through "4" are repeated for the needed number of cycles.



### 4.5.3 Output Readings

Upon completion of the required number of cycles, the data logger's readings are saved. At the end, the produced potable water from the condenser is collected and measured. The following equations are used to compute the specific daily water production.

$$SDWP = \frac{\text{collected potable water (litre)}}{\text{Adsorber mass (kg)} \times \text{No. of cycle} \times \text{Total time of cycle (min)}} \quad (4.1)$$

$$SCP = \frac{m'_{evap} C_p (T_{in,evap} - T_{out,vap})}{M_a} \quad (4.2)$$

### 4.6 Summary

All of the main parts of the 1-bed adsorption system for desalination and cooling, including the adsorber bed, evaporator, and condenser, as well as secondary equipment such as the electric boiler, cold water tank and the chiller/heater unit, and all measurement and control devices, are presented details in depth in this chapter. Along with the apparatus checking, approaches for detecting vacuum leakage were tested. Initial preparations, starting the test, and documenting the results have been described in detail. Calibration, uncertainty and error were made for each measurement device in the Ministry of Planning / Central Organization for Standardization and Quality Control (COSQC), (see Appendix B).

# CHAPTER FIVE

## Results and discussions

### 5.1 Introduction

This chapter shows the numerical and experimental results of the adsorption system for desalination and cooling system adopted in this study. The experimental apparatus consists mainly of an adsorbent bed, condenser and evaporator utilizing Silica-gel as an adsorbent material; however, the numerical study includes two adsorbent beds (for more realistic data) in addition to the condenser and evaporator utilizing Silica-gel. The experimental and numerical results were discussed and validated against experimental data taken from the literature,[1].

### 5.2 Numerical Results

Four variables were focused to study their roles on the specific daily water production (SDWP) and the specific cooling power (SCP) generated from the system. These variables are the half-cycle time, the temperature of the hot water entering the bed, the temperature of the water entering the evaporator and the temperature of the water entering condenser. The effect of each variable is studied separately, while the rest of the variables are kept fixed. Standard value for each variable is ( $T_b=90^\circ\text{C}$ ,  $T_{ch}=20^\circ\text{C}$ ,  $T_c=30^\circ\text{C}$ , and  $t_{\text{half cycle time}}=320$  sec). Matlab Simulink program was used to build

a simulation model, and, different values of main variables were used as in the table below.

Table (5.1): Values of variables used in simulation

Half cycle time (s)	Bed hot water inlet ( $T_b$ ) ( $^{\circ}\text{C}$ )	Condenser water inlet ( $T_c$ ) ( $^{\circ}\text{C}$ )	Evaporator water inlet ( $T_{ch}$ ) ( $^{\circ}\text{C}$ )
220	80	22	12
320	90	26	16
420	100	30	20
520	110	34	24
		38	

### 5.2.1 Half Cycle Time Effect

In Figures (5.1) and (5.2), the effect of half-cycle time on system outputs is discussed. The half-cycle time is increased from (220 to 520 sec) with the remaining operating conditions fixed. At the beginning of the operation, the outputs of the cycle increase with half cycle time, up to a certain time (220 sec), in which the outputs of the system are as high as possible. After this time, the outputs of the cycle gradually decrease with time. That is attributed to a large quantity of desorbed vapor from the Silica gel from (0 to 220 sec), and then begins to decrease with the rest of the cycle time. This indicates that just a little amount of vapor is desorbed after the (220 sec). The action in Figure (5.2) is due to the evaporator

temperature profile, which declines with faster rate at the start point than at the end of the adsorption period, resulting in a lower average evaporator temperature for shorter cycle durations, which improves (SCP).

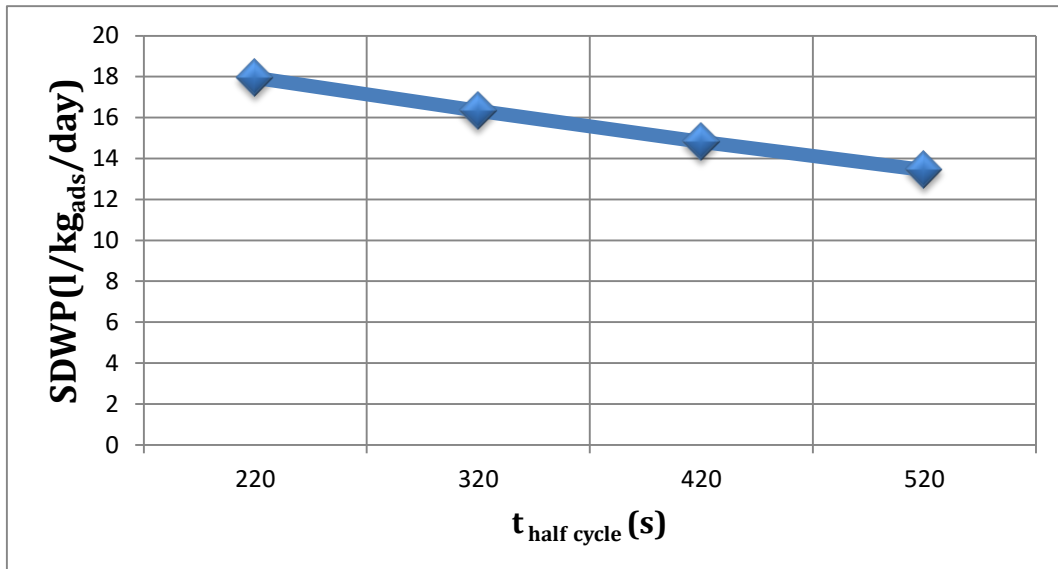


Figure (5.1): Effect of half cycle time on SDWP (numerical)

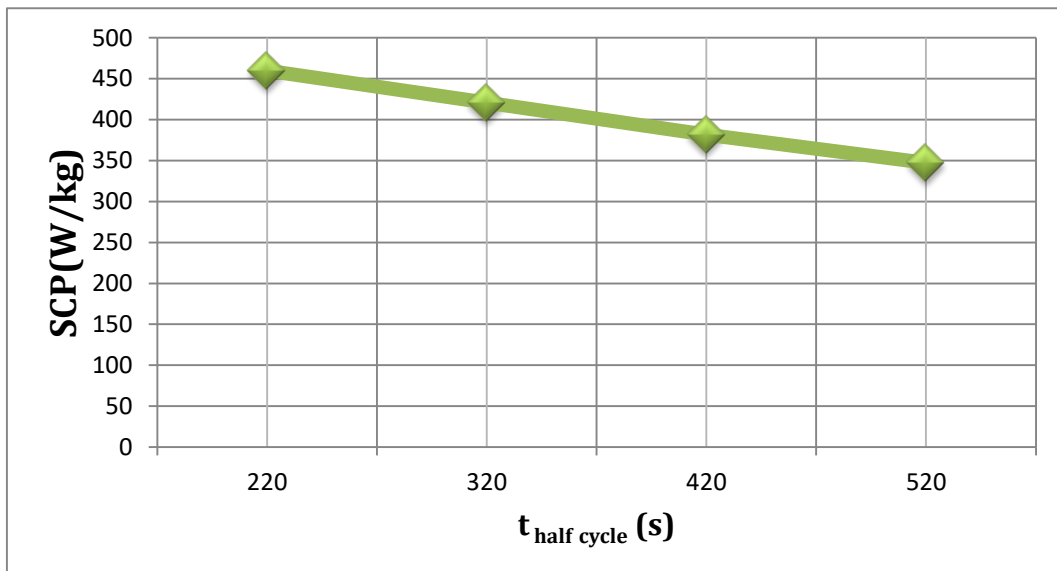


Figure (5.2): Half cycle time effect on SCP (numerical)

## 5.2.2 Bed Hot Water Temperature Effect

Figure (5.3) and Figure (5.4) investigate numerically the effect of the hot bed temperature on the (SDWP) and (SCP), respectively. In these Figures, the temperature was increased from (80 to 110°C), while the rest of the operating conditions are kept constant. With increasing temperature, an increase in (SDWP) and (SCP) was observed. High heating water temperatures lead to more desorbed water vapor and a large amount of desorped vapor is produced from the adsorber bed to the condenser as the desorption temperature increases as shown in Figure (5.5).

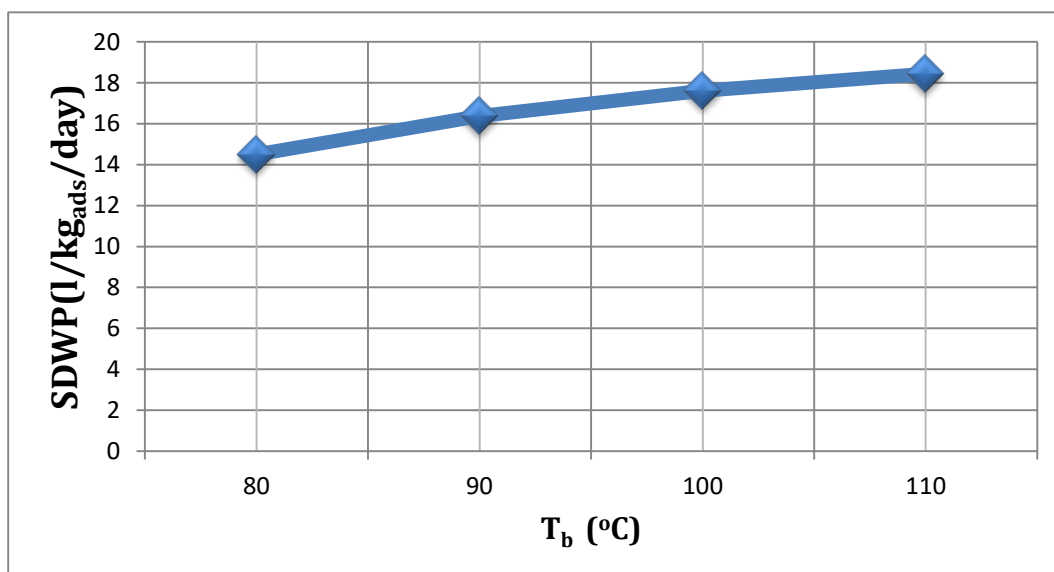


Figure (5.3): Effect of bed hot water temperature on SDWP (numerical)

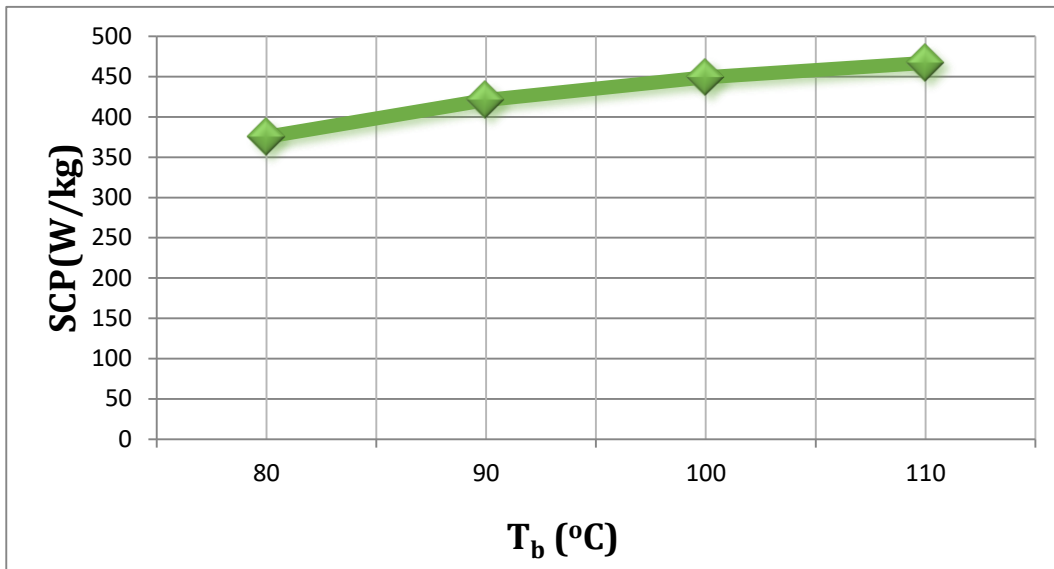


Figure (5.4): Effect of bed hot water temperature on SCP (numerical)

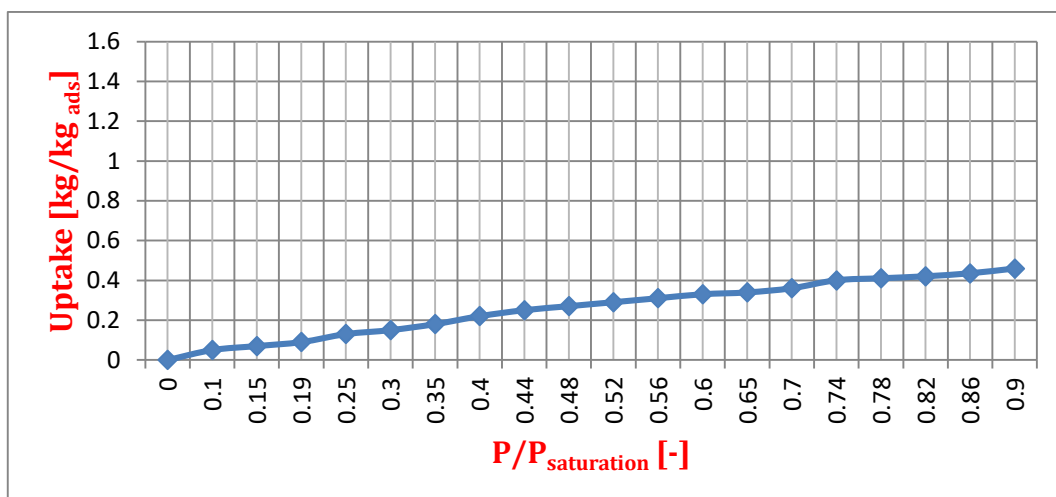


Figure (5.5): Silica-gel isotherms at 25°C

### 5.2.3 Condenser Inlet Water Temperature Effect

Figures (5.6) and (5.7) examine the effect of condenser water temperature on the (SDWP) and (SCP). The condenser water temperature gradually rises from (22 to 38°C), with the remaining operating conditions fixed. (SDWP) and (SCP) are inversely proportional to the temperature of the condenser water, as it was observed that these outputs decreased with the increase in the temperature of the evaporator water. The value for the

considerable fall in (SDWP) is the condensation rate which is quite small at great condensing temperatures due to limited water absorption under these conditions, and high condenser temperature leads to low water uptake too.

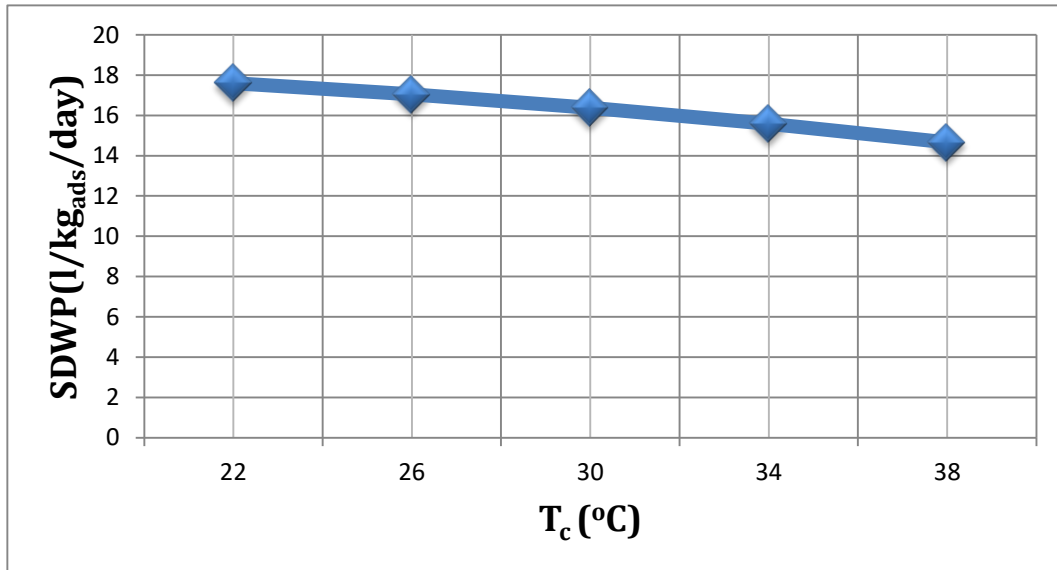


Figure (5.6): Effect of condenser water temperature on SDWP (numerical)

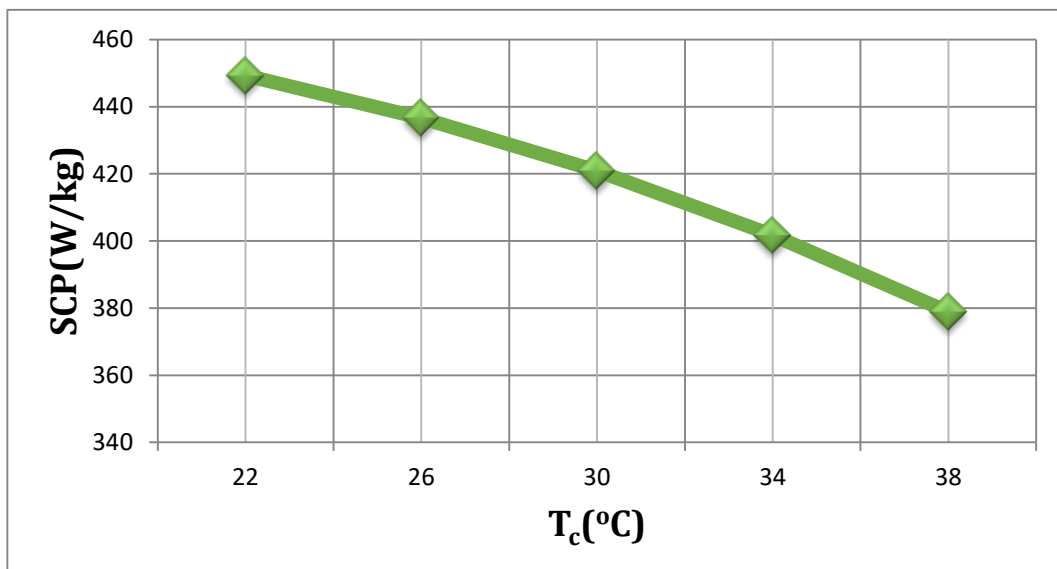


Figure (5.7): Effect of condenser water temperature on SCP (numerical)

### 5.2.4 Evaporator Inlet Water Temperature Effect

Figures (5.8) and (5.9) investigate the effect of evaporator water temperature on the (SDWP) and (SCP), respectively. When the evaporator temperature increases gradually from (12 to 24°C) the (SDWP) and (SCP) increase. The value for this behavior is related to the quantity of water vapor produced in the evaporator, which rises with the temperature of the evaporator water as a result of increased water absorption due to the transfer of vapor from the high pressure in the evaporator to the low pressure in the adsorption bed, which led to an increase in the relative pressure between the evaporator and the adsorption bed ( $P_{\text{evap}}/P_{\text{saturation}}$ ), according to the linear relationship of the isotherm of silica gel as shown in Figure (5.5).

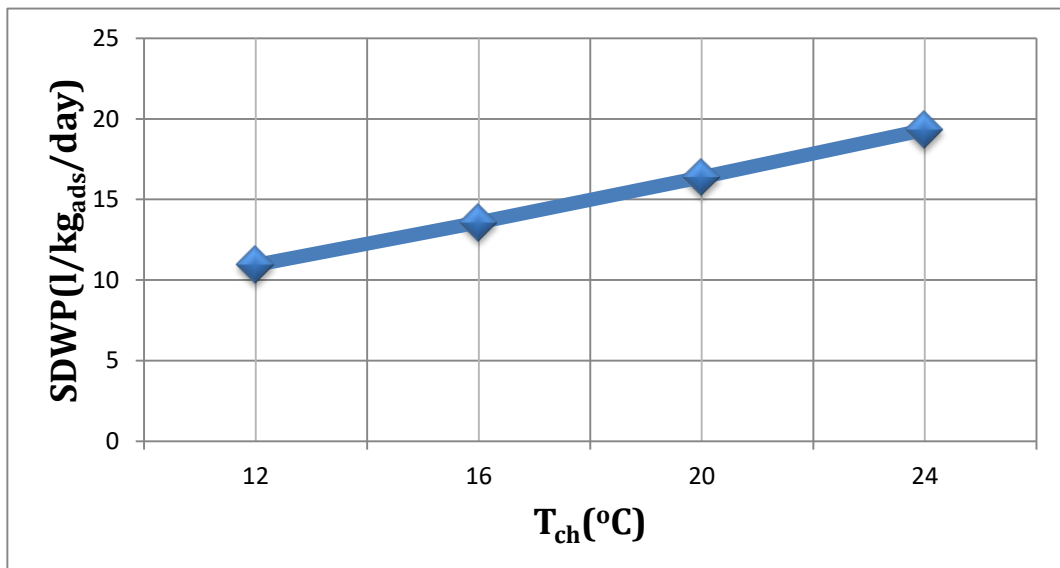


Figure (5.8): Effect of evaporator water temperature on SDWP (numerical)



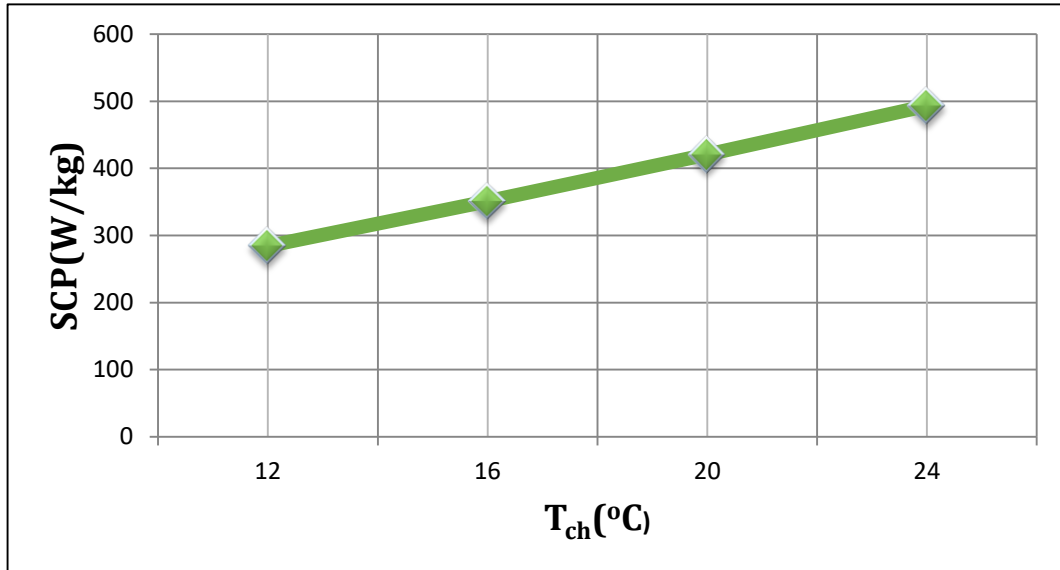


Figure (5.9): Effect of evaporator water temperature on SCP (numerical)

### 5.3 Experimental results

In the experimental work, a single-bed system was used with Silica gel and water as an adsorption pair. Similar to the numerical work, four variables were chosen to evaluate the performance of the current system. The standard value for each variable is ( $T_b= 90^{\circ}\text{C}$ ,  $T_{ch}=38^{\circ}\text{C}$ ,  $T_c= 14^{\circ}\text{C}$  and  $t_{\text{half cycle time}} =320$  sec). The condensation process appears in the bottom of Figure (5.10).

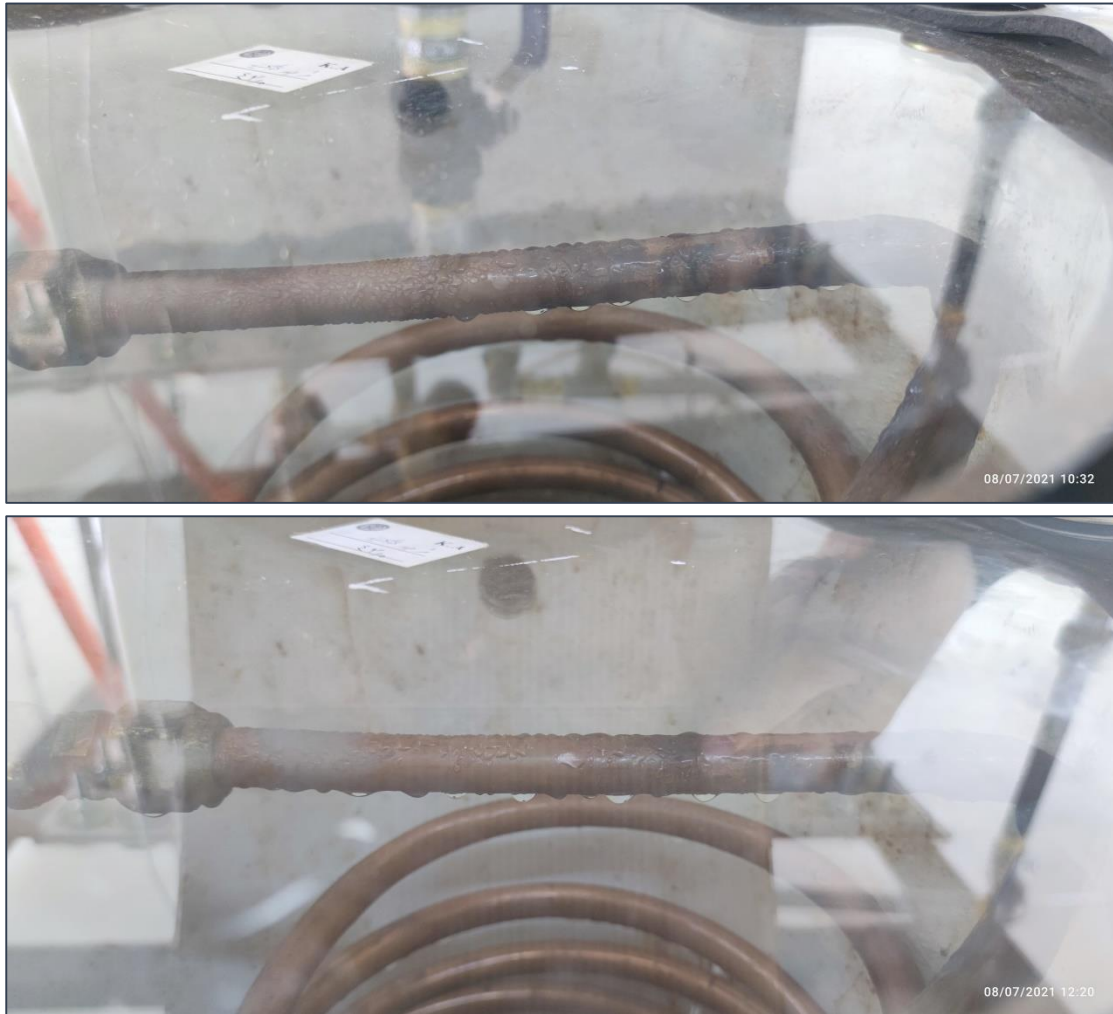


Figure (5.10): Pictures of water condensation inside the condenser

### 5.3.1 Half cycle time effect

The effect of the half-cycle time on the (SDWP) and (SCP) of the system is shown in Figures (5.11) and (5.12). The half-cycle time is increased from (320 to 520 sec). Cycle (SDWP) and (SCP) grow over time, up to a point (320 sec.) where the system of (SDWP) and (SCP) are as high as possible (4.59 l/kg<sub>ads</sub> per day), (95.71W/kg<sub>ads</sub>), respectively. After this period, the cycle output steadily decreases with time. It indicates large volume of vapor desorbed from the Silica gel, which then began to decrease

as the cycle progressed. This shows that the adsorption/desorption processes become slower at the end of the half cycle time.

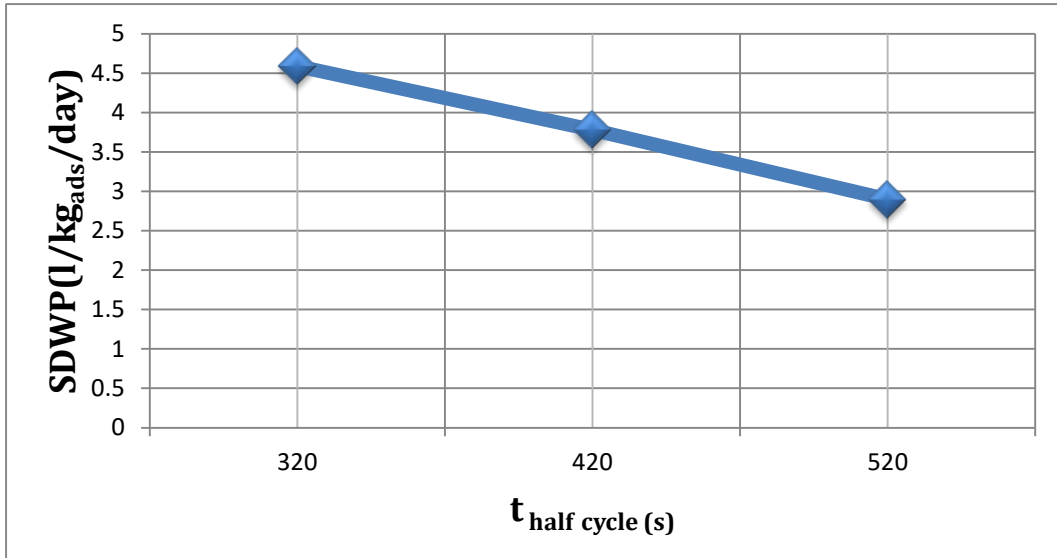


Figure (5.11): Effect of half cycle time on SDWP (Exp.)

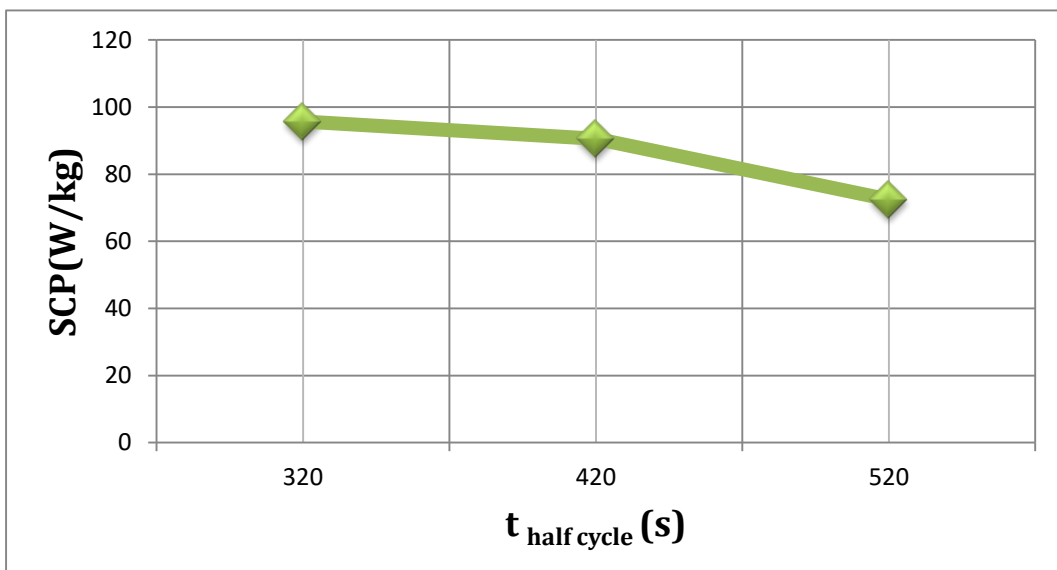


Figure (5.12): Effect of half cycle time on SCP (Exp.)

### 5.3.2 Bed Hot Water Temperature Effect

In Figures (5.13) and (5.14) the change of (SDWP) and (SCP) is shown with the increase of the hot water temperature of the adsorption bed, respectively, it is noted that the (SDWP) value increased from (2.43 to 6.21) ( $\text{l/kg}_{\text{ads}}$  per day) with an increase in temperature from ( $70^{\circ}\text{C}$  -  $90^{\circ}\text{C}$ ). The SCP also raised from (87.95 to  $100.88 \text{ W} / \text{kg}_{\text{ads}}$ ) for the same range of Temperatures. The behavior of these two Figures is attributed to as the desorption temperature rises, more desorbed water vapor is produced owing to higher silica-gel absorption as the relative pressure and temperature rise, as illustrated in Figure (5.5), and a substantial volume of refrigerant vapor is produced from the adsorber bed to the condenser.

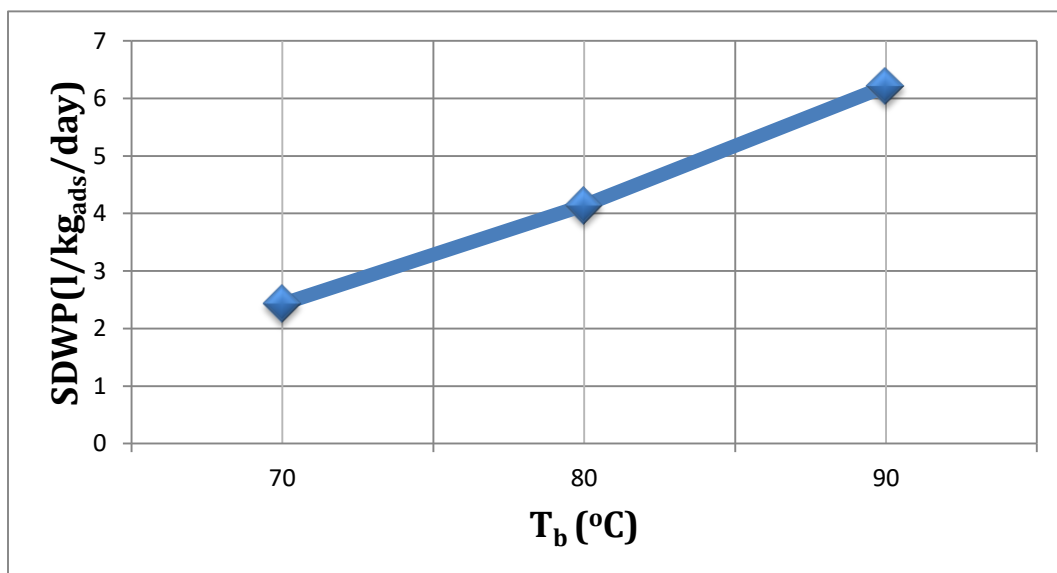


Figure (5.13): Effect of bed hot water temperature on SDWP (Exp.)

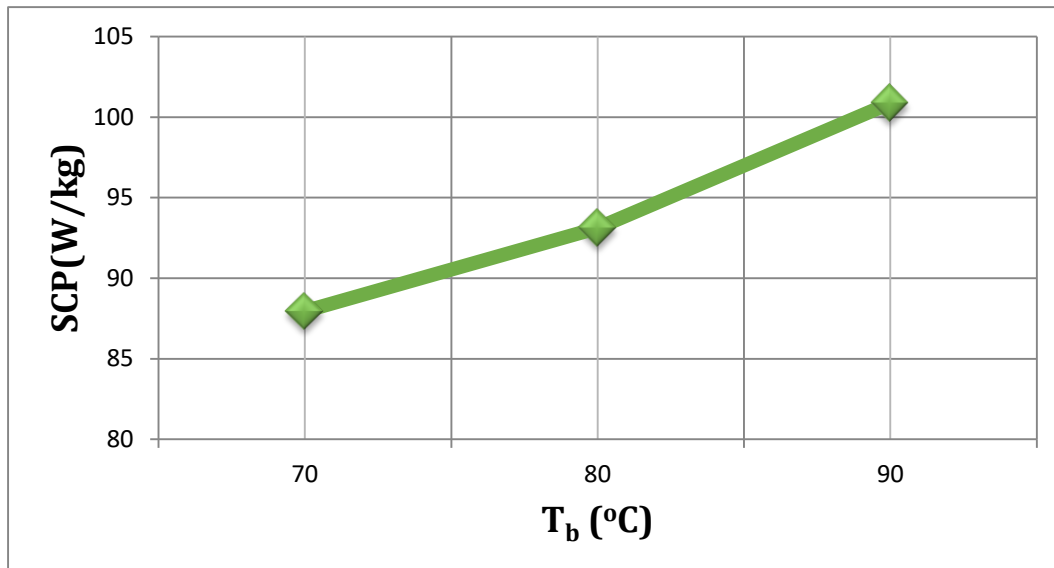


Figure (5.14): Effect of bed hot water temperature on SCP (Exp.)

### 5.3.3 Condenser Inlet Water Temperature Effect

The effect of condenser water temperature on (SDWP) and (SCP) is shown in Figures (5.15) and (5.16), respectively. The temperature of the condenser increases from (14 to 18°C). It is noted that the (SDWP) decreased from (6.03 to 5.49 l/kg<sub>ads</sub> per day), and the (SCP) decreased from (99.59 to 98.3 W/kg<sub>ads</sub>) with the rise in temperature. The behavior of these two Figures is due to restricted water absorption at high condensing temperatures, and the condensation rate is relatively low, resulting in considerable drop in (SDWP) and (SCP).

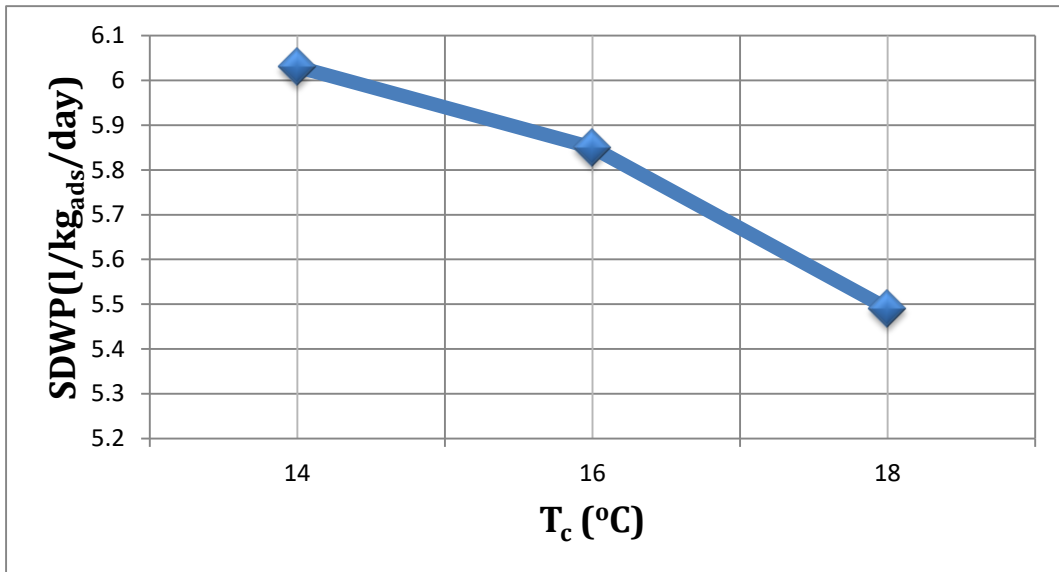


Figure (5.15): Effect of condenser water temperature on SDWP (Exp.)

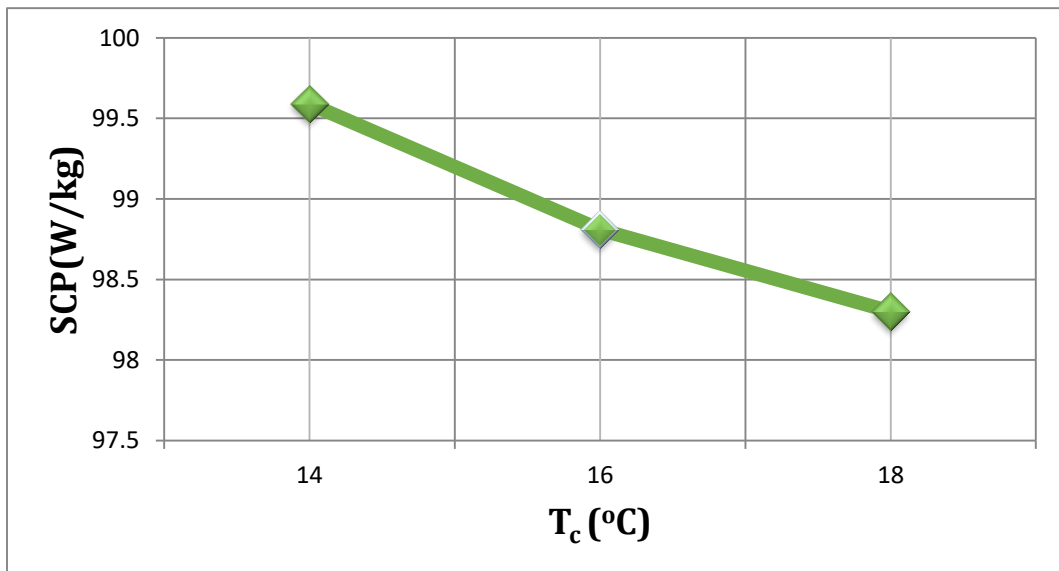


Figure (5.16): Condenser water temperature effect on SCP (Exp.)

### 5.3.4 Evaporator Inlet Water Temperature Effect

The effect of the evaporator water temperature on the (SDWP and SCP) is illustrated in Figures (5.17) and (5.18), respectively. The temperature was increased from (30 to 38°C). An increase in the value of the (SDWP) and

(SCP) is observed. The value of (SDWP) increases from (4.5 to 6.3 l/kg<sub>ads</sub> per day), and (SCP) increases from (72.43 to 103.47 W/ kg<sub>ads</sub>). This behavior is linked to the amount of water vapor produced in the evaporator, which rises with the temperature of the evaporator water as a result of increased water absorption due to increasing relative pressure and the linear shape of silica-gel isotherms.

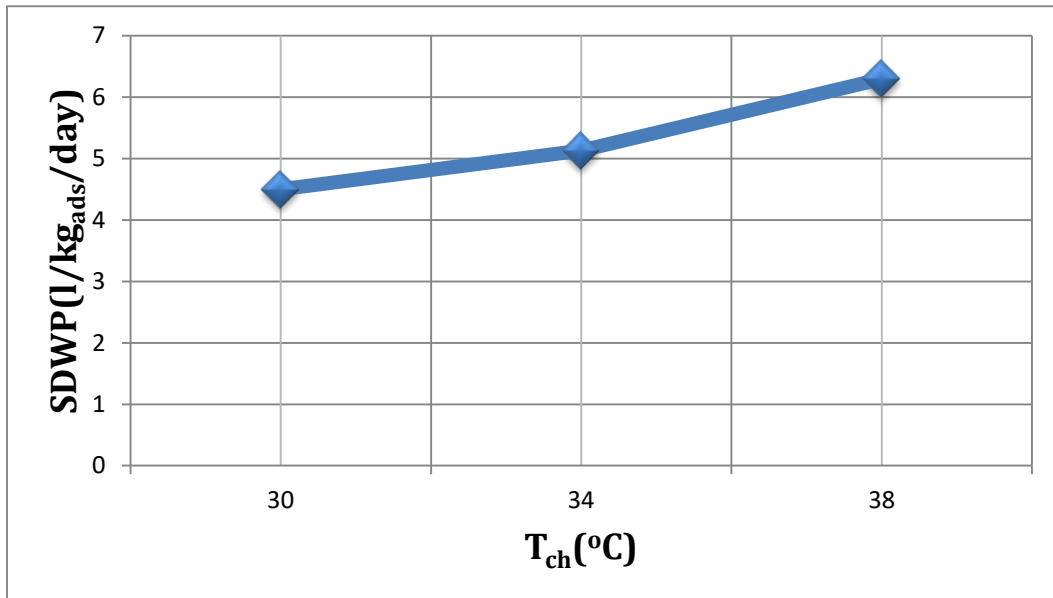


Figure (5.17): Effect of evaporator water temperature on SDWP (Exp.)

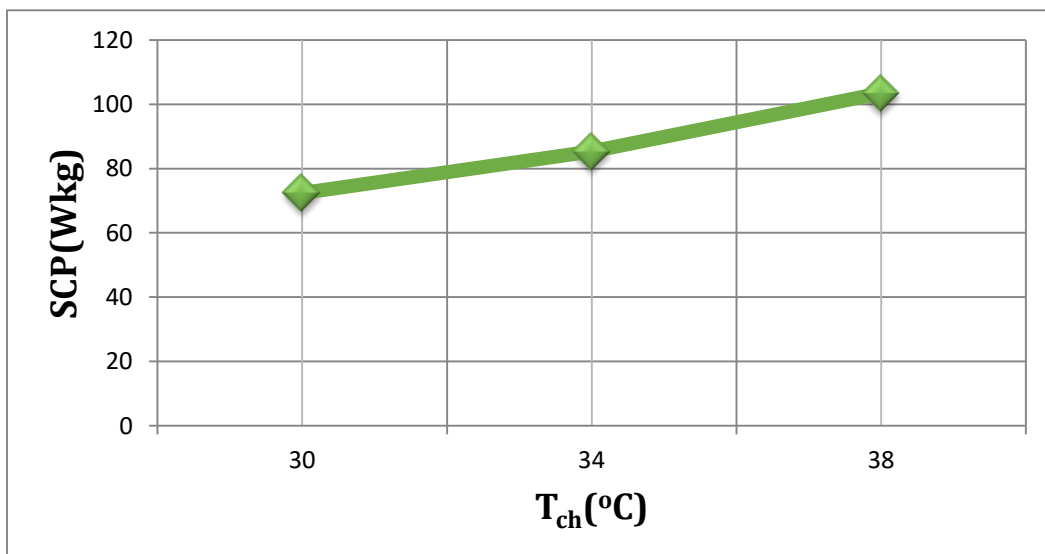


Figure (5.18): Effect of evaporator water temperature on SCP (Exp.)

## **5.4 Summary**

The impact of altering operational situations on cycle specific daily water production (SDWP) and specific cooling power (SCP) was explored in this chapter. These parameters include desorption water temperature, evaporator water input temperature, condenser inlet cooling water temperature, and half cycle time. Silica gel has been studied as an adsorbent. At lower desorption temperatures, longer cycle periods are required, and greater evaporator inlet water temperatures result in greater (SDWP) and (SCP). It was discovered that the temperature of the condenser cooling water had almost no effect on the Silica gel performance at higher desorption temperatures.



# CHAPTER SIX

## Conclusions and Suggestion for Future Works

### 6.1 Conclusions

The main conclusions can be summarized as follows:

- 1- A numerical model was created using Simulink to determine the performance of two-bed adsorption desalination and cooling system employing one adsorbent "Silica-gel" under various operating environments.
- 2- The suggested 2-bed Simulink model was validated against published Silica-gel experimental data using actual and approximated temperatures measured in Celsius degrees, with an instantaneous error of  $\pm 9.7\%$ .
- 3- Maximum SDWP (19.322 l / kg silica-gel/ day) using  $T_b= 90^\circ\text{C}$ ,  $T_c= 30^\circ\text{C}$ ,  $T_{ch}= 24^\circ\text{C}$  and half cycle time= 320 s and SCP (493.1831 W/kg) using  $T_b= 90^\circ\text{C}$ ,  $T_c= 30^\circ\text{C}$ ,  $T_{ch}= 24^\circ\text{C}$  and half cycle time= 320 s. As heating temperature increases, SDWP increases by 21% and SCP by 23.4%. As evaporator temperature increases, SDWP and SCP increase by 43% and 42% respectively. As condenser temperature increases, SDWP and SCP drop by 20% and 18.6%

respectively. As half cycle time increases, SDWP and SCP decrease by 33.4% and 32.5%.

- 4- A single-bed adsorption test apparatus was built to function as a desalination/cooling system, and Silica gel material was evaluated for desalination purposes under various working circumstances, with cooling load produced as a byproduct.
- 5- Raising the adsorption water temperature from 70°C to 90°C leads to an improvement in SDWP by 60% and an improvement in SCP by 12.8%. Raising the evaporator water temperature from 30°C to 38°C leads to an improvement in SDWP and SCP by 28.5% and 30%, respectively. Raising the half-cycle time from 300 to 500 sec leads to a decrease in SDWP and SCP values by 55% and 32%, respectively.

## **6.2 Suggestion for Future Works**

1. It is recommended to use modern adsorbent materials that have a large uptake of vapour and work at high temperatures compared to Silica gel, which has limited uptake and low temperature range in which it works.
2. The study of various adsorber bed designs and the method of integrating the adsorber materials are necessary to help improving the heat transfer between the adsorbent material grains and the adsorption bed during heating/cooling processes.

3. Various evaporator designs should be investigated to increase the evaporation heat transfer coefficient, such as inventing a mechanism for circulating sea water inside the evaporator to make continuous sea water spraying.
4. Other alternative condenser designs can be tested should be investigated to obtain greater heat transfer coefficients, as well as evaluating the influence of accumulation of potable water level.

## References

- [1] P. G. A. Youssef, "EXPERIMENTAL AND NUMERICAL INVESTIGATION OF A NEW MOF BASED ADSORPTION WATER DESALINATION SYSTEM," Doctor of Philosophy, Department of Mechanical Engineering School of Engineering College of Engineering and Physical Sciences, University of Birmingham, 2017.
- [2] T. Distefano and S. Kelly, "Are we in deep water? Water scarcity and its limits to economic growth," *Ecological Economics*, vol. 142, pp. 130-147, 2017.
- [3] T. L. Anderson, B. Scarborough, and L. R. Watson, "Water Crises, Water Rights, and Water Markets\*\*Excerpted from Tapping Water Markets, by Terry L. Anderson, Brandon Scarborough, and L. Reed Watson (2012, Routledge)," in *Encyclopedia of Energy, Natural Resource, and Environmental Economics*, 2013, pp. 248-254.
- [4] J. W. WU, "A Study of Silica Gel Adsorption Desalination System," degree of Doctor of Philosophy, School of Mechanical Engineering, The University of Adelaide, 2012.
- [5] S. M. M. a. R. K. A.-D. Peter G. Youssef, "SEAWATER DESALINATION TECHNOLOGIES," *International Journal of Innovation Sciences and Research*, vol. Vol.4, p. 21, 2015.
- [6] K. C. Ng, K. Thu, B. B. Saha, and A. Chakraborty, "Study on a waste heat-driven adsorption cooling cum desalination cycle," *International Journal of refrigeration*, vol. 35, no. 3, pp. 685-693, 2012.
- [7] X. Wang and K. C. Ng, "Experimental investigation of an adsorption desalination plant using low-temperature waste heat," *Applied Thermal Engineering*, vol. 25, no. 17-18, pp. 2780-2789, 2005, doi: 10.1016/j.applthermaleng.2005.02.011.
- [8] P. G. Youssef, R. K. Al-Dadah, and S. M. Mahmoud, "Comparative Analysis of Desalination Technologies," *Energy Procedia*, vol. 61, pp. 2604-2607, 2014, doi: 10.1016/j.egypro.2014.12.258.
- [9] K. E. T. Tamim Younos, "Overview of Desalination Techniques," *JOURNAL OF CONTEMPORARY WATER RESEARCH & EDUCATION*, no. 132, pp. 3-10, 2005.

- [10] M. S. M. Al-Shammiri, "Multi-effect distillation plants: state of the art," *Desalination*, vol. 126, pp. 45-59, 1999.
- [11] I. A. Hisham El-Dessouky, S. Bingulac and Hisham Ettouney, "Steady-State Analysis of the Multiple Effect Evaporation Desalination Process," *Chem. Eng. Technol*, 1998.
- [12] P. Druetta, P. Aguirre, and S. Mussati, "Optimization of Multi-Effect Evaporation desalination plants," *Desalination*, vol. 311, pp. 1-15, 2013, doi: 10.1016/j.desal.2012.10.03.
- [13] H. M. E. Hisham T. El-Dessouky, Faisal Mandani, "Performance of parallel feed multiple effect evaporation system for seawater desalination," *Applied Thermal Engineering*, vol. 20, pp. 1679-1706, 2000.
- [14] N. Misdan, W. J. Lau, and A. F. Ismail, "Seawater Reverse Osmosis (SWRO) desalination by thin-film composite membrane—Current development, challenges and future prospects," *Desalination*, vol. 287, pp. 228-237, 2012, doi: 10.1016/j.desal.2011.11.001.
- [15] A. D. Khawaji, I. K. Kutubkhanah, and J.-M. Wie, "Advances in seawater desalination technologies," *Desalination*, vol. 221, no. 1-3, pp. 47-69, 2008, doi: 10.1016/j.desal.2007.01.067.
- [16] K. H. E. B.A. BOLTO, M.B. JACKSON AND R.V. SIWDAK, "an ion-exchange process with thermal regeneration xvi\* oxygen-resistant polyamine resins," *Desalination*, vol. 42, pp. 273-290, 1982.
- [17] A. N. A. Mabrouk, "Technoeconomic analysis of once through long tube MSF process for high capacity desalination plants," *Desalination*, vol. 317, pp. 84-94, 2013, doi: 10.1016/j.desal.2013.03.002.
- [18] M. Shatat, M. Worall, and S. Riffat, "Opportunities for solar water desalination worldwide: Review," *Sustainable Cities and Society*, vol. 9, pp. 67-80, 2013, doi: 10.1016/j.scs.2013.03.004.
- [19] A. Naeimi, S. M. Nowee, and H. A. Akhlaghi Amiri, "Numerical simulation and theoretical investigation of a multi-cycle dual-evaporator adsorption desalination and cooling system," *Chemical Engineering Research and Design*, vol. 156, pp. 402-413, 2020, doi: 10.1016/j.cherd.2020.02.016.

- [20] R. H. Mohammed, "Experimental and Numerical Investigation of a Novel Adsorption Bed Design for Cooling Applications," degree of Doctor of Philosophy, Department of Mechanical and Aerospace Engineering in the College of Engineering and Computer Science, University of Central Florida, 2019.
- [21] Y. I. Aristov, "Challenging offers of material science for adsorption heat transformation: A review," *Applied Thermal Engineering*, vol. 50, no. 2, pp. 1610-1618, 2013, doi: 10.1016/j.applthermaleng.2011.09.003.
- [22] K. Daou, R. Z. Wang, and Z. Z. Xia, "Development of a new synthesized adsorbent for refrigeration and air conditioning applications," *Applied Thermal Engineering*, vol. 26, no. 1, pp. 56-65, 2006, doi: 10.1016/j.applthermaleng.2005.04.024.
- [23] A. A. Askalany, M. Salem, I. M. Ismael, A. H. H. Ali, M. G. Morsy, and B. B. Saha, "An overview on adsorption pairs for cooling," *Renewable and Sustainable Energy Reviews*, vol. 19, pp. 565-572, 2013, doi: 10.1016/j.rser.2012.11.037.
- [24] F. N. A. Al-Mousawi, "ADSORPTION SYSTEM FOR COOLING AND POWER GENERATION USING ADVANCED ADSORBENT MATERIALS," Degree of Doctor of Philosophy, Mechanical Engineering School of Engineering College of Engineering and Physical Sciences, University of Birmingham, 2018.
- [25] F. N. Al-Mousawi, R. Al-Dadah, and S. Mahmoud, "Novel system for cooling and electricity: Four different integrated adsorption-ORC configurations with two expanders," *Energy Conversion and Management*, vol. 152, pp. 72-87, 2017, doi: 10.1016/j.enconman.2017.09.044.
- [26] V. Palomba, S. Vasta, A. Freni, Q. Pan, R. Wang, and X. Zhai, "Increasing the share of renewables through adsorption solar cooling: A validated case study," *Renewable Energy*, vol. 110, pp. 126-140, 2017, doi: 10.1016/j.renene.2016.12.016.
- [27] R. P. Sah, B. Choudhury, and R. K. Das, "A review on adsorption cooling systems with silica gel and carbon as adsorbents," *Renewable and Sustainable Energy Reviews*, vol. 45, pp. 123-134, 2015, doi: 10.1016/j.rser.2015.01.039.

- [28] O. Labban, T. Chen, A. F. Ghoniem, J. H. Lienhard, and L. K. Norford, "Next-generation HVAC: Prospects for and limitations of desiccant and membrane-based dehumidification and cooling," *Applied Energy*, vol. 200, pp. 330-346, 2017, doi: 10.1016/j.apenergy.2017.05.051.
- [29] H. Bao, Y. Wang, and A. P. Roskilly, "Modelling of a chemisorption refrigeration and power cogeneration system," *Applied Energy*, vol. 119, pp. 351-362, 2014, doi: 10.1016/j.apenergy.2014.01.012.
- [30] A. Shekari Namin, H. Rostamzadeh, and P. Nourani, "Thermodynamic and thermoeconomic analysis of three cascade power plants coupled with RO desalination unit, driven by a salinity-gradient solar pond," *Thermal Science and Engineering Progress*, vol. 18, 2020, doi: 10.1016/j.tsep.2020.100562.
- [31] K. Park, L. Burlace, N. Dhakal, A. Mudgal, N. A. Stewart, and P. A. Davies, "Design, modelling and optimisation of a batch reverse osmosis (RO) desalination system using a free piston for brackish water treatment," *Desalination*, vol. 494, 2020, doi: 10.1016/j.desal.2020.114625.
- [32] A. K. Singh, R. K. Yadav, D. Mishra, R. Prasad, L. K. Gupta, and P. Kumar, "Active solar distillation technology: A wide overview," *Desalination*, vol. 493, 2020, doi: 10.1016/j.desal.2020.114652.
- [33] L. Chen, P. Xu, K. Kota, S. Kuravi, and H. Wang, "Solar distillation of highly saline produced water using low-cost and high-performance carbon black and airlaid paper-based evaporator (CAPER)," *Chemosphere*, vol. 269, p. 129372, Apr 2021, doi: 10.1016/j.chemosphere.2020.129372.
- [34] K. Thu, A. Chakraborty, Y.-D. Kim, A. Myat, B. B. Saha, and K. C. Ng, "Numerical simulation and performance investigation of an advanced adsorption desalination cycle," *Desalination*, vol. 308, pp. 209-218, 2013, doi: 10.1016/j.desal.2012.04.021.
- [35] S. Mitra, K. Srinivasan, P. Kumar, S. S. Murthy, and P. Dutta, "Solar Driven Adsorption Desalination System," *Energy Procedia*, vol. 49, pp. 2261-2269, 2014, doi: 10.1016/j.egypro.2014.03.239.
- [36] P. G. Youssef, S. M. Mahmoud, and R. K. Al-Dadah, "Numerical simulation of combined adsorption desalination and cooling cycles

- with integrated evaporator/condenser," *Desalination*, vol. 392, pp. 14-24, 2016, doi: 10.1016/j.desal.2016.04.011.
- [37] S. M. Ali and A. Chakraborty, "Adsorption assisted double stage cooling and desalination employing silica gel + water and AQSOA-Z02 + water systems," *Energy Conversion and Management*, vol. 117, pp. 193-205, 2016, doi: 10.1016/j.enconman.2016.03.007.
- [38] K. Thu, B. B. Saha, K. J. Chua, and K. C. Ng, "Performance investigation of a waste heat-driven 3-bed 2-evaporator adsorption cycle for cooling and desalination," *International Journal of Heat and Mass Transfer*, vol. 101, pp. 1111-1122, 2016, doi: 10.1016/j.ijheatmasstransfer.2016.05.127.
- [39] E. Elsayed, R. Al-Dadah, S. Mahmoud, P. A. Anderson, A. Elsayed, and P. G. Youssef, "CPO-27(Ni), aluminium fumarate and MIL-101(Cr) MOF materials for adsorption water desalination," *Desalination*, vol. 406, pp. 25-36, 2017, doi: 10.1016/j.desal.2016.07.030.
- [40] S. M. M. Peter G. Youssef, Raya K. AL-Dadah, Eman Elsayed and Osman El-Samni, "Numerical Investigation of Aluminum Fumarate MOF adsorbent material for adsorption desalination/cooling application," *energy Procedia*, vol. 142, pp. 1693-1698, 2017.
- [41] E. S. Ali, A. S. Alsaman, K. Harby, A. A. Askalany, M. R. Diab, and S. M. Ebrahim Yakoot, "Recycling brine water of reverse osmosis desalination employing adsorption desalination: A theoretical simulation," *Desalination*, vol. 408, pp. 13-24, 2017, doi: 10.1016/j.desal.2016.12.002.
- [42] H. Rezk, A. S. Alsaman, M. Al-Dhaifallah, A. A. Askalany, M. A. Abdelkareem, and A. M. Nassef, "Identifying optimal operating conditions of solar-driven silica gel based adsorption desalination cooling system via modern optimization," *Solar Energy*, vol. 181, pp. 475-489, 2019, doi: 10.1016/j.solener.2019.02.024.
- [43] A. Amirfakhraei, T. Zarei, and J. Khorshidi, "Performance improvement of adsorption desalination system by applying mass and heat recovery processes," *Thermal Science and Engineering Progress*, vol. 18, 2020, doi: 10.1016/j.tsep.2020.100516.
- [44] A. Askalany, E. S. Ali, and R. H. Mohammed, "A novel cycle for adsorption desalination system with two stages-ejector for higher



- water production and efficiency," *Desalination*, vol. 496, 2020, doi: 10.1016/j.desal.2020.114753.
- [45] M. H. Elbassoussi, R. H. Mohammed, and S. M. Zubair, "Thermoeconomic assessment of an adsorption cooling/desalination cycle coupled with a water-heated humidification-dehumidification desalination unit," *Energy Conversion and Management*, vol. 223, 2020, doi: 10.1016/j.enconman.2020.113270.
- [46] C. Ghenai, D. Kabakebji, I. Douba, and A. Yassin, "Performance analysis and optimization of hybrid multi-effect distillation adsorption desalination system powered with solar thermal energy for high salinity sea water," *Energy*, vol. 215, 2021, doi: 10.1016/j.energy.2020.119212.
- [47] K. Thu, B. B. Saha, A. Chakraborty, W. G. Chun, and K. C. Ng, "Study on an advanced adsorption desalination cycle with evaporator–condenser heat recovery circuit," *International Journal of heat and mass transfer*, vol. 54, no. 1-3, pp. 43-51, 2011.
- [48] P. G. Youssef, H. Dakkama, S. M. Mahmoud, and R. K. Al-Dadah, "Experimental investigation of adsorption water desalination/cooling system using CPO-27Ni MOF," *Desalination*, vol. 404, pp. 192-199, 2017, doi: 10.1016/j.desal.2016.11.008.
- [49] H. J. Dakkama, P. G. Youssef, R. K. Al-Dadah, and S. Mahmoud, "Adsorption ice making and water desalination system using metal organic frameworks/water pair," *Energy Conversion and Management*, vol. 142, pp. 53-61, 2017, doi: 10.1016/j.enconman.2017.03.036.
- [50] K. Thu, H. Yanagi, B. B. Saha, and K. C. Ng, "Performance investigation on a 4-bed adsorption desalination cycle with internal heat recovery scheme," *Desalination*, vol. 402, pp. 88-96, 2017.
- [51] H. Zhang, H. Ma, S. Liu, H. Wang, Y. Sun, and D. Qi, "Investigation on the operating characteristics of a pilot-scale adsorption desalination system," *Desalination*, vol. 473, 2020, doi: 10.1016/j.desal.2019.114196.
- [52] S. Bai, T. C. Ho, J. Ha, A. K. An, and C. Y. Tso, "Study of the salinity effects on the cooling and desalination performance of an adsorption cooling cum desalination system with a novel composite

adsorbent," *Applied Thermal Engineering*, vol. 181, 2020, doi: 10.1016/j.applthermaleng.2020.115879.

- [53] E. Elsayed, R. Al-Dadah, S. Mahmoud, P. Anderson, and A. Elsayed, "Experimental testing of aluminium fumarate MOF for adsorption desalination," *Desalination*, vol. 475, 2020, doi: 10.1016/j.desal.2019.114170.
- [54] H. S. Son, M. W. Shahzad, N. Ghaffour, and K. C. Ng, "Pilot studies on synergetic impacts of energy utilization in hybrid desalination system: Multi-effect distillation and adsorption cycle (MED-AD)," *Desalination*, vol. 477, 2020, doi: 10.1016/j.desal.2019.114266.

## Appendix A

Adsorbent type: Silica gel

Silica gel mass: 3.2 kg

$C_{p, \text{Silica gel}}$ : 0.934 @ 30°C

### **A-1 Adsorption Bed Design**

Heat exchanger dimensions

HX Fin width = 590 mm

HX Fin height = 330 mm

HX Fin thickness = 0.5 mm

HX Fin pitch = 1.25 mm

HX Tube width = 25 mm

HX Tube height = 2.5 mm

HX Tube thickness = 0.8 mm

HX Tube length = 550 mm

Number of tubes per fin area in HX = 30

Number of passes = 2

Fins and tubes are made of Aluminum.

#### **A-1.1 Mass calculations:**

##### **A-1.1.1 Fins**

No. fins /long of tube =  $550 / 1.25 = 440$  fins per tube length

Fin side area =  $(26 \times 330) - (30 \times 25 \times 2.5) = 6705 \text{ mm}^2$

Fins volume =  $6705 \times 0.5 \times 440 = 1475100 \text{ mm}^3 = 1.4751 \times 10^{-3} \text{ m}^3$

Mass of fins/pass =  $V \times \rho_{\text{aluminum}}$  (2721 kg/m<sup>3</sup>)

=  $1.4751 \times 10^{-3} \times 2720 = 4.012272 \text{ kg}$

Fins total mass = 4.012272 x 2= 8.024544 kg

### **A-1.1.2 Tubes**

Volume of tube = 25 x 2.5 x 550 = 34375 mm<sup>3</sup> = 3.437x10<sup>-5</sup> m<sup>3</sup>

Mass of tubes /pass = No. of tubes / pass x V x  $\rho_{aluminum}$  (2721 kg/m<sup>3</sup>)

30 x 3.437x10<sup>-5</sup> x 2721 = 2.805 kg

Total mass of tubes = 2.805 x 2= 5.61 kg

### **A-1.2 Heat of adsorbent:**

$$\begin{aligned} Q_{ads} &= M_{ads} \times C_{ads} \times (T_{desorption} - T_{adsorption}) \\ &= 3.2 \times 0.934 \times (70 - 35) = 104.608 \text{ kJ} \end{aligned}$$

### **A-1.3 Heat of Metals:**

$$\begin{aligned} Q_{Metal} &= M_{fin} \times C_{Al} \times (T_{desorption} - T_{adsorption}) + (M_{tube}) \times C_{Al} (T_{desorption} - T_{adsorption}) \\ &= 434.260 \text{ kJ} \end{aligned}$$

### **A-1.4 Heat of adsorption:**

Isothermic heat of adsorption for Silica gel is 2430 kJ/kg of water vapor.

Change in uptake for Silica gel ( $\Delta w$ ) = 0.07

$$\begin{aligned} Q_{reaction} &= M_{ads} \times \Delta w \times h_{ads} \\ &= 3.2 \times 0.07 \times 2500 = 560 \text{ kJ} \end{aligned}$$

### **1.5 Total Heat supplied:**

Total heat needed = 104.608 + 434.260 + 560 = 1098.86 kJ

For 520 (s) half cycle time

$$Q_{Heating} = 1098.86 \text{ kJ} / 520 \text{ sec} = 2.113 \text{ kW} = 2113 \text{ W}$$

### **A-2 Condenser Design**

Water created per second is:

$$\begin{aligned} \dot{m} &= 0.07 * 3.2 \text{ (kg}_{adsorbent} \text{ in bed)} / 520 \text{ (sec. cycle time)} \\ &= 0.00004307 \text{ kg/s} \end{aligned}$$

= 3.7212 kg – water/day for the 1 kg of adsorbent.

Heat of condensation is:

$$Q_{cond} = m_{water} \times h_{fg}$$

Where  $h_{fg} = 2458.8$  kJ/kg at  $T_{cond} = 18^\circ\text{C}$ , then

$$Q_{cond} = 2458.8 \times 3.7212 = 9149.68 \text{ kJ/day} = 0.1058 \text{ kW} = Q_{cond}$$

Coil designs:

$$Q_{cond} = UA\Delta T_{cw}$$

$$Q = 105.8 \text{ W}, U = 300 \text{ W}/(\text{m}^2\text{K}), \Delta T_{cw} = 1^\circ\text{C}, \text{ then } A = 0.3526 \text{ m}^2$$

Coil length is calculated by:

$$A = (\pi \times d_{coil}) \times l \quad d_{coil} = 0.0158 \text{ m}$$

Coil long is  $l = 7.1 \text{ m}$

### A-3 Evaporator Design

$$\dot{m}_{\text{created water}} = 0.07 \times 3.2 \text{ (kg adsorbent in bed)}/520 \text{ (sec. cycle time)}$$

$$= 0.00004307 \text{ kg/s}$$

$$Q_{evap} = m_{water} \times h_{fg}$$

Where  $h_{fg} = 2406.7$  kJ/kg at  $T_{evap} = 40^\circ\text{C}$ , then

$$Q_{evap} = 2406.7 \times 0.00004307 = 0.10365 \text{ kW} = Q_{evap}$$

Coil designs:

$$Q_{evap} = UA\Delta T_{chilled\_w}$$

Where  $Q = 103.65 \text{ W}$

$$U = 300 \text{ W}/(\text{m}^2\text{K}) [51]$$

$$\Delta T_{chilled\_w} = 1.1^\circ\text{C}, \text{ then } A = 0.31409 \text{ m}^2$$

Coil length is calculated by:

$$A = (\pi \times d_{coil}) \times l \quad \text{Then the length of coils is } l = 6.56 \text{ m}$$

## Appendix B

### The Calibration of Instruments used in Thesis:

جمهورية العراق

وزارة التخطيط  
الجهاز المركزي للقياس والسيطرة النوعية

العدد : ٨٤٨١  
التاريخ م : ٢٠٢١/١٠/٤  
هـ : ١١



الدائرة : التقييس  
القسم : المقاييس

إلى / جامعة كربلاء - كلية الهندسة - الموارد البشرية

م / معايرة أجهزة

يهدى الجهاز أطيب تحياته .....  
أشارة إلى كتابكم ذي العدد د/٣/ ٢٠١٤ في ٢٠٢١/٨/١ نود اعلامكم الاتي :  
١- تمت معايرة الجهاز العائد لكم وكانت النتائج كما مبينة في شهادة المعايرة و ينبغي الاخذ بنظر الاعتبار النتائج و التصحيحات عند القياس علما ان المعايرة نافذة لمدة سنة .  
٢- نعتذر عن معايرة الاجهزة الواردة في الفقرات (٣، ٤، ٥) لعدم وجود الامكانية في الوقت الحاضر .  
٣- تم تسديد أجور المعايرة البالغة (٧٧٠٠٠) سبعة وسبعون الف دينار فقط بموجب وصل القبض المرقم (٣٥٠٨٣) في ٢٠٢١/٨/٣ .


الأجهزة :

Data Logger مع مزدوج حراري نوع (K) عدد ٧/

مع التقدير ....

المراقبات /

شهادة معايرة عدد (١) فقط .

  
المهندسة

خلود خالد شكري  
ع/ مدير عام دائرة التقييس  
٢٠٢١/١٠/٤



نسخة منه إلى /

- مكتب المدير العام /للتفضل بالاطلاع ..... مع التقدير
- شعبة القياسات الفيزيائية لطفًا.


هناء محمد قانر



**Calibration Certificate**  
**Central Organization for Standardization and Quality Control (COSQC)**  
**Metrology Department - Physics Section** (FOR-TC-012)  
 P.O. Box13032 Aljadriya street, Baghdad , Tel:7785180 - E-Mail : cosqc@cosqc.gov.iq

Certificate No.: PHT 677 / 2021  
 Date of issue : 12/08/2021

Customer		
Name:	جامعة كربلاء / كلية الهندسة	
Address:	العراق - كربلاء المقدسة	
Item under calibration		
Description:	Temperature Recorder 12 CH With TC ( K )	Res. : 0.1 ° C
Manufacturer:	LUTRON	
Model:	BTM - 4208SD	
Serial number:	I.144597	
Other identification:	(-200 ----- 1370) °C	
Date of reception:	Order no. : (260) , Date of Reception : 3/08/2021	
Condition of reception:	As Found	
Standard(s) used in the calibration		
Description:	Digital Nano volt / Micro Ohm meter	PT100
Manufacturer:	Agilent	---
Model:	34420A	---
Serial number:	MY42000734	( 1 , 3 )
Other identification:	ID : PHT-01- 17	ID : PHT-01-84 , 86
Calibration information		
Date of calibration:	10/08/2021 , Due to: 10/08/2022	
Place of calibration:	PH LAB. 1	
Method(s) of calibration:	Calibration method using - PROC-TC-012 ( C )	
Calibrated quantity:	Temperature ° C	
Results of calibration:	Attached a complete result in Annex 1 of this certificate	
Measurement uncertainty:	The reported expanded uncertainty is based on UKAS M3003 Standard and the standard Uncertainty multiplied by coverage factor k=2 to give confidence level of 95%	
Metrological traceability:	The traceability of measurement results to the SI units is assured by the National standard maintained at Central Organization for standardization and Quality Control through calibration at :- UME /CER. NO (G1KS-0127)	
Environmental conditions of calibration:	Temp. 37.51° C	RH. 23.5%
Observations, opinions or recommendations:	The results in Annex 1 should be taken into consideration	

Approved by:  
  
 Eng. Moyasser Ali Taher  
 Head Of Physics Section  
 12/08/2021

1 of 2

This certificate is issued in accordance with the laboratory accreditation requirements. It provides traceability of measurement to recognized national standards, and to the units of measurement realized at the COSQC or other recognized national standards laboratories. This certificate may not be reproduced other than in full by photographic process. This certificate refers only to the particular item submitted for calibration.

Ref. Proc.Tc-012

**Figure (B.1): Data logger and thermocouples calibration**



**Calibration Certificate**  
**Central Organization for Standardization and Quality Control**  
**Metrology Department - Physics Section** (FOR-TC-012)  
P.O. Box13032 Aljadriya street, Baghdad , Tel:7785180 - - E-Mail : cosqc@cosqc.gov.iq


Certificate No.: PHT 677 / 2021  
Date of issue : 12/08/2021

**Annex 1**

**Results**

The results of the measurements are given on table below.

TC No.	Set. Value C°	Ref. ( R ) C°	UUC (M) C°	Error (M)-(R) C°	Uncertainty ± C°
TC 1	25	25.01	25.9	0.85	1.04
TC 2	35	34.98	35.7	0.74	0.95
TC 3	45	45.04	45.8	0.76	0.88
TC 4	55	55.01	55.80	0.79	0.92
TC 5	65	65.02	65.70	0.68	0.79
TC 6	75	23.02	23.40	0.38	0.45
TC 7	95	94.19	95.00	0.81	0.94

  
Calibrated by :  
Khalid Naser  
12/08/2021

  
Revised by:  
Hanaa Mohammed  
12/08/2021

  
Approved by:  
Moyasser Ali Taher  
12/08/2021

2 of 2

This certificate is issued in accordance with the laboratory accreditation requirements.It provides traciability of measurement to recognized national standards,and to the units of measurement realized at the COSQC or other recognized national standards laboratories.This certificate may not be reproduced other than in full by photographic process.This certificate refers only to the particular item submitted for calibration

Ref. Proc.Tc-012

**Figure (B.2): Results of calibration**



## Appendix C

### Published Research



*Kerbala Journal for Engineering Sciences*  
*Refereed Scholarly Journal*  
ISSN: 2709-6718

---

---

**Manuscript Acceptance Letter**

Dear Authors, Mohammed Al-Jibory, Fadhel Al-Mousawi and Esraa Abbas,

I am pleased to inform you that based on the recommendations of the reviewers and the editorial board members, your manuscript entitled:

**Numerical Study of an Adsorption Water Desalination System Utilizing Low-grade Heat Sources**

has been accepted for publication in the (Kerbala Journal of Engineering Sciences). The manuscript will be published in Vol. (02), Issue (01), on 03/2022.

Thanks for submitting your manuscript to our journal. Please do not hesitate to contact us if you have any questions regarding the publication process.

Best wishes,



**Prof. Dr. Basim K. Nile**  
Editor-in-Chief  
Kerbala Journal of Engineering Sciences (KJES)  
Date: 02/06/2022

---

*Published by College of Engineering, University of Kerbala, Iraq*  
Email: [kjes@uokerbala.edu.iq](mailto:kjes@uokerbala.edu.iq)

## Published Conference



### ICEAT 2022

### The 2<sup>nd</sup> International Conference on Engineering and Advanced Technology

28-29 March 2022, Turkey- Istanbul



Paper ID: 297

March 10, 2022

Esraa Abbas<sup>1, a)</sup>, Fadhel Al-Mousawi<sup>1, b)</sup> and Mohammed Al-Jibory<sup>1, c)</sup>

<sup>1</sup>Mechanical Engineering Department, College of Engineering, University of Kerbala, Kerbala, Iraq.

Dear Authors,

Herewith, we are happy to inform you that the peer-reviewed paper entitled: "**Experimental and Numerical Study On a Low Grade Heat Driven Adsorption Desalination and Cooling System Performance**" has been accepted for oral presentation as well as inclusion in the conference proceedings in the *2<sup>nd</sup> International Conference on Engineering and Advanced Technology (ICEAT 2022)* which is organized by Al-Qadisiyah University, Mustansiriyah University and the University of Warith Al-Anbiyaa, Iraq in collaboration with the University of Birmingham, UK, Hacettepe University -Turkey and Taras Shevchenko National University of Kyiv-Ukraine.

The conference ICEAT2022 will be held in Turkey- Istanbul on 28-29 March 2022. Due to the Coronavirus situation, the conference sessions will be held virtually depending on the Covid-19 circumstances.

The high-impact conference papers will also be considered for publication in the AIP Conference Proceeding: which are indexed by Scopus.

As this is an International Conference, we request you to present your paper and take part in the oral discussion.

We look forward to meeting you at the ICEAT 2022 Conference.

Yours sincerely,

Prof. Dr. Salih A. Rushdi  
Conference Organizing Committee Chairman  
Al-Qadisiyah University

Assist. Prof. Dr. Zainab T. Al-Sharify  
Conference Organizing Committee Chairman  
Mustansiriyah University

## Appendix D

### **D-1 Sample Example to Calculate (SDWP)**

$m'$  for fresh water collected from condenser = 0.7 liter

No. of cycle = 5

Adsorber mass ( $M_a$ ) = 3.2 Kg

Total time of cycle = half cycle time x 2 = 300 x 2

$$SDWP = \frac{\text{collected potable water (litre)}}{\text{Adsorber mass (kg)} \times \text{No. of cycle} \times \text{Total time of cycle (sec)}}$$

$$SDWP = \frac{0.7}{3.2 \times 5 \times 600} \times 3600 \times 24 = 6.3 \text{ liter/Kg}_{ads} / \text{day}$$

### **D-2 Sample Example to Calculate (SCP)**

Mass flow rate for chilled water pass through evaporator coil

$$m' = 11.8 \text{ liter / min} \Rightarrow m' = 0.1971 \text{ Kg/s}$$

specific heat capacity for water @ 38°C = 4.2 kJ. K<sup>-1</sup>.kg<sup>-1</sup>

$$\Delta T_{evap} = T_{w,in} - T_{w,out} \Rightarrow \Delta T_{evap} = 38^\circ - 37.6^\circ = 0.4^\circ \text{ C}$$

$$SCP = \frac{m'_{evap} C_p (T_{out,evap} - T_{ine,vap})}{M_a}$$

$$SCP = \frac{0.1971 \times 4.2 \times 0.4}{3.2} = 0.1034 \text{ kW/kg}_{ads} \Rightarrow 103.4 \text{ W/kg}_{ads}$$

## Appendix E

To calculate the uncertainty of the experimental results the following parameter is concerned:

1) The mean value of the variable  $x$  calculated as:

$$X_{mean} = X_{avaregr} = \frac{\sum_1^n x_i}{n}$$

2) The standard deviation of  $x$ , given by:  $\sigma = \sqrt{\frac{\sum_1^n (x_i - x_{mean})^2}{n-1}}$

3) The standard error is given by:  $\sigma_m = \frac{\sigma}{\sqrt{n}}$

4) The uncertainty of variable  $x$  given by:

$$x = X_{mean} \pm \sigma_m = X_{mean} \pm \frac{\sigma}{\sqrt{n}}$$

While the variables which are measured their uncertainty are specific daily water production (SDWP) and specific cooling power (SCP)

; the calculation shown in the table (E-1).

Table (A-1) The uncertainty calculations

no	The variable	Number of values	The tested value	$X_{mean}$	$\sigma$	$\sigma_m$	$x$
1	$T_{bed}$	$X_1$	70	80	10	5.77	85.77
		$X_2$	80				74.23
		$X_3$	90				
2	$T_{evap}$	$X_1$	30	34	4	2.3	36.3
		$X_2$	34				
		$X_3$	38				31.7

3	$T_{\text{cond}}$	$X_1$	14	16	2	1.15	17.15
		$X_2$	16				14.85
		$X_3$	18				

## الخلاصة

تعتبر ندرة مياه الشرب مشكلة واسعة الانتشار في العديد من البلدان، وتؤثر على جودة حياة الملايين من الناس. على الرغم من أن تقنيات تحلية المياه يمكن أن تساعد في حل مشكلة ندرة المياه، إلا أنها تحتاج إلى الكثير من الطاقة وتصدر الكثير من (ثاني أكسيد الكربون). أجريت هذه الدراسة لبناء جهاز اختبار ونموذج (MATLAB SIMULINK) لتحلية وتبريد الامتزاز، ومراقبة أداء النظام في ظل ظروف تشغيل مختلفة، وتحديد أفضل ظروف التشغيل. تم فحص النظام تجريبياً وعددياً في ظل ظروف ثابتة.

يتكون جهاز الاختبار من الأجزاء والملحقات الرئيسية. سرير الامتزاز والمكثف والمبخر هي المكونات الرئيسية للنظام. بينما تعد المضخات والخزانات وأجهزة القياس بمختلف أنواعها أجزاء ثانوية.

تم استخدام (MATLAB Simulink) في هذا العمل لمحاكاة المكونات المختلفة للنظام المقترح باستخدام هلام السيليكا والماء ثنائي امتزاز. نظرًا لقيود المعمل والتكلفة، تحتوي المنشأة التجريبية على سرير ممتز واحد فقط بالإضافة إلى المكثف والمبخر، بينما يحاكي النموذج العددي سريرين ممتزين بجانب المكثف والمبخر.

تم التحقق من صحة نموذج المحاكاة من خلال البحث التجريبي المنشور مسبقاً. تتم مراقبة أداء النظام من خلال مخرجاته، وهي إنتاج المياه اليومي المحدد وطاقة التبريد المحددة. تمت دراسة تأثير درجات حرارة سائل العمل في المكثف والمبخر والسرير وكذلك زمن نصف الدورة.

أظهرت النتائج التجريبية أن (إنتاج الماء اليومي المحدد وطاقة التبريد المحددة) للنظام يزدادان مع درجة حرارة الطبقة الساخنة بمقدار (2.43-6.21 لتر / كجم / يوم)، (87.95-100.88 واط / كجم) على التوالي ومع درجة حرارة المبخر بمقدار (4.5-6.3 لتر / كجم / يوم)، (72.43-103.47 واط / كجم) على التوالي، بينما تنخفض مع درجة حرارة الماء للمكثف بمقدار (6.03-5.49 لتر / كجم / يوم)، (98.3-99.59 واط / كجم) على التوالي مع زمن نصف الدورة بمقدار (2.97-4.59 لتر / كجم / يوم)، (72.43-95.71 واط / كجم) على التوالي.

يؤدي ارتفاع درجة حرارة التسخين من (70 درجة مئوية إلى 90 درجة مئوية) إلى نمو (60٪) في (الإنتاج اليومي المحدد وزيادة (12.8٪) في (طاقة التبريد المحددة). تم تحسين (إنتاج الماء اليومي المحدد وطاقة التبريد المحددة) بنسبة (28.5٪) و (30٪) على التوالي عندما ترتفع درجة حرارة الماء في المبخر من (30 درجة مئوية إلى 38 درجة مئوية). تنخفض قيم (إنتاج الماء اليومي المحدد وطاقة التبريد المحددة) بنسبة (55٪ و 32٪) على التوالي عند زيادة فترة نصف الدورة من (300 إلى 500 ثانية).

تسلط النتائج الضوء على إمكانية إنتاج مياه الشرب ودرجات حرارة التبريد باستخدام درجة منخفضة لمساعدة ملايين الأشخاص حول العالم.



وزارة التعليم العالي والبحث العلمي  
جامعة كربلاء  
كلية الهندسة  
قسم الهندسة الميكانيكية

## دراسة تجريبية و عددية لنظام تحلية مياه بالامتزاز باستخدام مصادر حرارة منخفضة

رسالة مقدمة الى كلية الهندسة -جامعة كربلاء كجزء من متطلبات نيل  
درجة الماجستير في علوم الهندسة الميكانيكية  
( حراريات وموائع )

من قِبل

**إسراء عباس حسين**

بإشراف

**أ.م. د محمد وهاب الجبوري**

**أ.م. د فاضل نورالدين الموسوي**